A STUDY OF THE FACTORS INVOLVED IN THE DEOXIDATION OF MOLTEN IRON AND SOME OF ITS ALLOYS.

Thesis   Presented

by

Abou-Bakr A. Murad, B.Sc.

For the Degree of Doctor of Philosophy of The University of Glasgow.

June, 1951.

C O N T E N T S.

CHAPTER I.

INTRODUCTION.

1. Main Reactions in Steelmaking:

In most of the reactions involved in steel making, oxygen dissolved in the metal is the most active agent in eliminating the metalloids. Thus carbon removal proceeds according to the equation *

$$\underline{C} + \underline{O} = CO \text{ (gas)}.$$
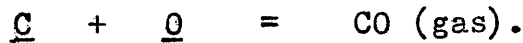
The carbon monoxide escapes into the furnace atmosphere. Silicon and manganese are oxidised by the reactions

$$\underline{Si} + 2\underline{O} = SiO_2$$

$$\underline{Mn} + \underline{O} = MnO$$
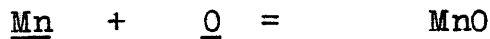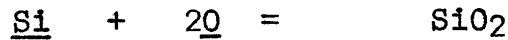
The oxides formed rise to the top of the bath to form part of the slag. The removal of phosphorus probably takes place in two steps.

$$(1) \quad 2\underline{P} + 5\underline{O} = P_2O_5$$

$$(2) \quad P_2O_5 + 3\, CaO = Ca_3(PO_4)_2$$
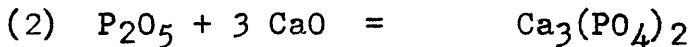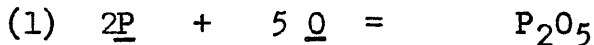
The possibility of the intermediate formations of $3\, FeO.P_2O_5$ seems unlikely; its stability, especially in contact with molten iron, has been questioned,[1] the following reaction probably occurring

$$3\, FeO.P_2O_5 + 11\, Fe = 2\, Fe_3P + 8\, FeO$$
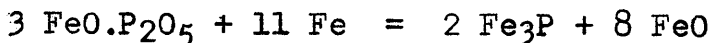
Oxygen has been shown by Carter [2] to play an important part in the removal of sulphur, where the reaction occurring is

$$MO + \underline{S} = MS + \underline{O}$$

MO/

MO is either CaO, MgO, MnO and FeO in the "uncombined" state, the desulphurising powers being approximately equal as all behave as a source of oxygen anions in the slag. It will be noted, however, that here oxygen in the metal hinders sulphur removal.

---

* Throughout this thesis, underlined reactants in chemical equations refer to the liquid metal (iron) phase. In the Mass Action Expression, square brackets will indicate concentra: :tions in the molten metal in percentage by weight, and round brackets will indicate concentrations in the slag in percentage by weight, unless stated otherwise.

---

2. Factors controlling the oxygen content of steel before Deoxidation:

Before considering the factors involved in the removal of oxygen from molten steel, it would seem of interest to consider briefly the factors controlling the oxygen content of steel prior to deoxidation.

(a) Sources of oxygen in the molten steel: The oxygen necessary for the above reactions is supplied to the metal both indirectly by the gas phase, the slag being the medium of transfer of oxygen, or by direct iron oxide additions. From the time the heat is melted, the oxygen content of the bath is gradually rising and the carbon content is decreasing. Carbon content may thus be considered a fair index of oxygen content.

(b) The carbon-oxygen equilibrium in the Bath: Since several workers have shown that there is a close relationship between the carbon/
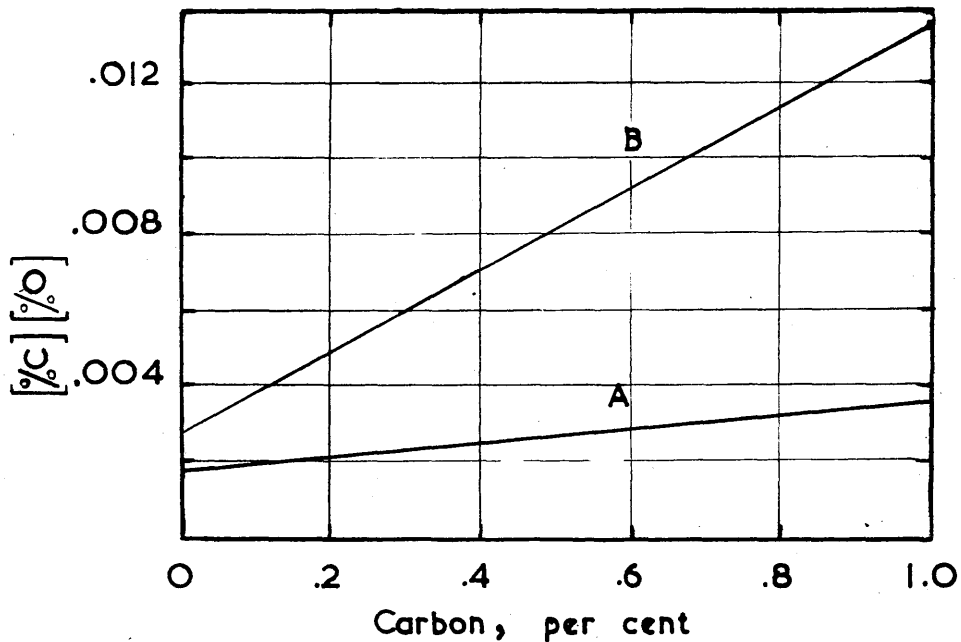
FIG.1. THE CARBON — OXYGEN PRODUCT at 1 atm.

A, at equilibrium   B, average in open hearth.
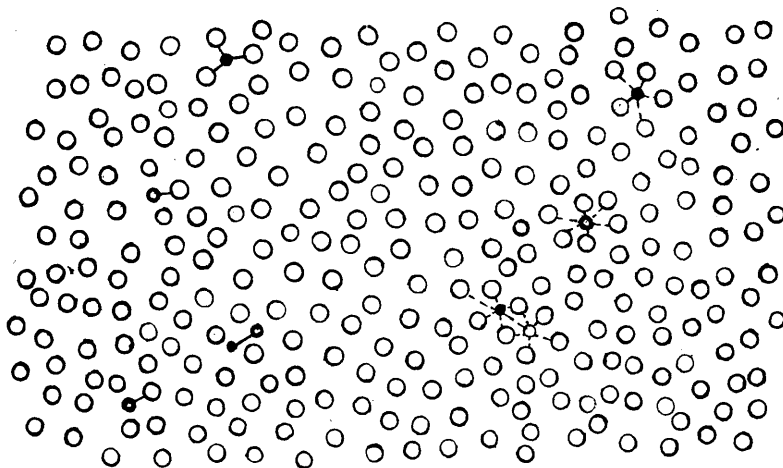
FIG. 2. ALTERNATIVE   ARRANGEMENTS OF   OXYGEN
ATOMS   (small open circle) & CARBON   ATOMS (small black
circle) IN LIQUID STEEL.

carbon and oxygen contents of the steel bath during the refining period it seems necessary to review the work done in studying their equilibrium. For the reaction:-

$$\underline{C} + \underline{O} \rightleftharpoons CO(gas)$$
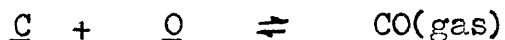
The equilibrium constant is given by

$$K = \frac{p_{CO}}{[C][O]}$$

The product $[C][O]$ should therefore be constant for a given pressure of carbon monoxide if one assumes that the activity of each element is equal to its percentage by weight. This reaction has been studied under equilibrium conditions by Vacher and Hamilton[3], Phragmen and Kalling[4] and Marshall and Chipman[5]. Their results, which are in very good agree:ment, are shown in Fig.1, line A, where the product $[C][O]$ is plotted as a function of the carbon content in the steel under equilibrium conditions while line B represents conditions in the open hearth. The data show that the product $[C][O]$ is not a constant under equilibrium conditions or during refining but it increases with increasing carbon content. Thus the addition of carbon to the bath not only reduces the quantity of oxygen remaining but it also renders less active that which remains. Fig.2 shows two alternative representations given by Chipman [6] of the behaviour of carbon and oxygen atoms in liquid steel. On the left each carbon atom is bonded to three iron atoms forming the molecule Fe_3C. Each oxygen atom is combined /

combined with an iron atom to form a molecule of FeO. In a
limited number of places a carbon and an oxygen atom may form a
molecule of CO. According to this picture the activities of
carbon and oxygen are both reduced because of the formation of
"molecules" of carbon monoxide in the molten steel. Chipman
in his earlier work by assuming a solubility of .0028 per cent
CO at $1600^{o}C$ under 1 atm. pressure in iron, and making the
necessary corrections to the total percentages of carbon and
oxygen dissolved in the iron, obtained a constant value for the
$[a_c]$ $[a_o]$ product.

The other representation is given on the right of Fig.2
where each carbon is bonded to all of its surrounding iron atoms.
The bond strength falls off with distance so that only nearest
neighbour atoms are effective. Each oxygen atom is similarly
bonded to its nearest neighbour iron atoms. When carbon and
oxygen atoms are close together, they may share the bonding of
nearby iron atoms and the carbon oxygen bonding may also become
effective. In the resulting complex it is clear that both
carbon and oxygen are held more firmly than when bonded to iron
alone, and the activity of each is reduced in proportion to the
number of such complexes present. In a steel of high carbon and
low oxygen content, a small fraction of the carbon atoms may
thus reduce the activity of a large fraction of the oxygen.
Thus the activity coefficient of oxygen is reduced by the pre:
:sence of carbon and vice versa. This picture leads to
similar results to the first but appears much more probable.
Many/

Many deoxidising elements have a similar effect to carbon and not only remove oxygen from steel but also have a pronounced lowering effect upon the activity of the oxygen remaining in solution in the steel.   This was predicted in a qualitative way by Zapffe and Sims[7] in their discussion on the existence of certain monoxides (e.g. silicon monoxide) in steel.   Quantit: :ative data are still scarce, although the subject has been excellently reviewed recently by Chipman[6] and Richardson[8]. The latter has shown that the deoxidising elements reduce the activity coefficient of the dissolved oxygen $\gamma_{[O]}$ below the value in pure iron.   The magnitude of the effect, increases markedly with the deoxidising power of the alloying element and the stability of its appropriate oxide.   This is shown in Table I.

Table I.

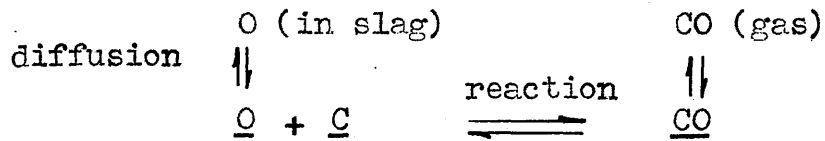| Deoxidiser X	Factor by which is lowered by ·5% X	Diff. between energies of association of O_2 with deoxidiser & with Fe Kg.cal/gram at. of O_2
Cr	.94	-27.6
Mn	.9	-30.0
V	.73	-36.9
Si	.8	-42.2
C	.7	+35.3
Al	.1	-71.0

The lowering of the activity coefficient of oxygen by the deoxidiser is probably due to some association between the atoms of oxygen and those of the deoxidiser, therefore the activity coefficients of the deoxidisers themselves should be lowered in the presence of dissolved oxygen.   Since oxygen is normally present /

present in far smaller quantities than the deoxidising element, its effect on the activity coefficient of the deoxidiser should be negligible.

Fig.1 also shows that the bath normally contains an excess of oxygen over the equilibrium value, so that the "boil" does not represent true equilibrium conditions. This has been ascribed to the difficulty of forming gas bubbles within the liquid steel and it is probable that such bubbles form most easily at a rough surface e.g., the tiny crevices of the dolomite bottom of an open hearth furnace. This was shown experimentally by Korber and Oelsen[9] who, using melts of iron with FeO in solution, held within crucible walls completely glazed over with a liquid slag layer, were able to introduce from 10 to 15 times the equilibrium amount. of carbon before any reaction occurred at all. An iron wire dipped in caused such melts to boil vigorously; dipping a rod of fused silica caused no effect but if the crucible walls under the liquid were scratched by the rod, vigor: :ous boiling again occurred. Melts in crucible walls not com: :pletely glazed over boiled with relatively little excess carbon.

(c) FeO content of slag. The representation of the carbon-oxygen reaction in the bath by the equation $\underline{C} + \underline{O} \rightleftharpoons$ CO (gas) is misleading since it does not represent the whole picture. The carbon is dissolved in the molten iron, while the main source of oxygen is in the slag and must be transferred to the metal; the product, CO, is liberated as a gas in the metal bath which later escapes to the furnace atmosphere. The whole/

whole process may then be represented as follows:-

diffusion   O (in slag)   CO (gas)

$$\text{diffusion} \quad \underset{\underline{O} + \underline{C}}{\overset{O \text{ (in slag)}}{\updownarrow}} \quad \xrightleftharpoons{\text{reaction}} \quad \underset{\underline{CO}}{\overset{CO \text{ (gas)}}{\updownarrow}}$$

At each of the three stages a process occurs which may control
the oxygen content of the metal. Korber and Oelsen [9] assumed
that the reaction between carbon and oxygen proceeded very rapidly
with the formation of the supersaturated solution of carbon
monoxide. According to these authors the slowest process in
the carbon reaction is the evaporation of the carbon monoxide
from such a supersaturated solution in steel. Korber and Oelsen
in assuming an instantaneous reaction between carbon and oxygen
have come to the conclusion that the oxygen content of the bath
is governed exclusively by the carbon reaction and that there is
therefore no direct equilibrium between the oxygen in steel and
the iron oxide in the slag. On the other hand Herasymenko [10]
assumed that the slowest reaction was that between carbon and
oxygen and that this required a considerable activation energy.
As a consequence the oxygen content of steel has no connection
with the carbon reaction, being influenced only indirectly by the
dissolved carbon, and depended mainly on the iron oxide content
of the slag.

The work of Fornander [11] indicates that the carbon
content of the bath is the factor which has the greatest influ:
:ence upon the oxygen content during the refining period.
Analysis of Fornander's data as indicated by Carter [12] suggests
that /

that towards the end of the refining period, i.e., at low [C], [O] is not entirely independent of the total FeO content of the slag. On the other hand recent investigations of actual open hearth heats by Speight[13] have shown that the oxygen contents of melted and tapped samples bear more or less the expected relationships to carbon content, yet consideration of the carbon content of the liquid steel bath alone does not give a sufficiently close indication of its oxygen content. A far better correlation appears to exist between the carbon content of the bath and the total iron in the slag, which show an almost straight line relat: :ionship. The melt samples show a greater degree of scatter from the straight line relationship.

The conclusion drawn from this argument is that the carbon content of the steel bath is a fair index of the oxygen content during the early stages of the refining period. At the end of the refining period when the carbon content is relatively low, the total iron content of the slag seems to give a better indication of the oxygen content of the bath since at this stage it would be expected that the metal and slag are approaching equilibrium. This might mean that at the beginning of the refining period the carbon-oxygen reaction in the bath proceeds faster than the diffusion of oxygen from the slag to the metal and vice versa towards the end of the refining period.

3. The form of oxygen in liquid Steel.

Before discussing deoxidation it is important to know the form in which oxygen exists in steel. Oxygen is always present/
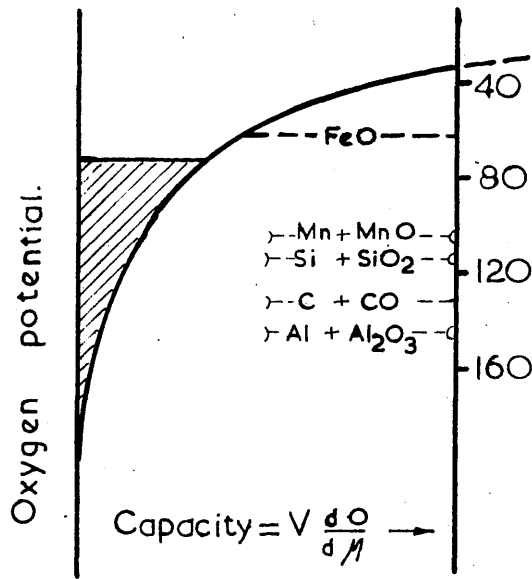
V volume of iron M potential of oxygen.

FIG. 3.
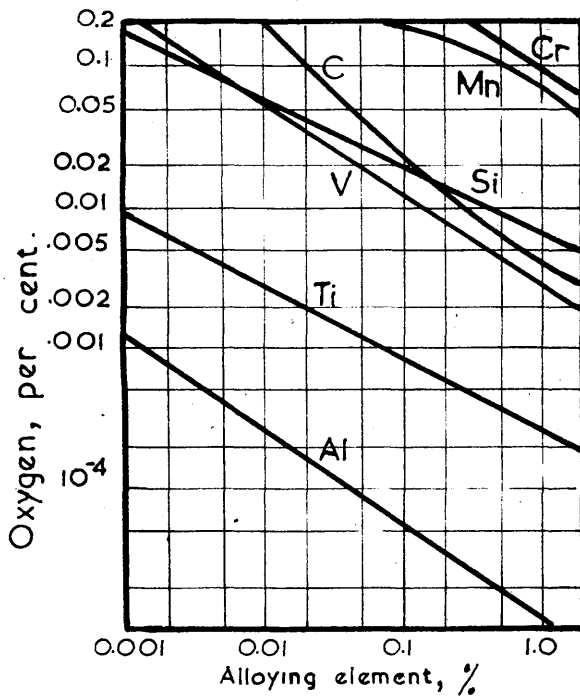
FIG. 4.

present in steels even in the dead killed variety. Chipman [14]
has shown from studies of the equilibrium of the reaction between
liquid iron and steam, forming hydrogen and oxygen dissolved in
liquid iron, that the solute is mono-atomic with respect to oxygen
Thermodynamically it is unnecessary to define the nature of the
solution any more exactly and any calculation based on the formula
FeO will not be appreciably in error.

4. Deoxidation.

(a) The need for deoxidation: The oxygen content of steel
as tapped from the furnace depends to a large extent on the carbon
content and also on the tapping temperature, high temperature
increasing the amount of oxygen. For most purposes the oxygen
content is excessive and would give rise to defective ingots and
inferior steels. It is also necessary to control the carbon-
oxygen reaction during freezing so that the right amount of gas is
evolved, resulting in a rimmed, semi-killed or killed ingot as
desired. The oxygen content is therefore usually reduced by the
addition of suitable deoxidisers.

(b) The meaning of deoxidation: Theoretically speaking,
the removal of oxygen is accomplished by the addition of elements
whose oxides have a higher free energy of formation that that of
iron. According to Goodeve [15] these elements would open a
"leak" in the potential capacity curve (Fig.3) and combine with all
the oxygen above the level of the leak forming an oxide which
separates as a distinct slag or gas phase. Many elements are
possible, among them being C, Mn, Si, Al, Ti, V, Cr, etc.
Fig.4 /

Fig.4 compares the deoxidising powers of these elements at 1600°C. The completeness of the reaction depends upon the stability of the oxide produced, i.e., its free energy of formation, and upon the concentration of the deoxidiser remaining in the metal when equilibrium is reached. The relationship between the percentage of oxygen and deoxidiser X which remain in the steel is summarised by the equilibrium constant K for the reaction

$$FeO + \underline{X} \rightleftharpoons XO + \underline{Fe} \qquad\qquad K = \frac{(XO)\,[\underline{Fe}]}{(FeO)\,[\underline{X}]}$$

The deoxidation process really takes place in two distinct stages
i) The reaction between the deoxidising element and the oxygen dissolved in the steel, forming a deoxidation product.
ii) The removal of the deoxidation product from the liquid steel. The occurrence of such a reaction as the above does not therefore necessarily mean that the oxygen content of the body of metal has decreased, as in many cases the deoxidation products remain sus: :pended in the steel. Nevertheless, even though these products may not be removed from the steel, the steel is usually superior to the untreated steel as oxygen combined in the form of deoxida: :tion products is normally less deleterious than oxygen in the form of FeO. It is, however, always preferable to aim at removal of the products of deoxidation.

Thus when aluminium is added to molten iron containing dissolved oxygen, the following reaction occurs:-

$$\underline{FeO} + \underline{Al} = \underline{Fe} + Al_2O_3 \text{ (solid)}$$
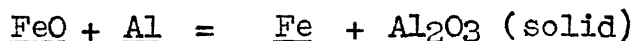
As /

As the deoxidation product, alumina, is solid at steel making temperatures, little or no coalescence occurs and the alumina is found in a state of fine dispersion in the solid ingot[16]. The state of the metal from the cleanliness point of view has not therefore been changed and we have simply replaced the FeO in the steel by Al_2O_3.

The rapid elimination of the products of deoxidation depends on the following factors:-

1. They should be liquid at steel making temperatures in order that the primary particles can coalesce into larger ones and so rise out of the bath more rapidly.   Whether or not the particles coalesce also depends on their viscosity

2. Stokes law which gives the velocity of spherical particles rising through a liquid is frequently encountered in the study of non-metallic inclusions in steel.   The law states that -

$$V = \frac{2}{9} gr^2 \frac{d_1 - d_2}{\gamma} \quad cm/sec.$$

where V is the final rising velocity , r is the radius of the particles in one, d_1 the density of the liquid in gm/cc, d_2 the density of the particle in gm/cc and γ is the viscosity of liquid in poise.   Although this law is not strictly followed by non-metallic inclusions rising in a steel bath because of complica: :tions caused by convection currents, etc., yet the following considerations follow from it:-

(a) The size of the deoxidation product should be as large as possible.

(b) /

(b) The density of the deoxidation products should be low.

5. <u>Theories of inclusion formation and growth:</u>

There appear to be two main schools of thought on the subject of coalescence and size of inclusions. Herty[17] stated that coalescence of non-metallic inclusions has been experiment: :ally demonstrated, one of his photomicrographs showing large silicate particles in the centre of an ingot and silica particles in the chilled crystal zone of the ingot. These silica partic: :les must have been present in the liquid steel in the same size as in solid steel and the larger particles in the center of the ingot are due solely to coalescence and to fluxing of FeO by the silica particles.

The other school is mainly supported by Sims and Lillieqvist[18] Sosman and Kearny[19] and Zapffe and Sims[7]. Sims and Lillieqvist visualised the formation of large inclusions in steel castings as due to growth by progressive precipitation of the inclusion substance during cooling on inclusions already present rather than the production of a large number of tiny inclusions, followed by coalescence of these during cooling in the mould. Sosman and Kearny[19] stated that there is no reason to expect any influence of one inclusion upon another when they are separated by a distance of more than a few thousandth of a millimeter. This statement was made during the discussion of a polished sect: :ion shown by Herty on which there was a large globular inclusion surrounded /

surrounded by a ring of small satellites, the inference by Herty being that the large inclusion was drawing in and absorbing the smaller ones. According to Sosman and Kearny [19] the logical deduction from Herty's photograph, was that the small satellites were on their way out from the central globule and not on their way in. In support of this they quoted the work of Rashevesky who, working on spontaneous dispersion of small drops of liquid, found that any suspended drops in which a chemical reaction is taking place has an upper limit of size and if larger than this, it tends to be dispersed. Metallurgists studying the rise of inclusions should, therefore, distinguish between a liquid inclus: :ion in internal equilibrium and one in which a reaction is taking place. The latter may be dispersing itself instead of coalescing with others to form larger drops.

The photomicrographs of Zapffe and Sims [7] reproduced in Fig.5 shows highly siliceous inclusions produced by quenching a melt contain: :ing 0.34% Si, 0.26% FeO. . The photomicrographs offer coales: :cence as a possible explanation of the peculiar form of inclusions On the other hand it could be explained by Sosman's theory which suggests it is a case of dispersion rather than coalescence. This would indicate a chemical or physical reaction producing a very low surface tension. Zapffe & Sims suggested that such a reaction might be the decomposition of precipitated SiO according to the equation

$$2 \, SiO \quad = \quad Si + SiO_2$$
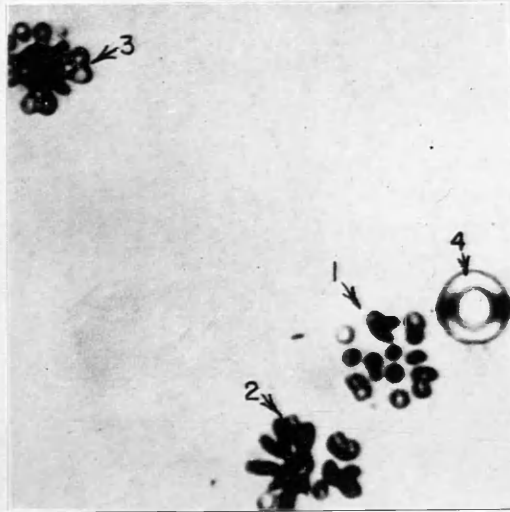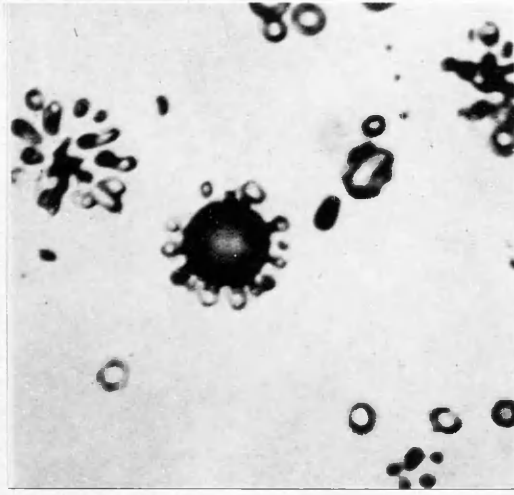
Another /

Fig. 5

Another possibility is that the round droplets with the protruber:
:ances are liquid SiO_2 inclusions on which cristobalite build up
by subsequent precipitation as the temperature decreased during
quenching.

According to any of the theories mentioned before, the growth of
inclusions is effected when they are in the liquid state at steel
making temperatures.   It is obvious therefore, that the two
important properties of the deoxidation products are their melting
points and fluidities.   The former necessitates a knowledge of the
thermal equilibrium diagrams of the various slag systems involved.
Since the present aim is to study   deoxidation with silicon and
manganese, a thorough knowledge of the following slag systems is
essential.

a.   Binary Systems $FeO-MnO$, $FeO-SiO_2$, $MnO-SiO_2$

b.   Ternary System $FeO-MnO-SiO_2$

It will be shown in a later chapter on slag-metal equilibrium
that these diagrams can be extremely useful in providing some
knowledge of the chemical constitution of liquid slags.

The plan of this research is to study the equilibrium
of molten iron-manganese alloys with $FeO-MnO-SiO_2$ slags which
are not saturated with SiO_2.   Owing to the time necessary for
the development of the vacuum fusion apparatus and the rotating
crucible furnace necessary for this work it was possible to
re-examine the $MnO-SiO_2$ and $FeO-MnO-SiO_2$ systems.   The results
obtained/

obtained will be described in the next four chapters, after
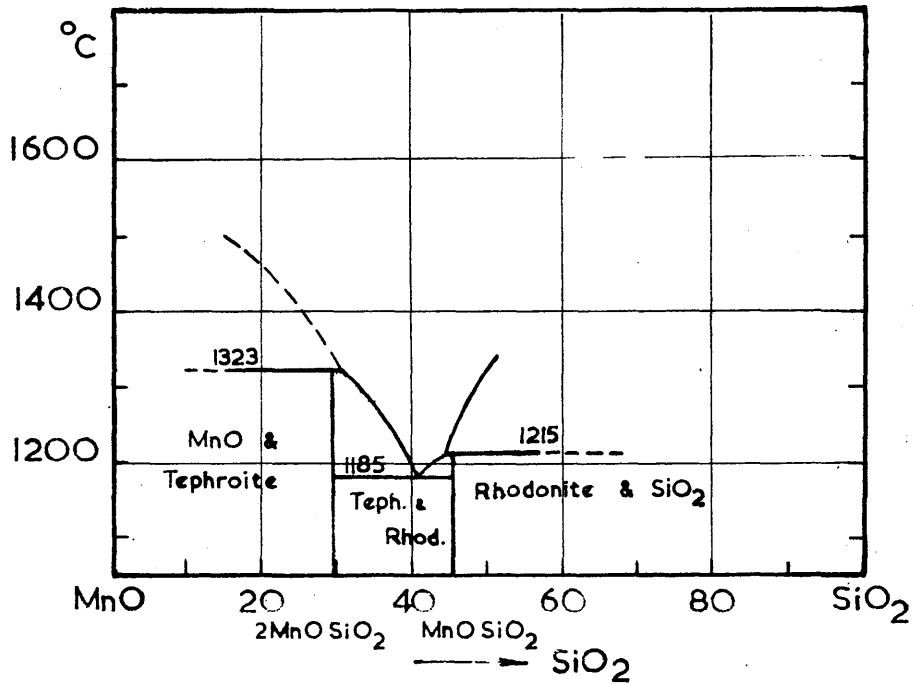which the main aim of the research will be considered.

FIG. 6a.   SYSTEM MnO —SiO₂   (Doerinkel.)
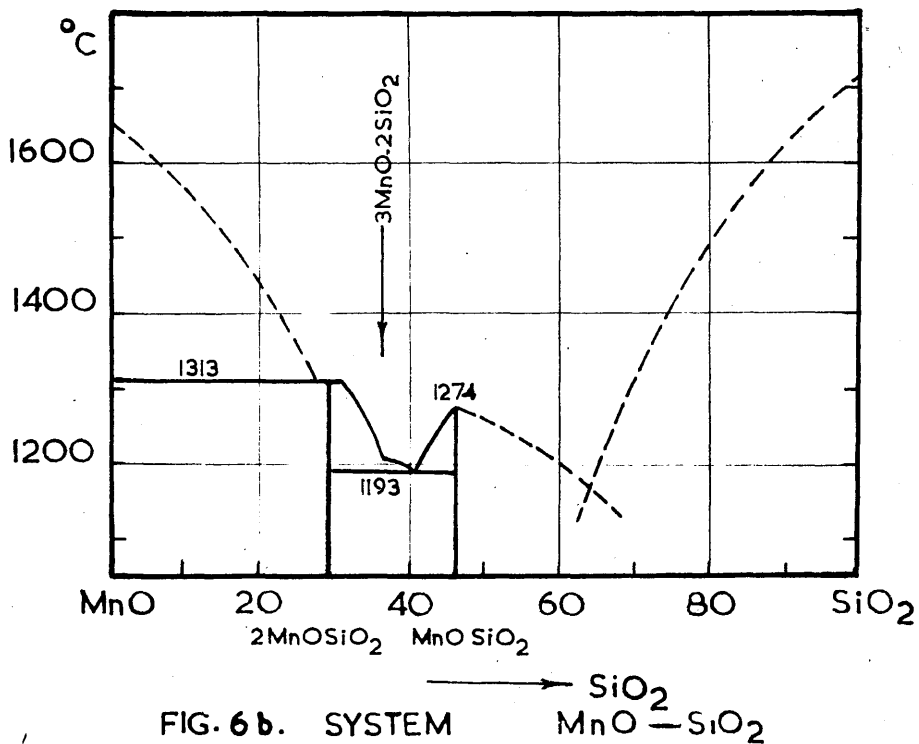
FIG. 6b.   SYSTEM   MnO — SiO₂

(O. Glaser.)

CHAPTER II.

THE BINARY SYSTEMS.

a. <u>Manganous oxide - Silica.</u>

This system was first investigated systematically by Doerinckel[20] in 1911. By means of thermal and microscopic examination, he established the presence of two silicates, tephroite (2 MnO SiO$_2$) and rhodonite (MnO.SiO$_2$), both melting incongruently . Cooling curves showed a eutectic between them at 41% SiO$_2$, melting at 1185°C, but microscopic examination of compositions on both sides of the eutectic point showed no eutectic structure. To explain this, Doerinckel suggested coalescence with the primary phase of the corresponding constituent in the eutectic. It should be mentioned here that no etching reagent was used for the microscopic examination. In the present work it was found that etching was very important in revealing the complete structure of these slags.

The results of Doerinckel are summarised in Fig.6a.

The diagram of Benedicks and Lofquist [21] shown in Fig.6c is based mainly on the results of Doerinckel, but also includes a region of immiscibility as given by Greig[22]. They also added narrow homogeneity ranges for all the solid phases.

Herty[23] also investigated the system and his diagram shown in Fig.6d bears the same features as those quoted above, but differs in many details. Because of these differences, the system was reinvestigated by White, Howat and Hay[24]. Their diagram, which is the one generally accepted now, is reproduced in/
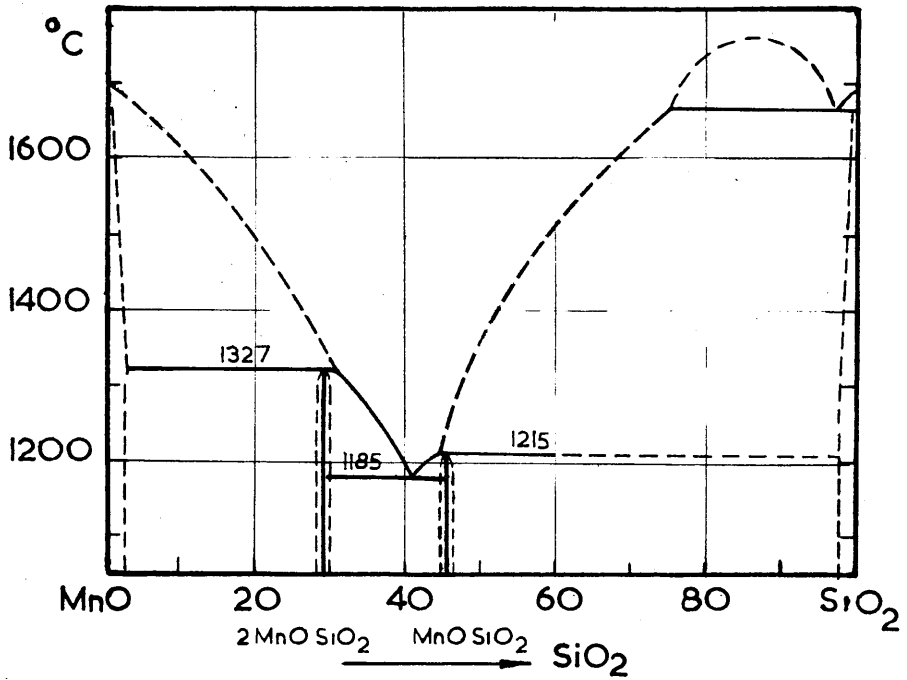
FIG. 6c. SYSTEM MnO — SiO₂

(Benedicks & Lofquist)
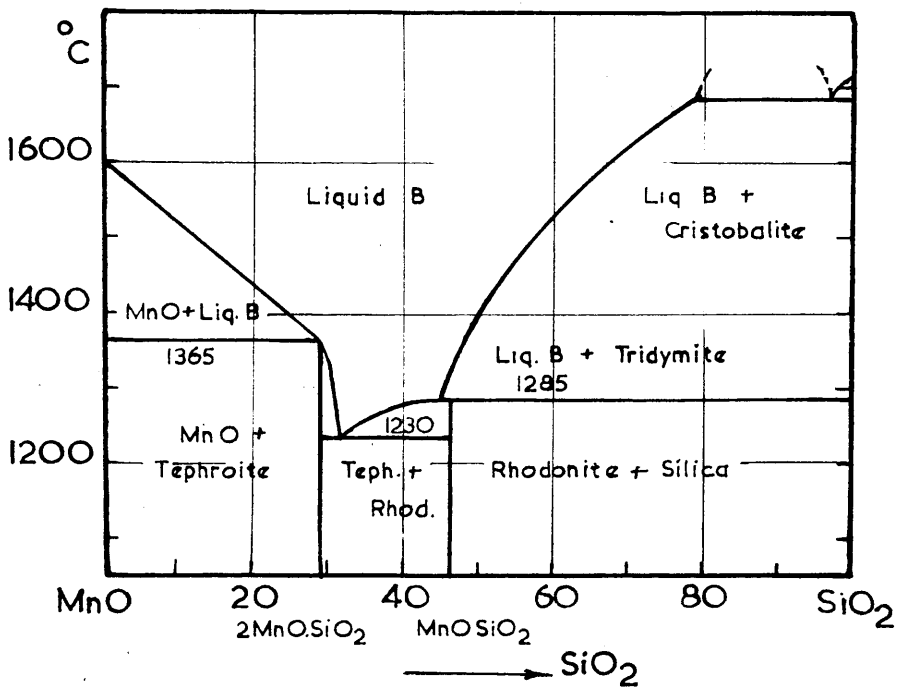
FIG. 6d. SYSTEM MnO — SiO₂

(Herty)

in Fig.6e.   Correction of the liquidus curve near its inter:
:section with the tephroite peritectic horizontal was found
necessary on theoretical grounds.   The diagram was based on the
results of heating and cooling curves, supplemented by observa:
:tion of the melting points with a high temperature microscope.
They experienced considerable difficulty in constructing the
part of the diagram between tephroite and rhodonite.   On all
their heating curves in this region, arrests occurred at 1280°C
and 1340°C.   It was suggested that this might be explained by
lack of homogeneity due to the slow rate of diffusion in silicate
materials.   The good agreement obtained with successive deter:
:minations did not support this theory.   A second explanation
put forward was that tephroite and rhodonite, whether in the
liquid or solid state, undergo a chemical dissociation at
invariant temperatures.   Neither of these explanations appeared
entirely satisfactory and this was one reason why it was consid:
:ered desirable to re-examine the system as described in the
next chapter.   Furthermore some of the data they obtained using
the high temperature microscope did not agree well with the
diagram as finally constructed by them.   Thus the eutectic
mixture which is supposed to melt at 1208°C, did not become
liquid until 1330°C.

The diagrams of Doerinckel, Herty, and White, Howat and
Hay are similar in form but a rather different diagram was put
forward by Glaser[25] in 1926 and is shown in Fig.6b.   Glaser
was/
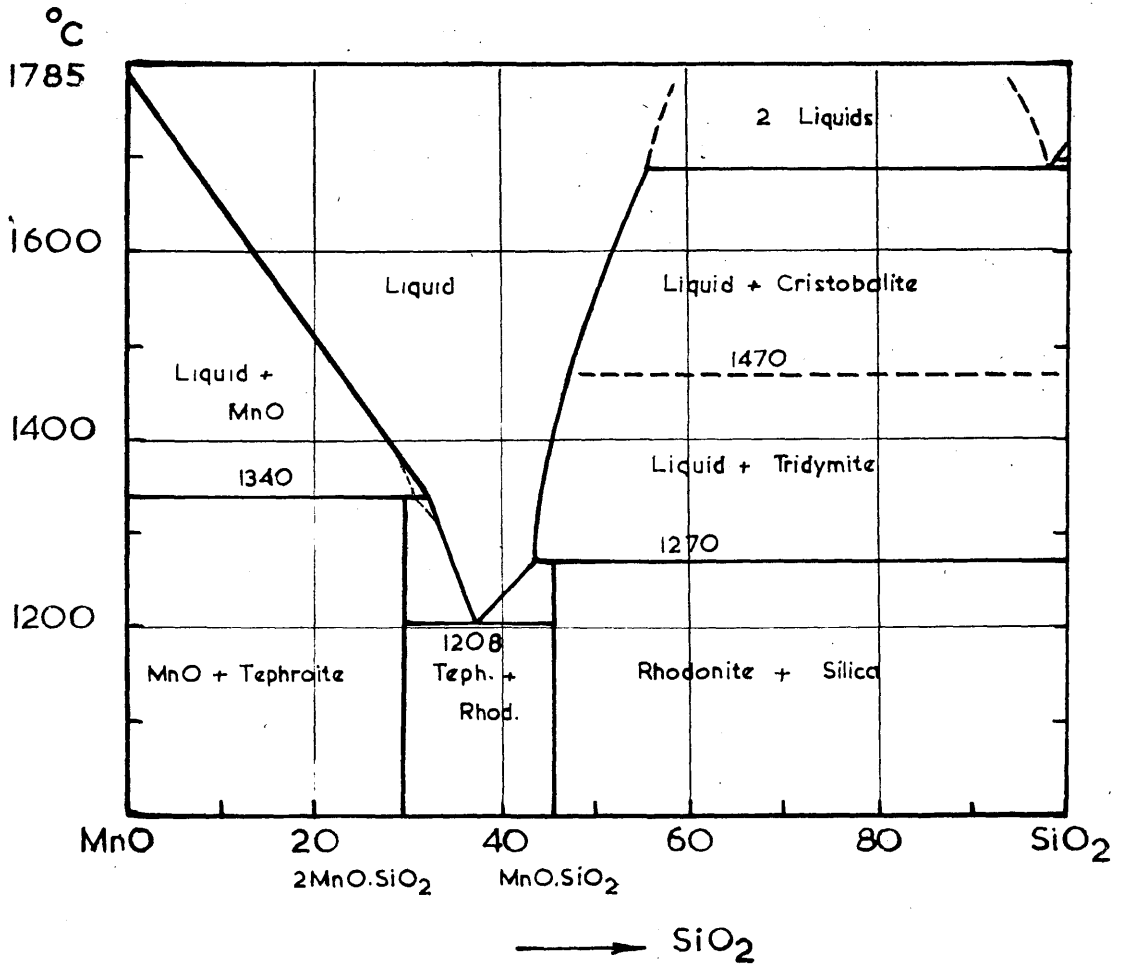
FIG. 6 e.   SYSTEM   MnO —SiO$_2$

(Hay, Howat & White)

was examining by thermal and microscopic methods cupola furnace slags corresponding to the $MnO-SiO_2-Al_2O_3$ system. He, therefore, re-examined the $MnO-SiO_2$ system. His melts were made in pythagoras crucibles. Thermal analysis were carried out using a Le Chatelier thermocouple protected by a sheath of refractory ware similar in composition to Pythagoras ware. The melting point of tephroite was found to be 1313^oC and that of rhodonite 1274^oC. (which he stated agreed with the melting point deter: :mination by Jager and Von Klooster[26]. The eutectic melted at 1193^oC.

A melt of the composition $3 MnO.2SiO_2$ was prepared and found to melt at $1194 - 1200^oC$. It was assumed that it had an incongruent melting point and was given the name manganiustite after a paper by Wulfing and Hofmann - Degenfeld[27].

Glaser mentioned the resemblance between the $MnO-SiO_2$ and $CaO-SiO_2$ systems. In both cases the ortho-and meta-silicates have congruent melting points and the compound $3 RO.2SiO_2$ where $RO = CaO$ or MnO decomposes on melting. A further melt was made of high silica content (64% SiO_2 and 36% MnO), which had a melting point between $1170 - 1160^oC$.

b. Ferrous oxide - Silica.

The history of the $FeO-SiO_2$ thermal equilibrium diagram started with the classical paper of Whiteley and Hallimond[28] who examined acid open hearth slags. These actually contained appreciable amounts of MnO. Their diagram shown in Fig.7a indicated/
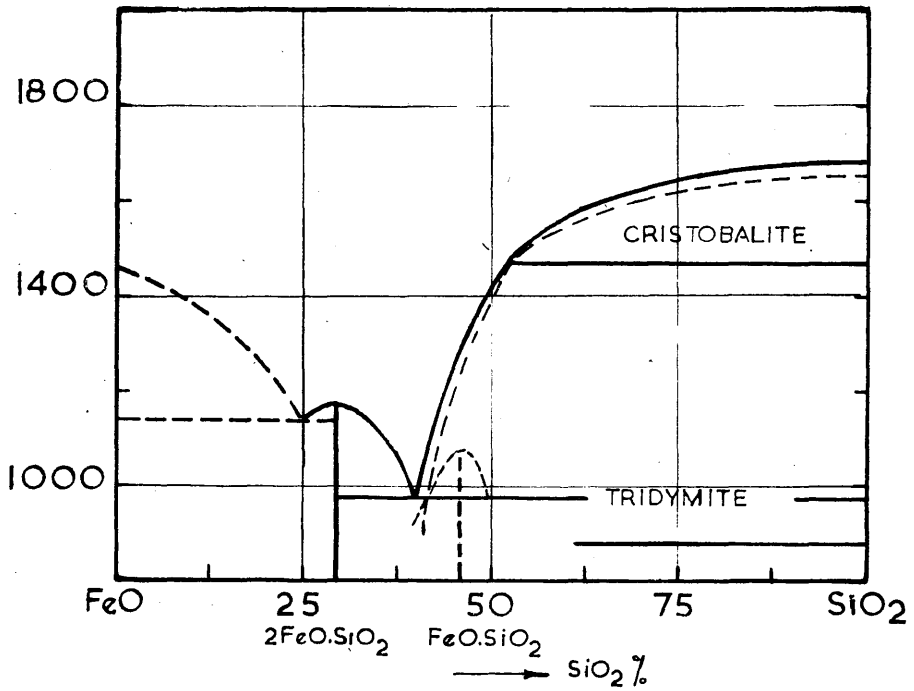
FIG. 7a. SYSTEM FeO — SiO$_2$ (Whiteley & Hallimond)
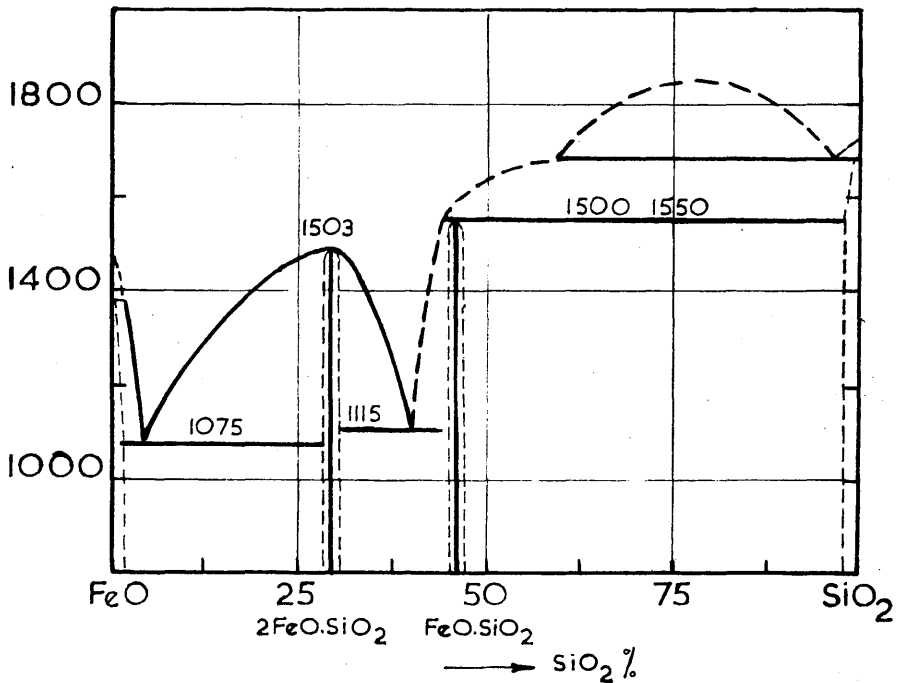
FIG. 7b. SYSTEM FeO — SiO$_2$ (Benedicks & Lofquist)

indicated the presence of the compound fayalite, $2 \, FeO.SiO_2$ melting at $1280^{\circ}C$ and forming a eutectic with each of the component oxides.

A subsequent diagram published by Benedicks and Lofquist[21] and shown in Fig.7b is based principally on the findings of Von Keil and Dammann[29]. Their samples were prepared by melting mixtures of SiO_2 and FeO, the latter contained about 7% Fe_2O_3. Their work, which actually represents the ternary system FeO-Fe_2O_3-SiO_2, confirmed the presence of fayalite, but in other respects their results differ considerably from those of Whiteley and Hallimond. The liquid immiscibility region was based on the results of Greig[22] (A later determination by Greig[30] placed the two liquid field between 58 per cent and 97 per cent silica, and the monotectic arrest at $1690^{\circ}C \pm 10^{\circ}C$.)

The results of a later investigation of the system by Herty and Fitterer [31] are shown in Fig.7c. These slags were prepared by heating mixtures of Fe_2O_3 and SiO_2 to $1600^{\circ}C$. in graphite crucibles. (Some reduction to Fe and even Fe_3C occurred. These were later separated magnetically.) Melting and softening point determinations were then carried out using a Burgess micropyrometer. The phases present were identified microscopically.

The above diagrams show considerable differences. A very accurate re-determination was carried out by Bowen and Schairer [32] using the "quenching" method for the determination of the liquidus and solidus lines. Thus if slags were quenched from/
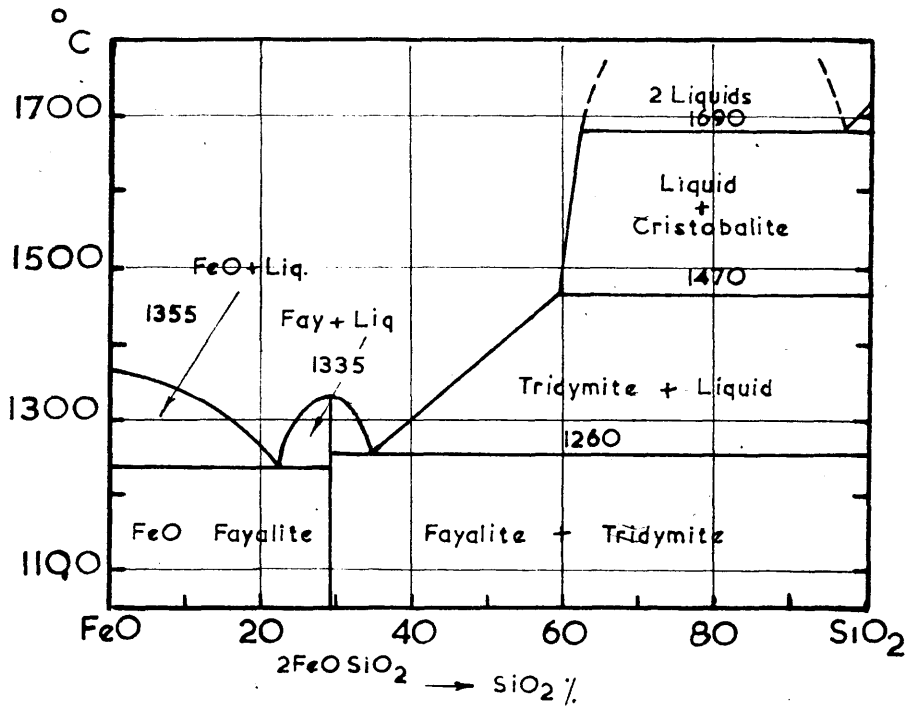
FIG. 7c. SYSTEM FeO — SiO₂ (Herty & Fitterer)
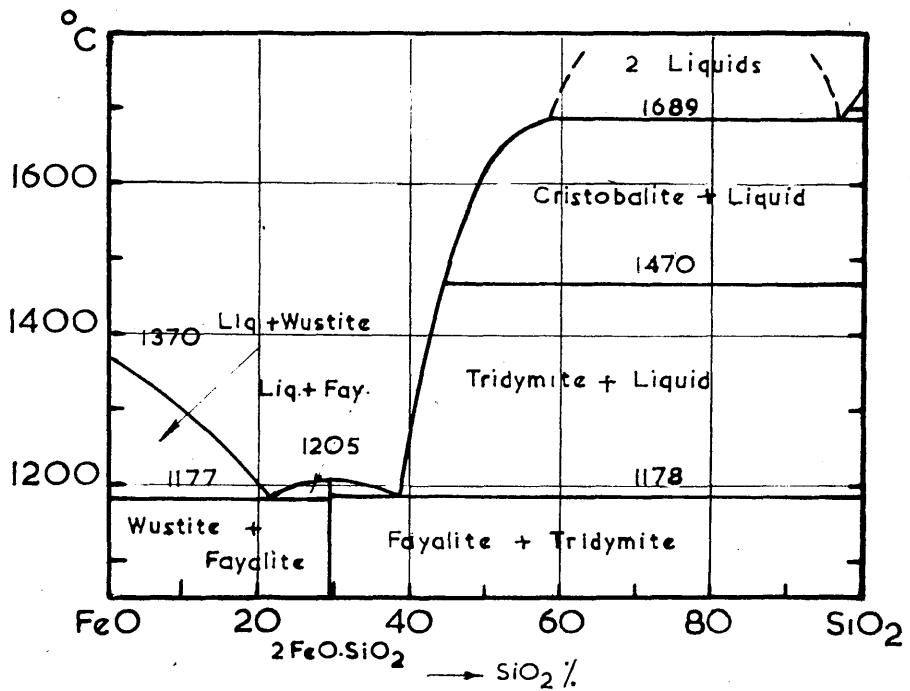
FIG. 7d. SYSTEM FeO — SiO₂ (Bowen & Schairer)

from above liquidus temperatures, microscopic examination should
reveal only glass; quenching from just below the liquidus
temperature should show the beginning of crystallisation.
Similarly quenching slags from below the solidus temperature
should show no glass. In the $FeO-SiO_2$ system quenching the
liquid to a glass - readily accomplished in most silicate
systems - was found possible only with the more siliceous melts.
The majority crystallised completely even with the most rapid
quenching, but the feathery aggregates so formed are readily
distinguished from primary crystals grown freely from the liquid.

Bowen and Schairer were unable to determine any point on
the cristobalite liquidus above 1515°C on account of the limit:
:ation imposed by the melting point of the iron crucible. They
extended their curve as a smooth curve meeting the point of
equilibrium of two liquids and cristobalite as determined by
Greig[30]. The diagram was finally constructed as shown in
Fig.7d for which they claimed an accuracy of $\pm$ 2°C.

The work of Bowen and Schairer[32] has been confirmed
by the subsequent work of Hay, Howat and White[33] and Ibrahim[34]
as shown in Table 2. The results of the previous workers
are also shown.

Table 2. /

Table 2.

Investi: :gator.	Melting Points °C				Composition SiO$_2$ per cent	
	FeO	2FeO.SiO$_2$	FeO- 2FeO.SiO$_2$ eutectic.	2FeO.SiO$_2$- SiO$_2$ eutectic	FeO- 2FeO.SiO$_2$ eutectic	2FeO.SiO$_2$- SiO$_2$ eutectic.
W.& H. [28]	1450	1280	1250	990	25	40
K.& D. [29]	1450	1075	1075	1115	4	40
B.& L. [21]						
H.& F. [31]	1355-1377	1335	1240	1260	22	35
B.& S. [32]	1380 ± 5	1205	1177	1178	22	38
H,H & W. [33]	1370	1225	1150	1155	24	38
I. [34]	1367	1263	1165	1170	22	38

The Existence of the compound "FeO.SiO$_2$"

About 20 years ago, the existence of the compound
FeO.SiO$_2$ now referred to as   ferrosilite became a subject of
some controversy.   Metasilicates approaching FeO.SiO$_2$ in
composition were already known to mineralogists.   One such
mineral is grunerite, belonging to the amphibole group, having
a double chain structure, which is different from the single
chain structure of the pyroxenes to which rhodonite, MnO.SiO$_2$
belongs.   X-ray studies by Warren[32] have shown that in
grunerite, one molecule of H$_2$O is associated with eight molecules
of SiO$_2$, the formula being Fe$_7$H$_2$ (SiO$_3$)$_8$, resembling that of
tremolite Ca$_2$ Mg$_5$ H$_2$ (SiO$_3$)$_8$.   The hydrogen ions occupy definite
positions in the amphibole structure.   (Most natural grunerites
also contain appreciable amounts of MgO and MnO).

Although/
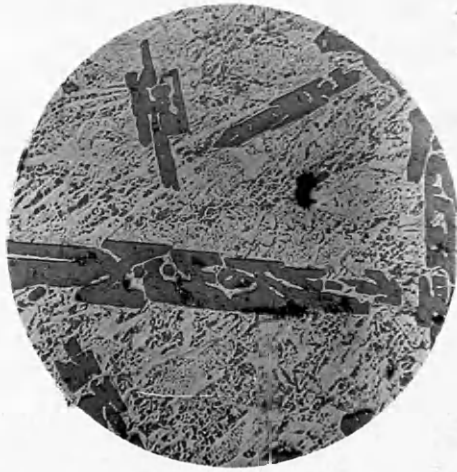
Fig. 8 - "FeO.SiO$_2$" x 100

Although $FeO.SiO_2$ did not appear in the slags they examin:
:ed, Whiteley and Hallimond[28] pointed out that the behaviour of
$FeO.SiO_2$ might be expected to be similar to that of $MnO.SiO_2$
which was then thought to have an incongruent melting point.
Benedicks and Lofquist stated that the existence of $FeO.SiO_2$
seemed probable and showed it melting incongruently at the arbit:
:rarily chosen temperature of 1500-1550°C.   Later investigators
were unable to substantiate the existence of $FeO.SiO_2$ (although
Bowen[35] reported the occurrence of minute crystals of the
monoclinic form of ferrosilite in an obsidian).   Thus Bowen and
Schairer[32] on annealing a glass of the composition $FeO.SiO_2$
at a temperature as low as 660°C obtained a feathery devitri:
:fication product, apparently completely crystalline but
unsuited for microscopic examination.   The X-ray powder pattern
showed only the lines of fayalite with a general blackening of
the film probably due to amorphous silica or glass.   In the
present work, a melt was made of the composition $FeO.SiO_2$ and
cooled slowly in the furnace.   This, melt when polished and
examined microscopically showed primary dendrites of silica in
a eutectic of silica and fayalite, (Fig.8).

c.   System FeO-MnO.

In spite of the many attempts which have been made to
construct the thermal equilibrium diagram of this system, its
exact form is still uncertain.
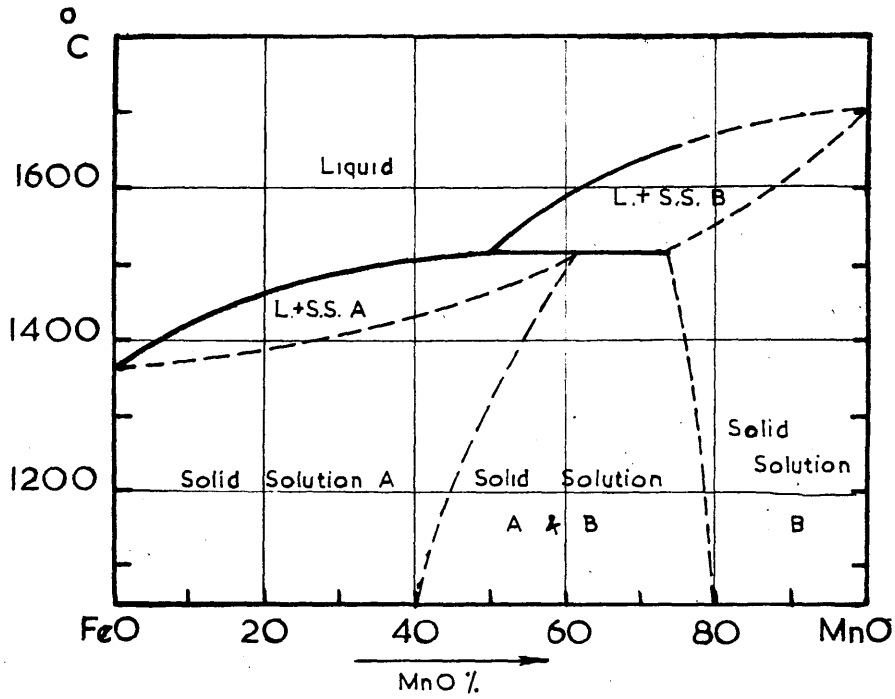
Benedicks /

FIG. 9a. SYSTEM   FeO — MnO (Benedicks & Lofquist.)
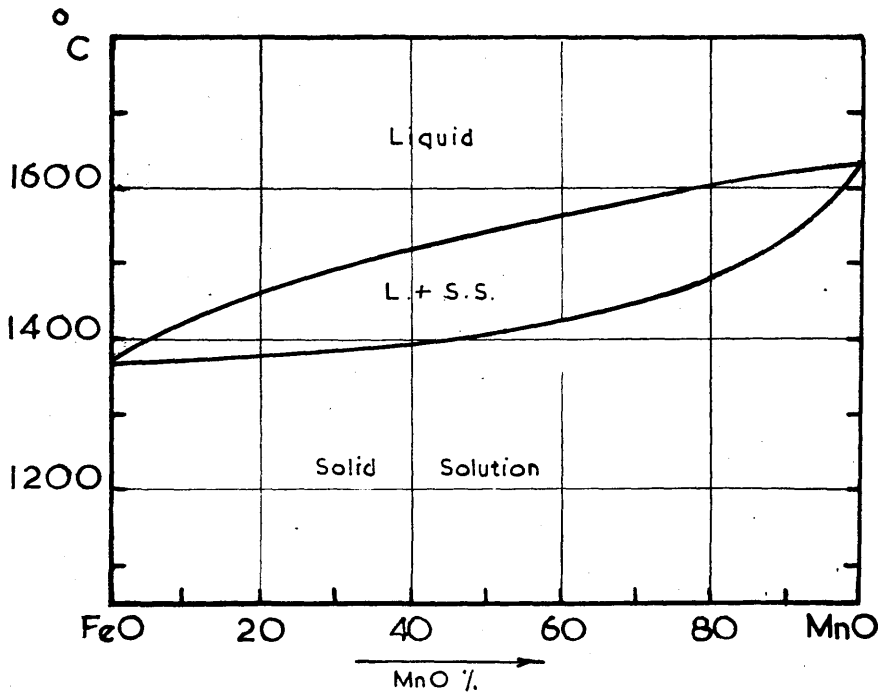
FIG 9b SYSTEM   FeO — MnO. (Danialoff)

Benedicks and Lofquist[21] used data published by Oberhoffer and Von Keil[36] on the melting points of FeO-MnO mixtures to construct the diagram shown in Fig.9a. No determinations were carried out with mixtures containing high percentages of MnO. It will be seen that the diagram indicates only partial mis::cibility between FeO and MnO.

The diagram shown in Fig.9b usually attributed to Herty[37] indicates complete miscibility in the solid state. According to Herty himself, this diagram was worked out by Daniloff[38] at the Pittsburgh Experimental Station of the United States Bureau of Mines. He concluded that the FeO-MnO system should be considered as a continuous solid solution series. The melting point of MnO was given as 1610°C and that of FeO as 1367°C.

Andrew, Maddocks and Howat[39] published a diagram for the system as shown in Fig.9c. It differs considerably from that suggested by Benedicks and Lofquist but is similar to that of Daniloff except that the melting point of FeO is given as 1410°C and that of MnO is 1585°C. These melting points are probably suspect on the ground that their experiments were carried out in alumina crucibles, which would flux considerably with the melts.

The diagram published by Hay, Howat and White[33] and shown in Fig.9d also indicates partial miscibility. It is based on evidence obtained from heating and cooling curves and petro::graphic examination of the powdered melts, and no examination of the actual structures obtained was made. The melts were prepared/
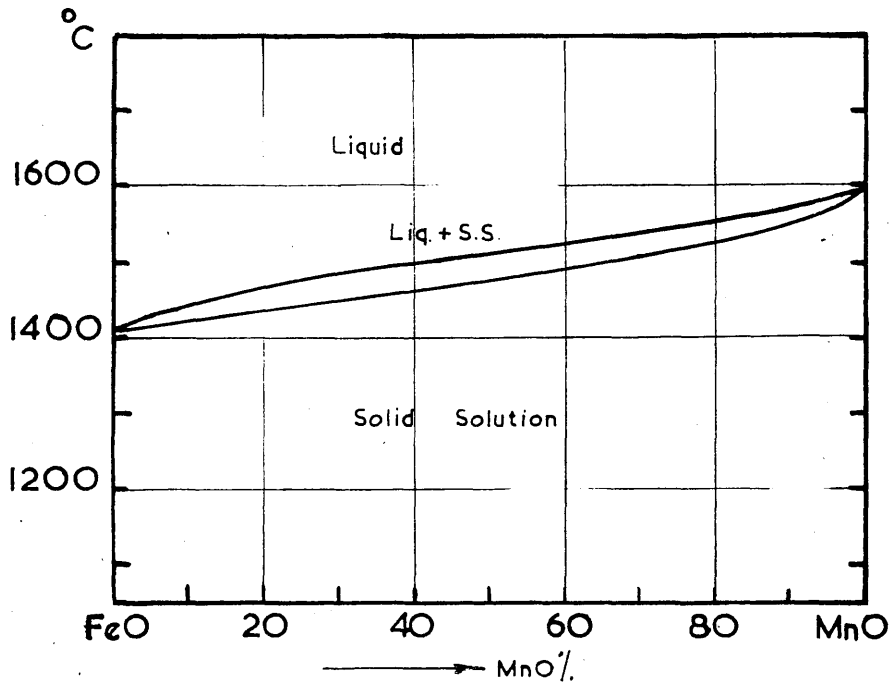
FIG.9c. SYSTEM FeO — MnO

(Andrew, Maddocks & Howat.)
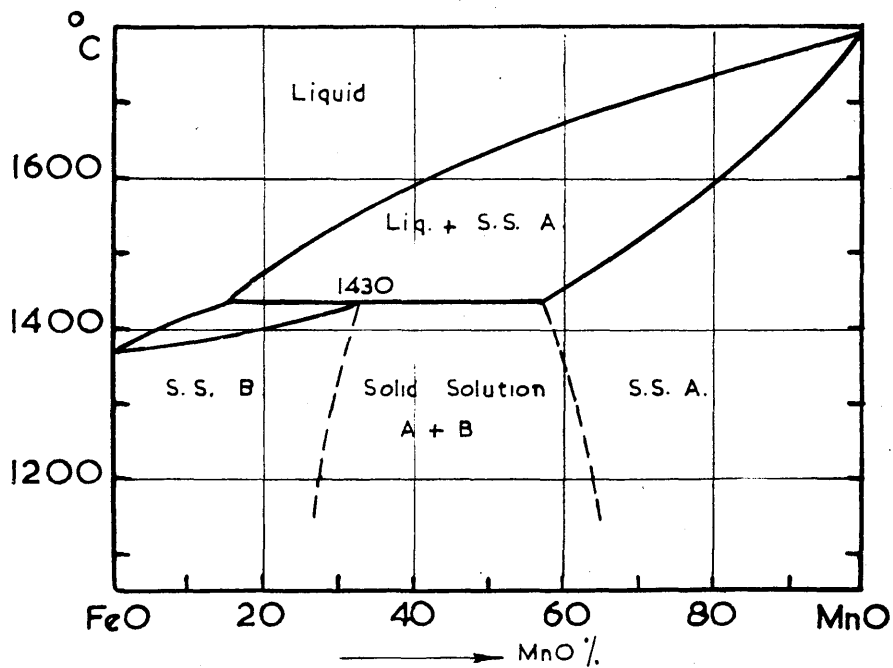
FIG.9d. SYSTEM FeO — MnO

(Hay, Howat & White.)

prepared by thoroughly mixing MnO and FeO to give the desired compositions and melting in a molybdenum crucible. The melting point of FeO was taken as $1370^{\circ}C$ and that of MnO as $1785^{\circ}C$.

White [40] stated that the structure of a few melts with: :in the suggested immiscibility range were later examined and the existence of two phases was confirmed. However, the appearance of a two-phase field could very easily result if any oxidation occurred, resulting in the formation of higher oxides of manganese and iron which might form a certain amount of $(Mn, Fe)_3O_4$ solid solution along with the MnO-FeO solid solution. This suggestion is supported by the fact that Whiteley[41] failed to find any evidence of immiscibility in examining a series of artifically produced FeO-MnO inclusions in steel, which having frozen in contact with metallic iron would probably contain a minimum of higher oxides.

More recent X-ray work by Jay and Andrews[42] has indicated that there is complete solid solubility between FeO and MnO in the temperature range $1350^{\circ}C$ and $1150^{\circ}C$. Their samples were not melted but merely sintered in the solid state. Further confirmation of the results of Jay and Andrews has been obtained by Pettersson[43] who also examined FeO-MnO sinters by means of X-rays.

In the discussion on the above paper by Jay and Andrews, White and Ford[44] supported these findings.

Thus, although views on the miscibility of FeO and MnO are/
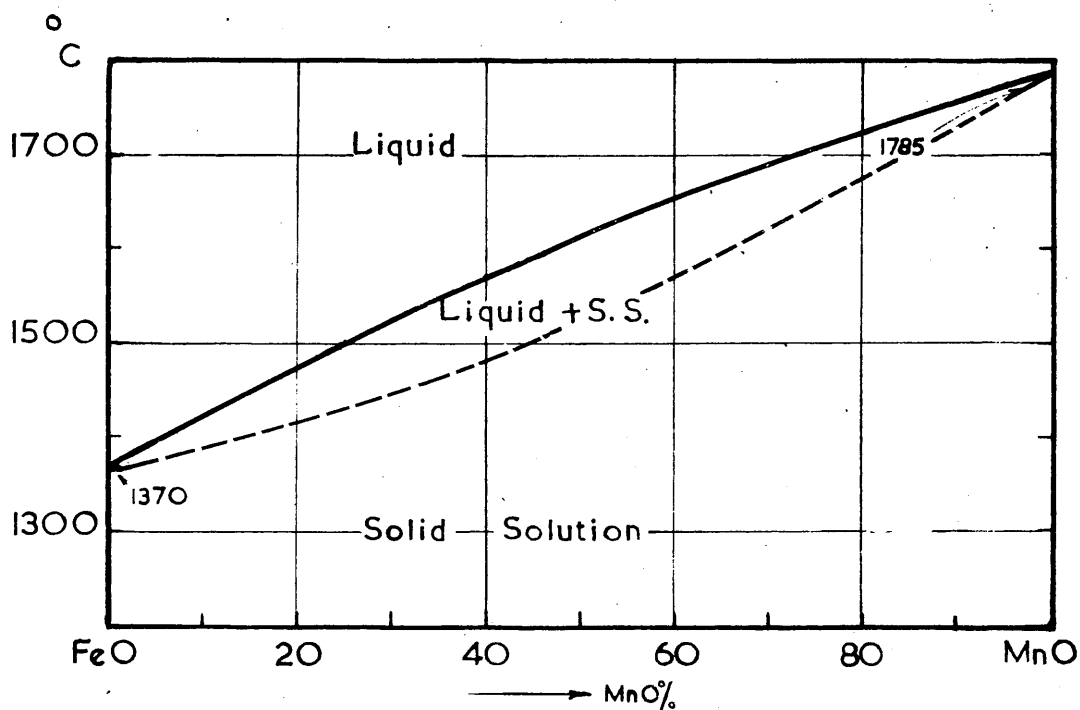
FIG.9 e. SYSTEM FeO-MnO

are conflicting, the later work appears to point to complete solid solubility. This might also be expected on theoretical grounds, as FeO and MnO have similar crystal lattices, both crystallising in the cubic system of the NaCl type, the sizes of the iron and manganese ions (Fe^{++}, 0.75^{o}_{A}, Mn^{++}, 0.80^{o}_{A}) are not greatly different, and there should be little expectation of compound formation between the two oxides.

In the light of the above evidence, a diagram showing complete solid solubility has been adopted in the present work. The diagram in Fig.9e has been constructed to agree as well as possible with the data of Hay, Howat and White but at best can only be regarded as an approximation.

CHAPTER III.

Experimental Investigation of the

Manganous Oxide - Silica System.

Certain difficulties in the interpretation of previously determined data relating to the $MnO-SiO_2$ system by means of a thermal equilibrium diagram have already been mentioned in the previous chapter. There were, however, other reasons for believing that the presently accepted diagram was incorrect and which justified a reinvestigation of this system.

1. Theoretical background.

The ability of the basic oxides CaO, MnO, MgO and FeO to break down the network structure of silica and form silicates is connected with the strength of the oxygen ion - metallic ion attraction. The less the oxygen is attracted to the metal ion the more it will be available for breaking the silica structure and forming the different silicate groupings, e.g. $(SiO_4)^{4-}$ $(n\ SiO_3)^{2n-}$ $(n\ Si_2O_7)^{6n-}$ etc. (Representing the tetrahedral structure in two dimensions for simplicity)
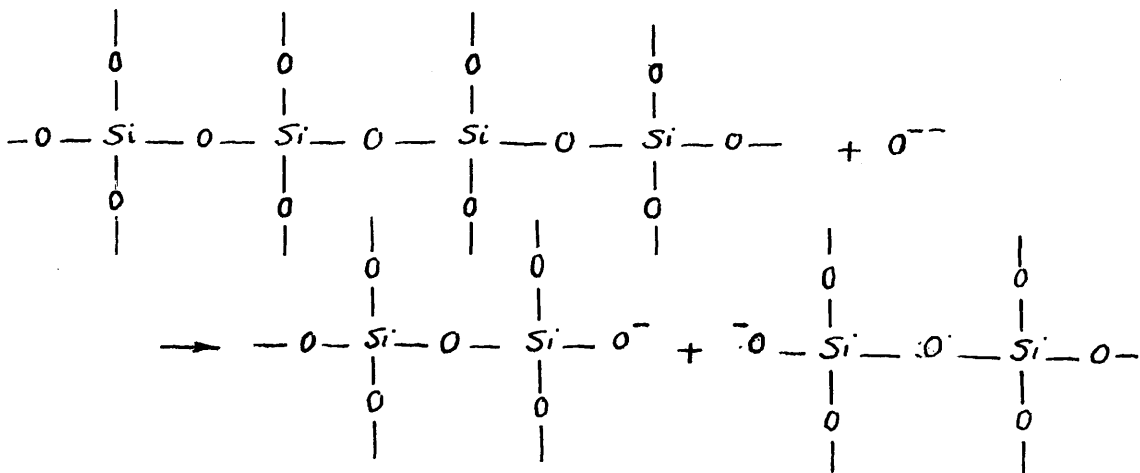
Since the ions Ca, Mn, Mg and Fe are all divalent, then the metallic ion-oxygen attraction is controlled by the radius of the metal ion and decreases as the metal ion radius increases as shown in Table 3.

Calcium has the largest metal ion and is the most strongly electro-positive of the four; CaO forms four silicates includ: :ing the ortho and meta silicates, while MgO and MnO form ortho and meta silicates only. It is generally accepted now that FeO forms only an orthosilicate in normally cooled $FeO-SiO_2$ melts. Although this looks exceptional since iron has a bigger ionic diameter than magnesium yet it should be remembered that magnesium is more electro positive than iron.

Table 3.

Metal.	Ionic Diam. $\overset{\circ}{A}$	Ion-Oxygen attraction $x10^{-16}$ E.S.U.	Electrode Pot. at $25^{\circ}C$.
Ca	1.06	0.69	Ca/Ca^{++} + 2.76
Mn	0.91	0.81	Mn/Mn^{++} + 1.1
Mg	0.76	0.91	Mg/Mg^{++} + 1.55
Fe	0.85	0.86	Fe/Fe^{++} + 0.441

If the system $MnO-SiO_2$ is compared with the binary systems $CaO-SiO_2$. $MgO-SiO_2$ and $FeO-SiO_2$ in the light of the above facts, two important points will be noticed.

1. Of all the four orthosilicates, tephroite, $2MnO.SiO_2$, is the only one which melts incongruently. One would certainly not expect tephroite to melt incongruently while the correspond: :ing iron compound, fayalite, has a congruent melting point, since/

since manganese has a bigger ionic diameter, is more electro-
positive and has a stronger ability to form silicates (which
is shown by the fact that manganese forms two silicates while
iron forms only one).

2.   Another anomalous feature is that in all the silicate
systems known, including alkali metals, alkaline earth metals,
alumina-silica, even SiO_2 - TiO_2, the only case reported of
silica taking part in a peritectic reaction is in the $MnO-SiO_2$
system.   In all other cases there is a eutectic between silica
and the compound richest in silica.   If rhodonite has an
incongruent melting point then one might expect it to be formed
by a peritectic reaction between tephroite and liquid.   The
diagram would then be similar to that of the $MgO-SiO_2$ system.

These two points, as well as previous considerations,
clearly justified a reinvestigation of this system.

11.   Experimental Work.
(a) The Preparation of Raw Material:

i) Manganous Oxide: The method of preparation of MnO
consisted of heating manganese oxalate in vacuum up to 800°C
and then holding it for an hour between 800 and 900°C where
most of the gases resulting from decomposition escape.   The
temperature was again raised to 1000 - 1050°C and finally the
product was allowed to cool to room temperature.   Decomposition
of the oxalate under vacuum helps to carry away the gases
evolved during decomposition and thus avoids any reaction which
might take place between the solid and the gaseous products.
If/

If, however, reaction occurs, higher oxides of manganese might form according to the equation.

$$3 \, MnO + CO_2 \; = \; Mn_3O_4 + CO$$
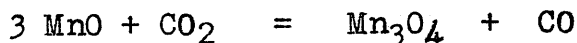
This usually resulted in a brownish appearance on the surface of the oxide which then had a dull green colour instead of a bright green one. This necessitated reheating the oxide to $1000^\circ C$ in a stream of cracked ammonia gas $(N_2 + 3H_2)$ to reduce the higher oxides of manganese. After this treatment the product was allowed to cool to room temperature with the gas still passing over it. Manganese oxide with a very bright green colour was obtained. Chemical analysis showed an average of 99.6 per cent purity.

Another factor which might affect the purity of manganous oxide is the method of preparation of manganese oxalate. This could be prepared by precipitation either from ammonium or sodium salts according to the equation.

$$Mn \, Cl_2 \; + \; (COO \, NH_4) \; = \; 2 \, NH_4Cl + Mn(COO)_2$$
$$or \quad Mn \, Cl_2 \; + \; (COO \, Na)_2 \; = \; 2 \, Na \, Cl + Mn(COO)_2$$
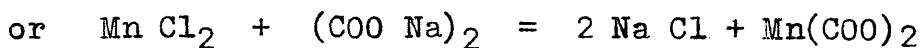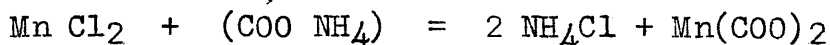
No serious effect would be expected if ammonium salts were used since they decompose very easily and at relatively low temperatures and the decomposition products are gaseous. On the other hand trouble might arise from the use of sodium salts. Although the effect of sodium oxide on manganese silicates has not yet been investigated, the recent investigation of the ternary system $Na_2O - FeO - SiO_2$ by Carter and Ibrahim (45) has /

FIG. 10. FURNACE ARRANGEMENT.
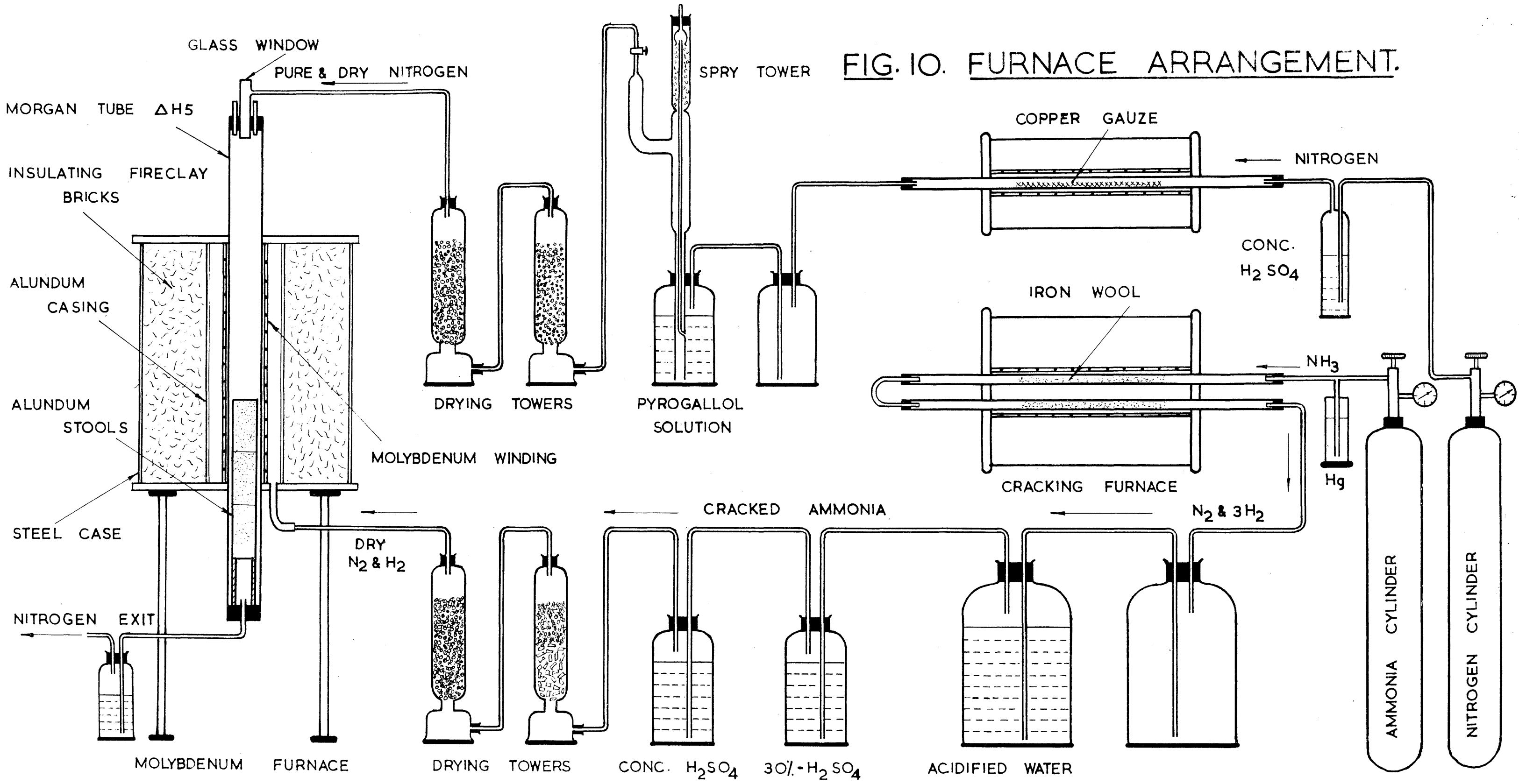
has shown that very small additions of Na_2O to $FeO-SiO_2$ melts may cause marked lowering of their melting points. Manganese oxalate prepared from ammonium salts was used in the present investigation.

ii) <u>Silica:</u> The purest available silica sand was used. Its purity can, however, be increased as follows. The sand was first ground to -200 mesh and then boiled for 3 to 4 hours with strong hydrochloric acid. The acid was decanted off and the silica washed thoroughly with hot water. Boiling with strong hydrochloric acid was repeated till the last traces of iron disappeared from the wash water. The product was finally washed, filtered, dried and ignited at $1000^{\circ}C$. Chemical analysis showed a purity of 99.9 per cent.

(b) <u>The Melting Furnace:</u>

A detailed drawing of the molybdenum furnace used is given in Fig.10.

Melting of the slags was carried out in an atmosphere of nitrogen. The nitrogen was first passed over copper gauze heated to $700^{\circ}C$ to remove oxygen. The partial pressure of oxygen is thus reduced to that corresponding to the equilibrium $2 Cu_2O = 4 Cu + O_2$ at the temperature of the gauze. From the data given by Richardson and Jeffes[46] the free energy of the above reaction is given by:-

$$\Delta G^{\circ}_{298-1357\,^{\circ}K} = 79,700 - 30.12\,T$$

$$\text{Hence } K_{973\,^{\circ}K} = 4.47 \times 10^{-12} \text{ atm.}$$

This/

This pressure is so low that for many purposes nitrogen so produced may be regarded as furnishing a neutral atmosphere. As a further precaution against any trace of oxygen being left in the gas, it was bubbled through an alkaline solution of pyrogallol and then finally dried. A continuous stream of this purified, dried nitrogen was passed through the furnace from the top. At the bottom it bubbled against 3" of water, thus avoiding any diffusion of atmospheric oxygen through the bottom.

(c) The Crucibles:

In studying slag systems, refractory crucibles are unsat: :isfactory due to unavoidable chemical attack. An attempt was, therefore, made to melt the slags in platinum foil. This was attacked by manganese silicate slags, which made fine holes from which the slag drained away leaving the foil empty. Similar trouble was also experienced with a thick walled crucible. Slags melted in iron crucibles were found to contain FeO of the order of 1 per cent. Another limitation to iron crucibles is the fact that they can only be used up to 1500°C.

Molybdenum was first used as a crucible material by White, Howat and Hay[24] in their study of the $MnO-SiO_2$ system. It was found to be very satisfactory, its chief advantages lying in its resistance to the corrosive attack of most oxides, and its high melting point (approximately 2620°C). Spectrographic analysis indicated negligible solution of molybdenum in the slag. This resistance of molybdenum to attack by slags was confirmed by Kitchener and Bockris (47) who heated a slag of composition /

composition 35 per cent CaO, 65 per cent SiO2 four times to 1800°C and only found 0.06 per cent MoO3 in the resultant slag. Moly: :bdenum has now been successfully used as a container for slags by several workers, notably by Maddocks [48] in his work on the ternary system FeO-MnO-SiO2, Rait, McMillan and Hay [49] in their determinations of the viscosity of MnO-SiO2 slags and Bockriss, Kitchener, Ignatowicz and Tomlinson [50] in their study of the electrical conductivity of silicates.

In the present investigation it was, therefore, decided to use molybdenum crucibles. (Some of the earlier slags were made in iron crucibles). The molybdenum crucibles were made by drilling molybdenum rod of $\frac{1}{2}$" diameter. The final crucible was $\frac{3}{8}$" inside diameter and 2" deep. The iron crucibles were made in the same way and with the same dimensions.

(d) Preparation of the slags:

A charge of four grams was prepared from the two oxides, MnO and SiO2 according to the composition required. After thorough mixing it was transferred to the crucible. The crucible was held in an alundum container with a hole in the middle for insertion of the thermocouple. The alundum container was supported in the hot zone on alundum stools as shown in Fig.10. The temperature was measured with a platinum/platinum 13% rhodium thermocouple. As a rule the slags were melted at a temperature 50 to 70°C higher than the melting point expected. The tempera: :ture was maintained there for 30 to 40 minutes to ensure complete homogeneity of the melt. The slags were then cooled slowly in

the/
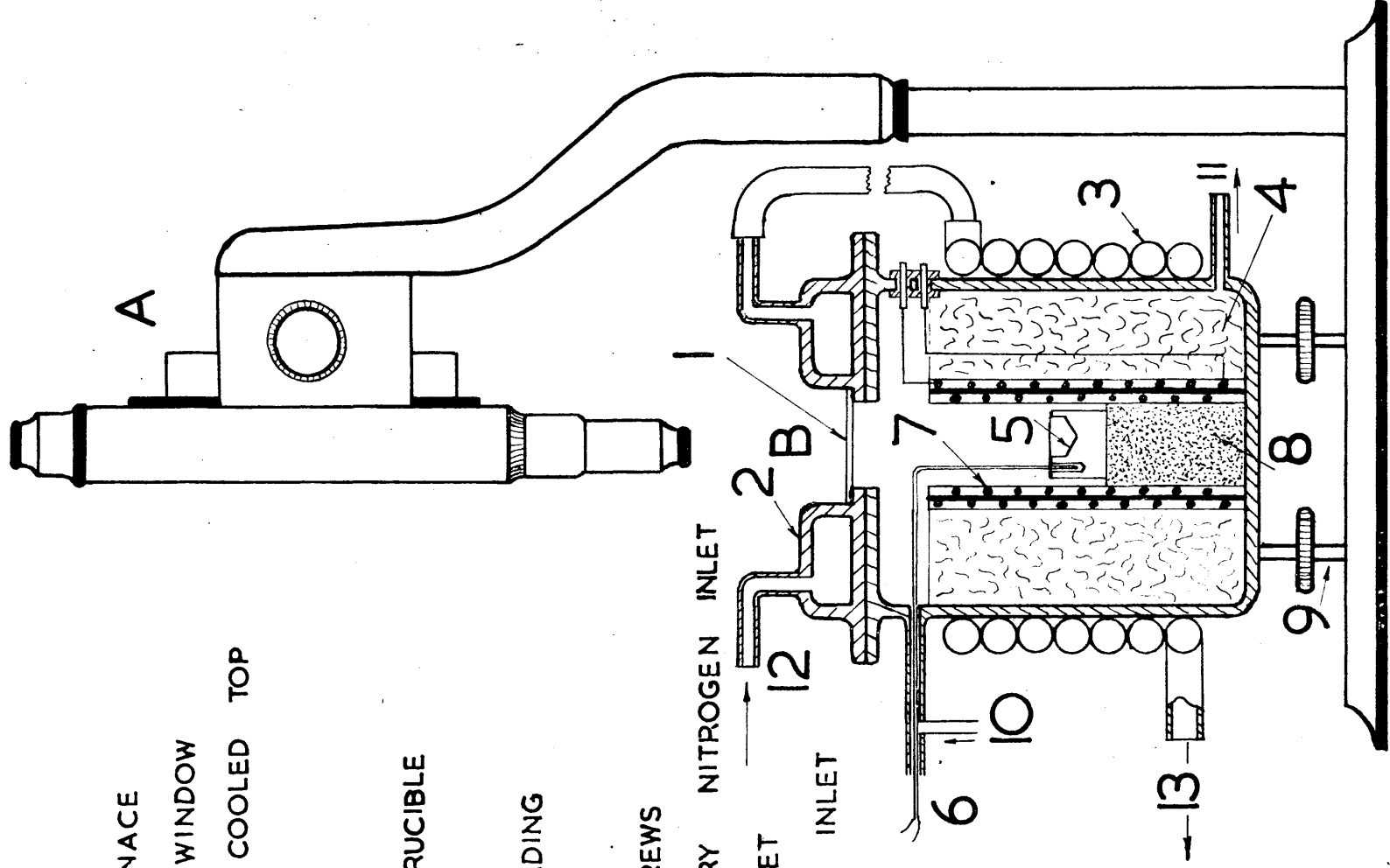
A   THE MICROSCOPE

B   THE MELTING FURNACE

1   QUARTZ GLASS WINDOW

2   BRASS WATER COOLED TOP

3   COOLING COIL

4   INSULATION

5   MOLYBDENUM CRUCIBLE

6   THERMOCOUPLE

7   DOUBLE Pt WINDING

8   FUSED ALUMINA

9   ADJUSTING SCREWS

10 OXYGEN FREE DRY NITROGEN INLET

11 NITROGEN OUTLET

12 COOLING WATER INLET

13 WATER OUTLET

FIG. II.   THE HIGH TEMPERATURE

MICROSCOPE

the furnace. The crucibles were then sectioned and the bottom half was kept for microscopic examination while the top was used for melting point determination and the subsequent chemical and X-ray analyses. It should be mentioned here that the ideal method of sampling is by sectioning the crucible lengthwise since segregation might happen and a less dense phase float to the top as shown later.

(e) Melting Point Determination:

The high temperature microscope shown in Fig.11 was used for the determination of the softening and melting points of the slags throughout this investigation.

The apparatus is a modification of that used by White, Howat and Hay[24]. The main change took place in the furnace tube which is made of alundum $\frac{3}{4}$" diameter and 5" long with two layers of platinum windings separated by a thin layer of alundum. Temperatures up to 1550°C were reached and the outer case became so hot that a cooling coil was fitted around it. The microscope had an objective lens of 2" focal length and 50 diameter magni: :fication.

The slags were melted in a nitrogen atmosphere in a molybdenum crucible drilled from $\frac{5}{8}$" rod. The crucible had two holes, a shallow and wide one for the slag powder and a narrow one for the thermocouple. A platinum/platinum 13 per cent rhodium thermocouple protected by a silica sheath was used for temperature measurement. It was found that the beginning of melting was best indicated by fine powder while coarser particles showed

the/

the end of melting more clearly.

The same apparatus was successfully used by Carter and Ibrahim[45] in the investigation of the ternary system FeO-Na$_2$O-SiO$_2$. The results they obtained by the high temperature micro:
:scope agreed reasonably well with those determined by the quench:
:ing method. The apparatus was standardised against the melting points of copper and fayalite. The accuracy obtained was $\pm$ 5°C.

(f) X-Ray Analysis:

The X-ray set used was a Philips Geiger Counter X-ray spectrometer, the tube being equipped with a copper target and operated at 30 K.V. and an average filament current of 6 m.A. (Certain difficulties were experienced due to fluctuations in the mains voltage, the current occasionally falling as low as 5.2 mA.)

Frequent checking of the "zero reading" was carried out by cutting off the X-ray beam from the Geiger tube. Normal values of 2 to 4 counts per 16 seconds were always obtained.

The technique used in preparation of the samples for X-ray examination was that described by Carter and Harris.[51] In any crushed sample the number of particles in a position to reflect X-radiation is inversely proportional to the particle size. Unless the size of the particles is exceedingly small, deviation can be expected to occur in the intensity of X-rays diffracted at a given angle from different samples of the same material. Carter and Harris found that grinding slag to -300 mesh gave good repro:
:ducibility. The slags were, therefore, ground in an agate

mortar/

mortar to -300 mesh.   The powdered sample was held in a small rectangular perspex slide in which a depression was filled with the powdered sample, which was pressed into position with a clean glass slide.   This pressure was found useful in reducing varia: :tions in readings caused by loose packing.   The same specimen thickness was used through.

The apparatus was standardised using a quartz sample.

III.   Results.

(a) Melting Points.

The melting points as determined by the high temperature microscope are given in Table 4 together with the corresponding slag composition.

Table 5 shows the chemical analysis of a few slags.   The results of the analyses indicate that there is no appreciable change in the composition of the slags prepared in molybdenum crucibles after melting, while those prepared in iron crucibles picked up FeO of the order of 1 per cent.

Table 4./

Table 4.

Slag No.	Made up composition		Melting Points °C.		Remarks.
	MnO	SiO$_2$%	starting	ending	
1	80	20	1327	1435	
2	75	25	1325	1340	
3	74	26	1323	1325	
4	72.5	27.5	1325	1350	
5	70.1	29.9	1350	1355	Tephroite
6	67	33	1270	1335	
7	65	35	1260	1303	
8	64	36	1260	1270	
9	63.5	36.5	1235	1260	
10	62	38	1231	1252	
11	60	40	1230	1240	
12	58	42	1235	1250	
13	54.1	45.9	1230(trace)	1280	Rhodonite
14	52	48	1275	1370	
15	50	50	1270	1450	

Table 5.

Slag No.	Made up Composition.		Analysis.			Remarks.
	MnO%	SiO$_2$%	MnO%	SiO$_2$%	FeO%	
2	75	25	74.8	25.1		Mo crucible.
5	70.1	29.9	70.0	30.0		" "
7	65	35	64.9	35.0		" "
11	60	40	60.2	39.8		" "
15	50	50	50.1	49.9		" "
	70.1	29.9	69.6	29.5	0.9	in Fe crucible.
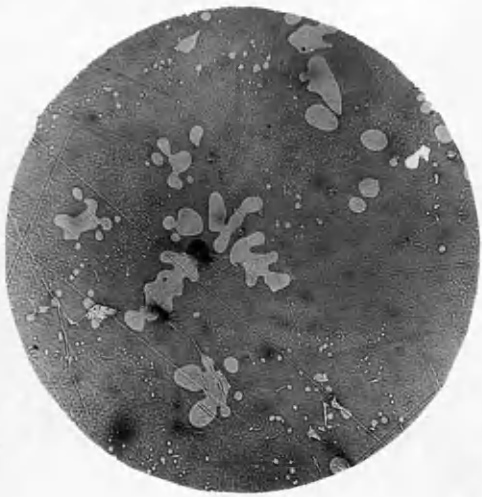
Fig. 12 - 75 MnO & 25% SiO₂ . x 100
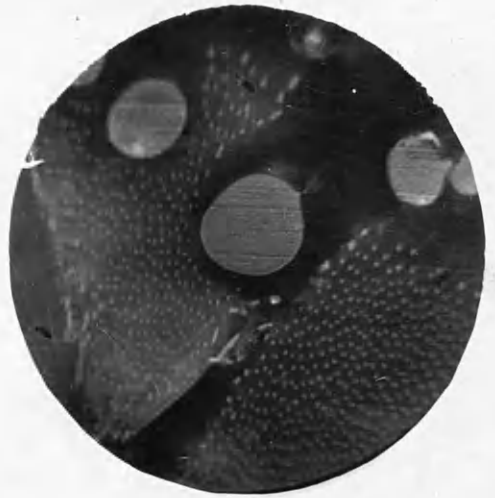
Fig. 13 - 75% MnO & 25% SiO₂ x 400

Fig. 14 - 74% MnO & 26% SiO₂. x 400
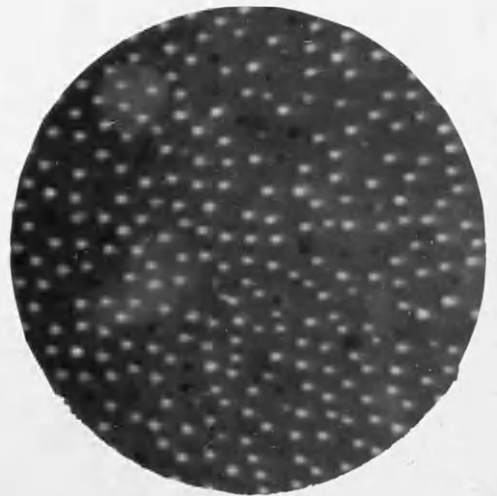
Fig. 15 - 74% MnO & 26% SiO₂. x 2000.

(b) Microstructure:

i)   Slags with composition between MnO & Tephroite:

Slags Nos.1 and 2 showed primary grains of MnO in a eutect:
:ic background. Fig.12 shows slag No.2.   This eutectic has not
been reported before by any of the earlier investigators.   It is
very fine and typical of eutectic structures, having a continuous
phase which is tephroite and a dispersed phase which is MnO.   It
should be mentioned here that it is not very easy to observe the
eutectic structure at low magnifications owing to its very fine
character and the lack of contrast in the colours of tephroite
and MnO.   Unless the specimen is very carefully polished, the
eutectic structure can be very easily missed.   Fig.13 shows the
same slag at a higher magnification where the eutectic is more
distinct .

Slag No.3 showed only eutectic of the same nature as that
observed in slag 2.   Fig.14 shows the eutectic at 400 magnifica:
:tion while Fig.15 shows it at 2000.

Slag No.4, Fig.16 showed primary tephroite in a background
of tephroite - MnO eutectic.

Slag No.5 is the tephroite composition and appeared greyish
green to the eye.   Under the microscope (Fig.17) it showed only
one phase.

To exclude any possibility of confusion due to glass forma:
:tion, the above four slags, although they were slowly cooled in
the furnace, were given an annealing treatment for 30 hours at
1250°C.   No change in the structure occurred, although the
colour/
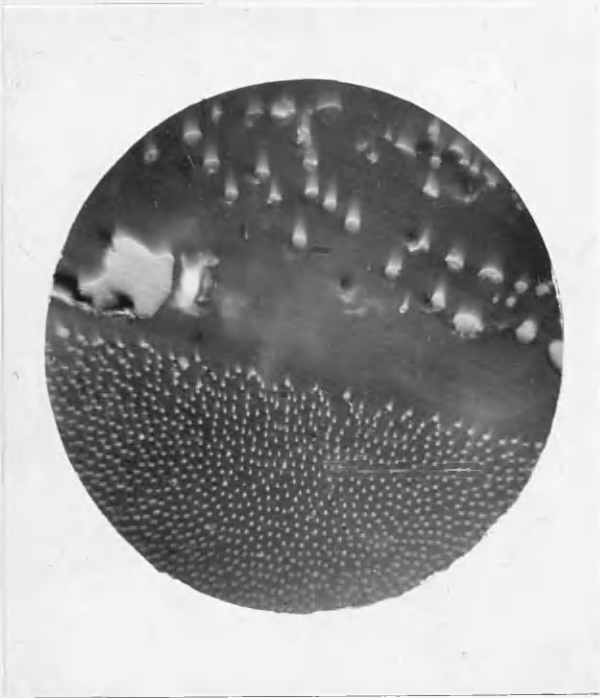
Fig. 16 - 72.5% MnO & 27.5% SiO₂ x400
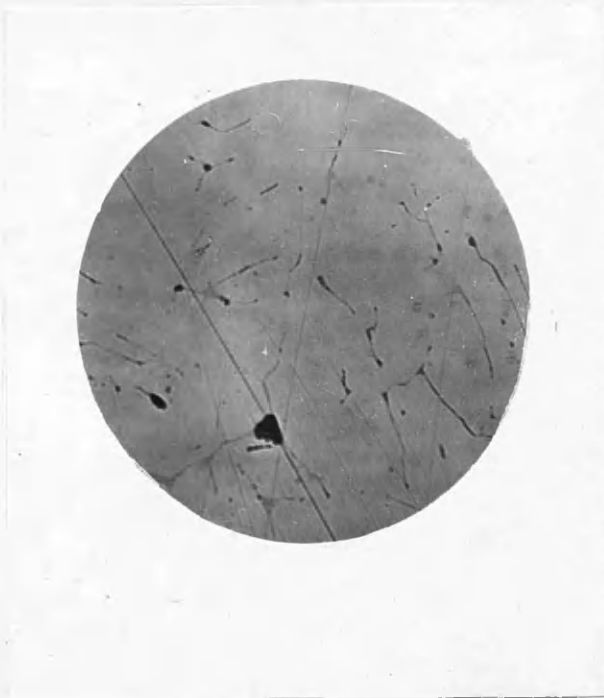
Fig. 17 - 70.1% MnO & 29.9% SiO₂. x100

Tephroite.

Fig. 18 - 67% MnO & 33% SiO₂. x100

unetched

Fig. 19 - 67% MnO & 33% SiO₂. x100

etched in HCl.

Fig. 20 _ 67% MnO & 33% SiO₂. x 400
etched in HCl.

Fig. 21 _ 65% MnO & 33% SiO₂. x 100
etched in HCl.
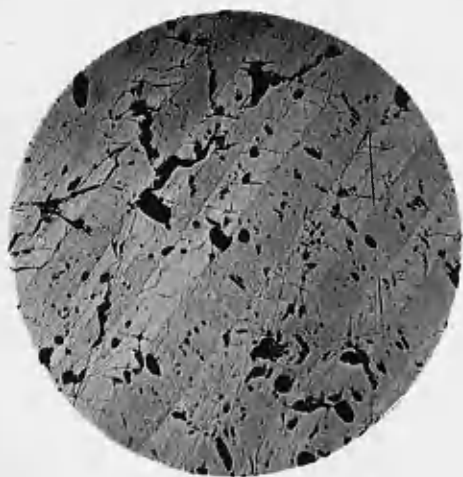
Fig. 22. 62% MnO & 38% SiO₂. x 100
unetched.
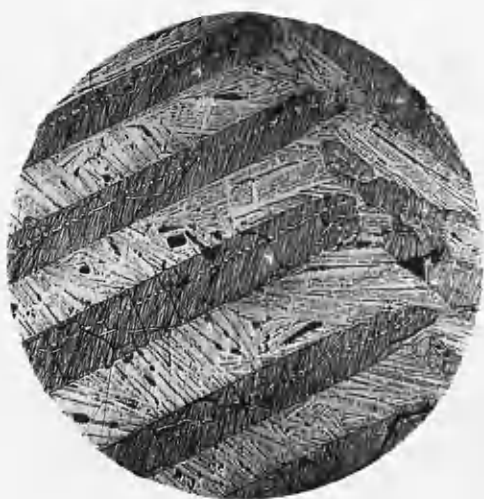
Fig. 23 _ 62% MnO & 33% SiO₂. x 100
etched in HCl.

colour changed from green to violet. As a result of this change in colour it was possible to take better photographs.

ii)   Slags with composition between tephroite and rhodonite:

These slags gave the greatest trouble during the present work in constructing the diagram. Similar difficulties were also reported by White, Howat and Hay[24].

Slag No.6, Fig.18, under the microscope showed only two phases, one a little darker than the other. No eutectic structure was observed. It was thought that etching might help in showing up better the structure of the slag; for this purpose 50 per cent HCl was used as an etchant. Fig.19 shows the same slag after etching for a few seconds. There are still only two phases present, the only change being that the light phase in the un: :etched slag became the dark one after etching. A peritectic reaction rim was also noticed round the light phase which is enlarged in Fig.20.

Slag No.7, Fig.21, shows almost one phase with a little of the light phase (after etching) at its grain boundaries. Thus the phase which became dark after etching increases as the silica content of the slag increases.

Slag No.10, Fig.22, without etching showed long crystals of the white phase and a eutectic. The latter was not very clear but it was easily seen under the microscope. After etching the white phase became dark and had the same appearance as that observed before in slags 6 and 7, while the eutectic became more distinct (Fig.23). The other phase which was present in slags 6 and 7 had disappeared completely.

Fig. 24 _ 60% MnO & 40% SiO₂. x 100
etched in HCl.
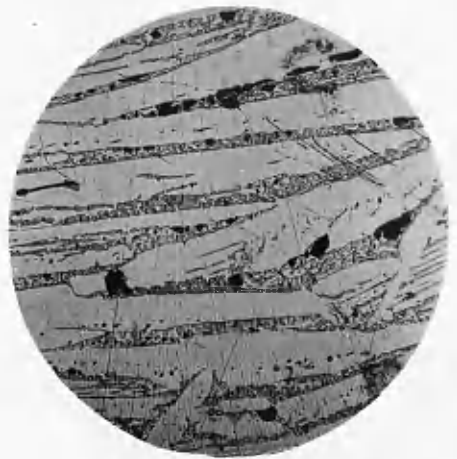
Fig. 25_ 58% MnO & 42% SiO₂ x 100
etched in HCl.
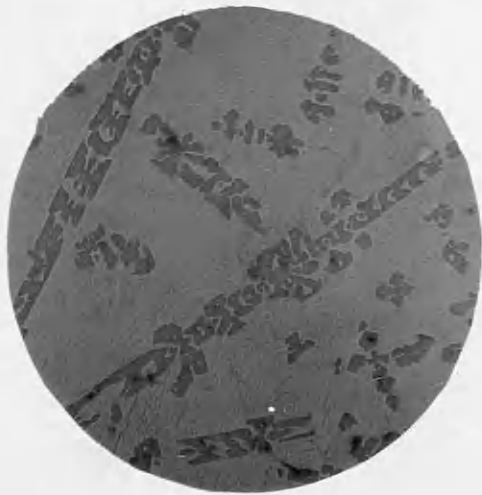
Fig. 26_ 50% MnO & 50% SiO₂. x 100
unetched

Fig. 27_ 50% MnO & 50% SiO₂. x 100
etched in HCl.

With increasing silica content, the amount of that phase which darkened on etching became less and less. At 40 per cent silica and 60 per cent MnO the structure showed only eutectic as shown in Fig.24. With more silica another primary phase began to appear which was unaffected by the etching reagent. This is seen in Fig.25 which shows slag No.12.

iii) Slags with composition between rhodonite and silica:

Slags No. 14 and 15 showed primary silica in a background of eutectic. Fig.28 shows slag No.15 in the unetched condition, while Fig.27 shows the same slag after etching, the eutectic structure being much clearer.

Fig.26, 27 and 28 show sections of the same specimen, No. 15 taken at three different levels (top, middle and bottom respect: :ively). They show the segregation of silica to the top of the crucible which takes place during cooling, due to its much lower density. The bottom thus shows only eutectic and no primary silica.

(c) The Compound 3 MnO.2 SiO2

The results of microscopic examination indicate the exist: :ence of three eutectics in the MnO-SiO2 system. They also in: :dicate that compositions between tephroite and rhodonite richer than 64 per cent MnO appear to undergo a peritectic reaction during freezing whereas compositions between 64 per cent MnO and rhodonite showed a primary phase and eutectic. This suggested that there may be an intermediate compound between tephroite and/

Fig. 28 _ 50% MnO & 50% SiO₂ , etched in HCl . x 100.
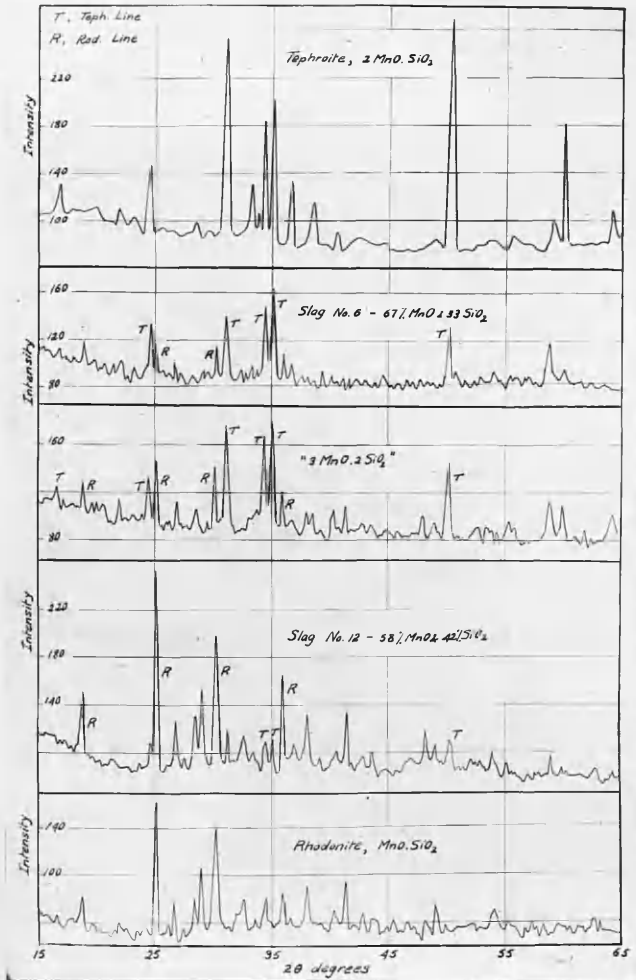
Fig. 29.

and rhodonite which melted incongruently to form tephroite and liquid. These results were confirmed by the data obtained using the high temperature microscope. These showed that compositions from 70.1 per cent MnO (tephroite) to about 64 per cent MnO began to melt at $1260^{\circ}C$, whereas those from 64 per cent MnO to 54.1 per cent MnO(rhodonite) started melting at $1230^{\circ}C$.

The thermal equilibrium diagram constructed from the com: :bined microscopic and thermal examinations is shown in Fig.31. This indicates that both tephroite and rhodonite melt congruently at $1355^{\circ}C$ and $1280^{\circ}C$ respectively, and the probable existence of a third compound, possibly $3 MnO. 2 SiO_2$ (by analogy with the $CaO-SiO_2$ system), which melts incongruently at $1260^{\circ}C$. Eutectics therefore occur between MnO and tephroite, the intermediate com: :pound ($3 MnO. 2 SiO_2$) and rhodonite, and rhodonite and silica.

Although the results of the thermal and microscopic examin: :ation seemed fairly conclusive in establishing the existence of a third compound in the $MnO-SiO_2$ system, an attempt was made to confirm this by X-ray examination

A slag was prepared corresponding to the composition $3 MnO. 2SiO_2$ by melting MnO and SiO_2 in a molybdenum crucible in the appropriate proportions and slowly cooling in the furnace as described earlier. This slag, as well as slags Nos.6 and 12 were examined by X-rays as described on page 34 . The results are shown in Fig.29 where intensity is plotted against diff: :raction angle. For comparison the curves obtained for tephroite and rhodonite are also shown.

It/
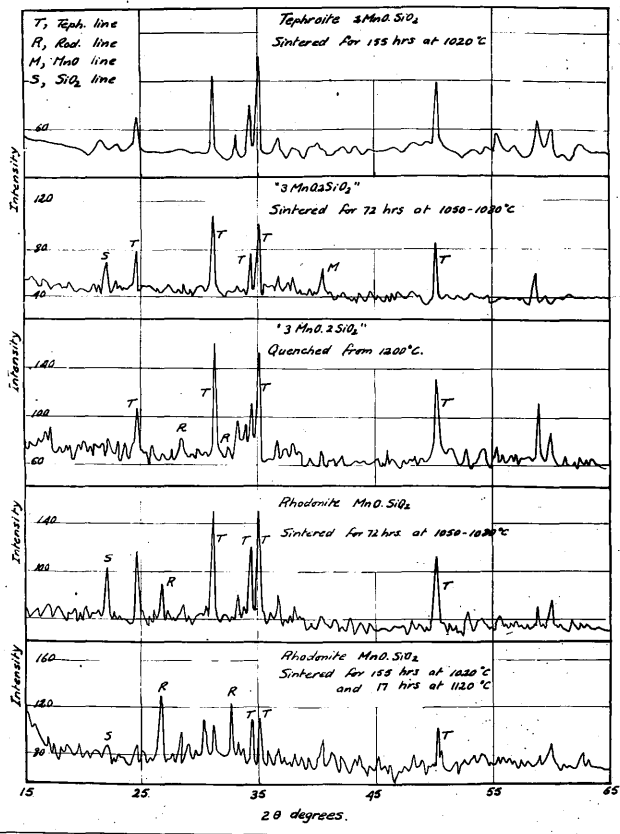
Fig. 30

It will be seen that the diffraction curves for the compositions between tephroite and rhodonite show only the lines of these two compounds. Thus the lines given by the composition $3 MnO. 2 SiO_2$ are mainly those of tephroite.

Mixtures of MnO and SiO_2 in proportions corresponding to $3 MnO. 2SiO_2$ were also sintered at $1050 - 1080^{\circ}C$ for 72 hours in an atmosphere of cracked ammonia gas in order to avoid contamina: :tion which might occur during melting. X-ray examination indicated only tephroite with a little unchanged MnO (Fig.30b).

The experiments suggest that if the compound $3 MnO.2 SiO_2$ is formed on freezing it is unstable and breaks down very easily on cooling in the solid state to tephroite and rhodonite.

Attempts were made to prevent the decomposition on cooling of the compound $3 MnO. 2SiO_2$ by rapid quenching. The compound was prepared by melting the two oxides in the right proportion, cooled slowly to $1260^{\circ}C$, the peritectic arrest, held there for 4 hours, cooled to $1200^{\circ}C$ and then quenched in cold water. No glass was found and the X-ray diffraction curve obtained was that of tephroite (Fig.30).

It would appear therefore, that the light coloured "phase" which darkened on etching, shown in Figs.18 - 23, is really duplex in nature and consists of a finely divided mixture of tephroite and rhodonite, probably lamellar in nature. The appearance of this "phase" in the etched condition under the microscope does not conflict with such a conclusion. High temperature X-ray examination might be necessary for the final/

final confirmation of the existence of this compound at high temperatures.

Similar conclusions were reached by Hart and Rennie[52] on the stability of the compound $3CaO.2SiO_2$. Their results showed only $2CaO.SiO_2$ and $CaO.SiO_2$ were present in a slag pre: :pared by slow cooling the composition $3CaO.2SiO_2$.

(d) <u>Investigation into possible existence of allotropic forms of Tephroite and Rhodonite.</u>

Since many of the silicates, e.g., those of calcium, exist in more than one form, the following experiments were carried out on tephroite.

1 - Tephroite was prepared by melting the oxides in the correct proportions, cooled slowly in the furnace to $1200°C$ and then quenched in cold water.

2 - Tephroite was prepared by sintering the two oxides MnO and SiO_2 in the right proportions at $1020°C$ for 155 hours.

3 - Premelted tephroite was annealed at $1150°C$ for 100 hours.

4 - Premelted tephroite was annealed at $550°C$ for 70 hours. All these gave a diffraction curve similar to that shown in Fig.29 corresponding to melted tephroite cooled slowly.

These results suggest that tephroite occurs in only one modification, at least at temperatures below $1200°C$.

Similar/

Similar experiments were carried out on rhodonite.

1 - Rhodonite was prepared by melting the two oxides in the right proportions, cooled slowly in the furnace to 1200°C and then quenched in cold water.

2 - Previously melted rhodonite was annealed at 1150°C for 100 hrs.

3 - Rhodonite was prepared by sintering the two oxides in the correct proportion at 1050°C for 72 hrs.

4 - Rhodonite was prepared by sintering the two oxides for 155 hours at 1020°C and 17 hours at 1120°C.

The first two showed the same curve as that indicated in Fig.29 corresponding to melted rhodonite cooled slowly.

The diffraction curve obtained from the sintered sample prepared at 1050°C for 72 hours was mainly that of tephroite, but with lines of silica.   This indicates that tephroite is easier to form than rhodonite and that the first stage of formation of rhodonite is tephroite, which by prolonged sintering will combine with more silica forming rhodonite, as shown in curves for samples 3 and 4, Fig.30.   Even sample 4 which was prepared at 1020°C for 155 hours and 17 hours at 1120°C still shows tephroite lines.

Table 6 gives the d values for the two compounds tephroite and rhodonite calculated from the curves given in Fig.29.

Table 6./

Table 6.

Tephroite			Rhodonite		
20	d	Relative Intensity.	20	d	Relative Intensity.
16.8	5.28	VW	18.8 (3)	4.720	M
21.97	4.046	VW	25.15 (1)	3.544	S
23.14	3.844	VW	26.8	3.327	W
24.6	3.618	MS	27.4	3.255	VVW
28.5	3.132	VVW	28.45	3.127	W
31.07 (2)	2.878	S	29.05	3.071	W
33.23	2.698	W	30.2 (2)	2.959	MS
33.80	2.753	VVW	32	2.798	VVW
34.38	2.608	MS	32.55	2.758	W
35.025 (3)	2.563	S	33.75	2.666	VVW
36.68	2.450	M	34.5	2.604	W
38.04	2.365	VVW	35.2	2.561	VW
38.52	2.336	W	35.95	2.50	W
40.08	2.228	W	38	2.368	VW
42.68	2.118	WVW	40.5	2.223	VW
48.1	1.892	WVW	41.35	2.187	W
48.88	1.863	VVW	42.7	2.22	VVW
50.29 (1)	1.814	S	43.5	2.084	VVW
50.62	1.803	VVW	48.5	1.88	VVW
52.78	1.736	VVW	48.55	1.862	VVW
52.88	1.731	VVW	49.9	1.827	VVW
53.76	1.705	VVW	54	1.697	VW
54.2	1.692	VVW	55.05	1.669	VW
55.42	1.658	VVW	65.4	1.428	VW
58.86	1.569	W			
59.89	1.544	M			
64.08	1.453	W			
64.31	1.448	VW			
64.76	1.440	VVW			
66.8	1.401	VVW			
68.05	1.378	VVW			
69.38	1.355	VVW			
72.2	1.308	VVW			
77.6	1.230	VVW			

S = Strong.
M = Medium.
W = Weak.
V = Very.
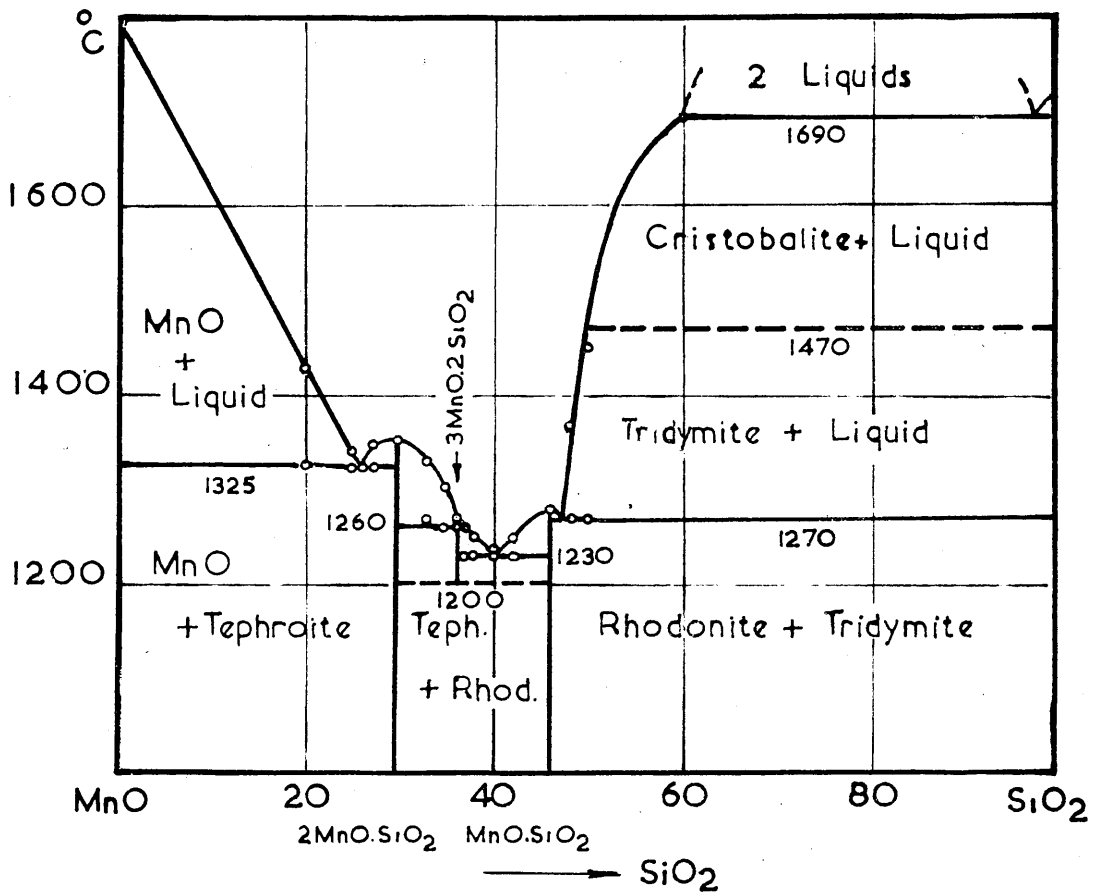
FIG. 31. SYSTEM   MnO — SiO₂
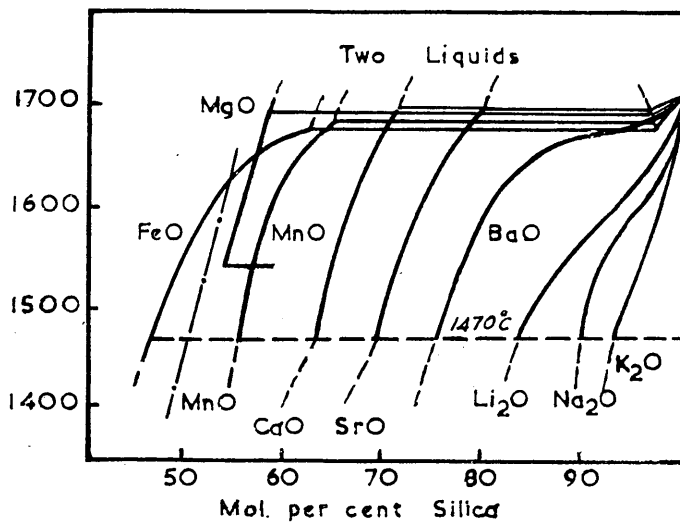
FIG. 32.

The d values obtained for tephroite agree fairly well with those of Harstigen[53] but differ appreciably from those of Ross and Keir[54] obtained for natural tephroite.

No data are available in the literature to check the d values obtained for rhodonite.

IV. MnO-SiO₂ Thermal Equilibrium Diagram.

The diagram as finally constructed is shown in Fig.31. The decomposition temperature of the compound 3MnO.2SiO2 is taken approximately at 1200°C. The arrest obtained at 1208°C by White Howat and Hay[24] for compositions between tephroite and rhodonite may in fact be due to the decomposition of 3MnO.2SiO2. The cristobalite liquidus was extended beyond 50 per cent silica (the highest silica percentage investigated) as a smooth curve to meet the point of equilibrium of two liquids and cristobalite as calculated recently by Murray and White[55]. These workers cal: :culated the silica saturation curve for the systems CaO-SiO2, MnO-SiO2 and FeO-SiO2 and only in the case of MnO-SiO2 was there any appreciable difference from the experimental curve. Comment: :ing on this, they pointed out that the MnO-SiO2 diagram had been determined by the method of heating and cooling curves and was probably somewhat qualitative.

Warren and Pincus[55a] have pointed out that the order of the silica saturation curves for the alkali and alkaline earth oxides as shown in Fig.32 is of the same order as z/R where z is the valency of the cation and R its radius as given in Table 7.

The/

The ratio z/R also indicates the relative attraction of the oxygen atom for the metallic cation, which increases as we go down the table. Although the relationship is only qualitative it suggests that the greater the bond strength of the oxygen to the metal ion, the more important it is that the cation should be fully co-ordinated with unsaturated oxygen ions and the greater therefore i the tendency for the melt to separate into two immiscible liquid phases. One of these is rich in metallic oxide, with the co-ordination of the metallic ion fully saturated and the other is rich in silica.

Table 7.

Metal	R	Z	Z/R	Type of Curve.
Cs	1.65	1	0.61	nearly straight.
Rb	1.49	1	0.67	
K	1.33	1	0.75	
Na	0.98	1	1.02	S - shaped.
Li	0.78	1	1.28	
Ba	1.43	2	1.4	
Sr	1.27	2	1.57	
Ca	1.06	2	1.89	Immiscibility
Mn	0.91	2	2.2	
Fe	0.85	2	2.36	
Mg	0.78	2	2.56	

The curve of silica saturation for the system $MnO-SiO_2$ as given here fits in very well with the conclusions of Warren and Pincus as shown in Fig.32. The dotted curve is the experimental curve of White, Howat and Hay.[24]

V. Summary: /

V.   Summary:

The diagram as given in Fig.31 indicates that both tephroite and rhodonite have congruent melting points.   It would be inferred from the flatness of the maximum at the rhodonite composition as compared with that of tephroite that the rhodonite structure breaks down more easily in the liquid state.

The sintering experiments have also shown that tephroite is easier to form and that the first stage in the preparation of these silicates by sintering is the formation of the ortho: :silicate.

Both microstructure and melting point data favour the existence of the compound $3MnO.2SiO_2$ at high temperatures and suggest that it decomposes on cooling to give tephroite and rhodonite as shown by X-ray results.

The diagram agrees very well with what would be expected from theoretical considerations.   It also explains some of the arrests obtained by White, Howat and Hay[24] in the region between tephroite and rhodonite which were not accounted for in their diagram.
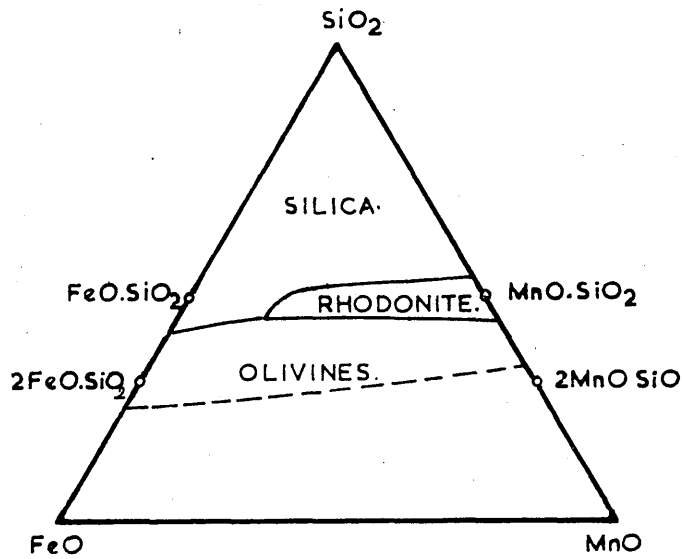
FIG. 33. SYSTEM MnO — FeO—SiO₂.
(WHITELEY & HALLIMOND)
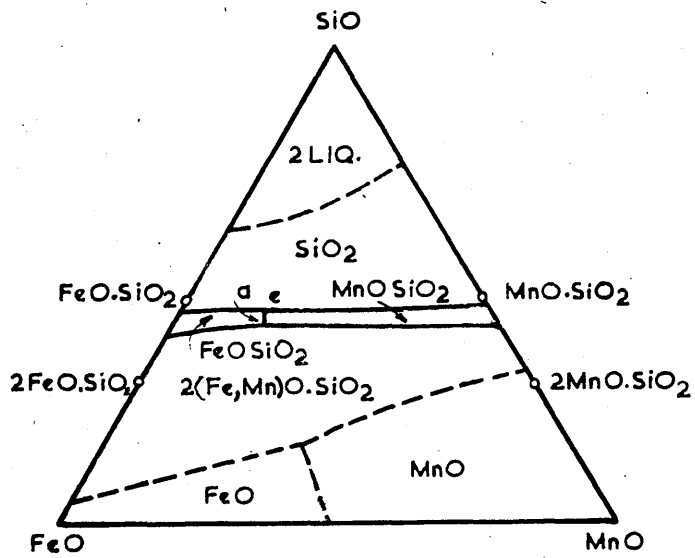
FIG. 34. SYSTEM MnO—FeO—SiO₂.
(BENEDICKS & LOFQUIST)

CHAPTER IV.

The Ternary System   FeO-MnO-SiO2.

Because of the importance of the FeO-MnO-SiO$_2$ system in both acid steelmaking and deoxidation practice many attempts have been made to construct its thermal equilibrium diagram. In the light of the work recorded in the previous chapter it is necessary to reconsider this ternary system.

The first attempt to construct the FeO-MnO-SiO$_2$ diagram was that of Whiteley and Hallimond[28]. Their diagram which is shown in Fig.33 was constructed from an examination of acid open hearth slags.   These slags consist mainly of FeO, MnO and SiO$_2$ with small amounts of Al$_2$O$_3$, Fe$_2$O$_3$, MgO, TiO$_2$ and CaO up to 5%.   Thin sections of the slags were examined by transmitted light by the usual petrographic method.   Polished sections were also examined microscopically.   Owing to the presence of other substances, they adopted the following method for plotting their slag compositions.   The FeO/MnO ratio was plotted along the base of the triangle.   The point representing the slag composition was marked off on the line joining the apex of the triangle to the appropriate FeO/MnO ratio along the base, according to the percentage of silica present.

They found that "rhodonite" appeared in acid furnace slags at FeO/MnO ratios up to 73/21.   The point where the three curves separating the primary fields of olivine, silica and

rhodonite/
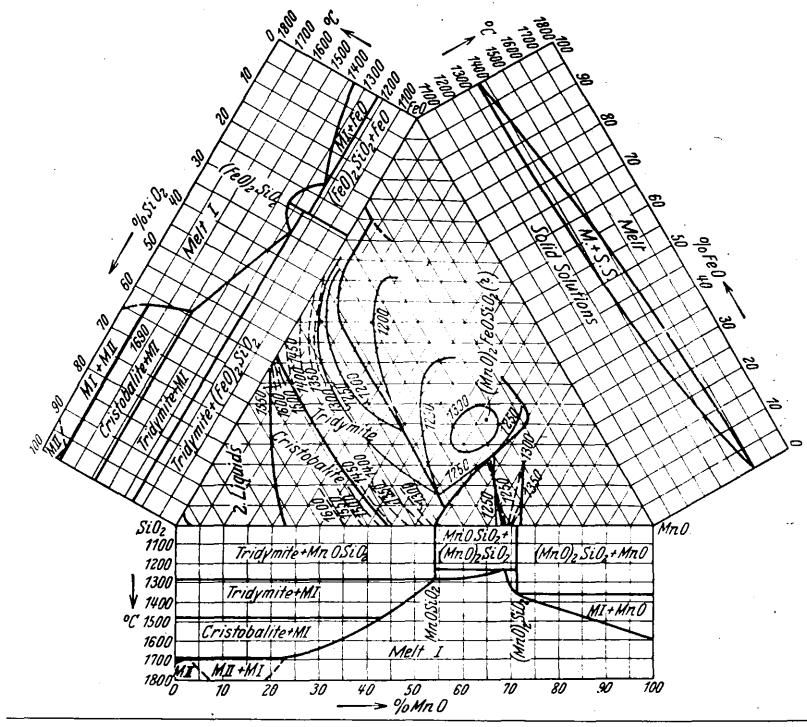
Fig. 35 — System FeO-MnO-SiO₂

(Herty and co-workers)

rhodonite met was found to be a ternary eutectic point.   No
ternary compounds were formed although they were uncertain
whether the mineral knebelite, which contains equimolecular
amounts of fayalite and tephroite, should be regarded as a
definite compound or not.

The diagram shown in Fig.34 given by Benedicks and
Lofquist[21] is based mainly on the work of Whiteley and
Hallimond[28] and Grieg[30]. The point "a" corresponds to a
ternary eutectic.   A continuous series of solid solutions was
postulated between tephroite $2MnO.SiO_2$ and fayalite $2FeO.SiO_2$
with knebelite as an intermediate link.   Obviously the diagram
is based on three wrong binary systems and the knowledge
derived from such a diagram will not be of great use.

A more thorough investigation was made by Herty, Conley
and Roger[56] who prepared synthetic $FeO-MnO-SiO_2$ slags by
melting MnO (from $MnCO_3$), Fe_2O_3 and SiO_2 in graphite crucibles
in a high frequency induction furnace.   Reduction of the oxides
by the graphite was allowed for in preparing the charge. After
cooling, the samples were crushed, free metal removed with
a magnet and analysed for FeO, Fe_2O_3, MnO and SiO_2.   The
analyses were recalculated to a three component basis of FeO,
MnO and SiO_2.   The liquidus surface for the system was then
determined by measuring melting points using a Burgess micro:
:pyrometer, as was done in the $FeO-SiO_2$ system examined by
Herty and Fitterer[31].   Their results are shown in Fig.35.
Apart/
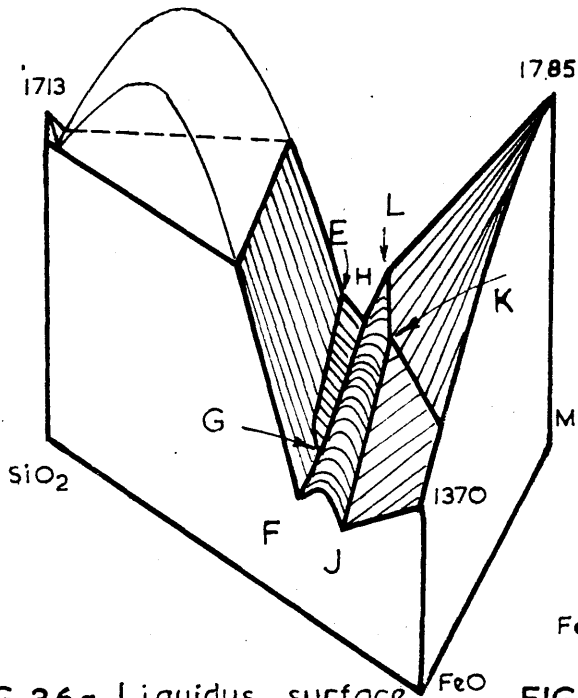
FIG. 36a. Liquidus surface.
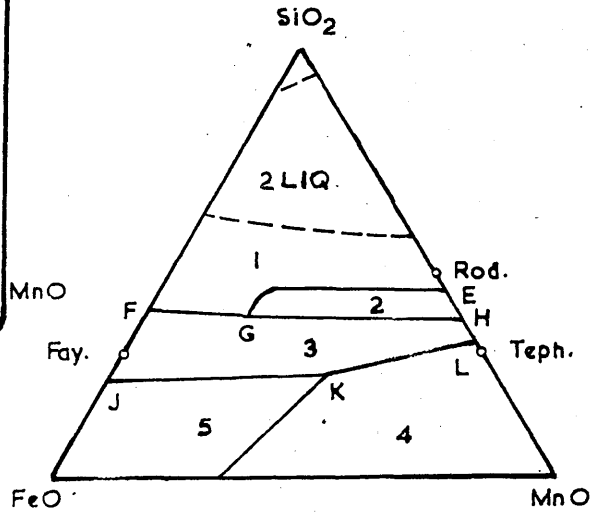
FIG. 36b. Projection of liquidus surface.

FIG. 37a. Phase Distribution.
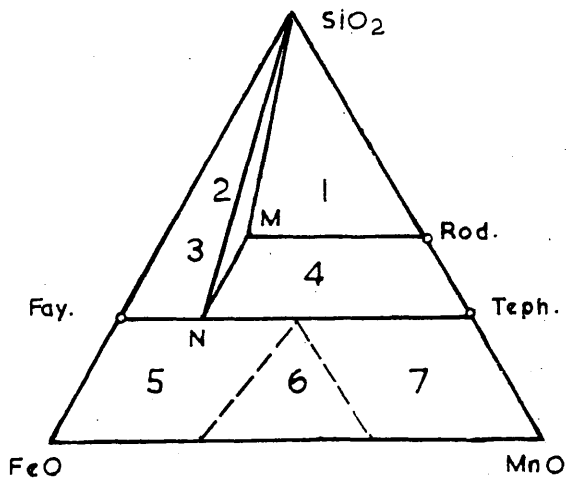
1 — Silica   2 — Rhodonites

3 — Orthosilicates

4 — MnO — FeO   S.S.

5 — FeO — MnO   S.S.

1-SiO₂ & rhodonites   2-SiO₂ & orthosilicates   3-SiO₂, rhodonite & orthosilicate
4-rhodonites & orthosilicates   5-orthosilicates & FeO—MnO S.S.
6-orthosilicates , FeO—MnO S.S & MnO—FeO S.S
7-orthosilicates & MnO—FeO   S.S.

Apart from the inaccuracies indicated in the three binary systems shown in Fig.35, their work suggested the probable existence of the compound $2MnO.FeO.SiO_2$ as is indicated by the maximum on the liquidus surface at this composition.

Their work also seems to suggest the existence of a ternary eutectic point at about $1100 - 1150^{o}C$ and 75 per cent FeO, 3 per cent MnO and 22 per cent silica, the three phases separating being $2FeO.SiO_2$, FeO and $2MnO.FeO.SiO_2$.

A further examination of the system was carried out by Hay, White and McIntosh[57]. Their results, as given in Fig.36a & b, showed two eutectic troughs, FGH & JKL, the latter of which becomes a binary peritectic curve near the tephroite composition and crosses the diagram approximately parallel to the direction of the solid solution series $2FeO.SiO_2 - 2MnO.SiO_2$. Both G & K appear to be reaction points. No ternary eutectic point was found in this system. The trough FGH has a gradual rise in melting point from $1178^{o}C$ on the $FeO-SiO_2$ side to $1208^{o}C$ on the $MnO-SiO_2$ side. Evidence of the existence of this low melting range was found by the above workers in the low temperature melting of slags of compositions near 15% MnO, 40% SiO_2 and 45% FeO. This composition melted at $1170^{o}C$. In general their diagram does not differ greatly from Benedicks and Lofquist[21].

White[40] constructed a diagram (Fig.37a) showing the distribution of phases in the solid state from the above work, and that of Whiteley and Hallimond (28). Tentative diagram for/
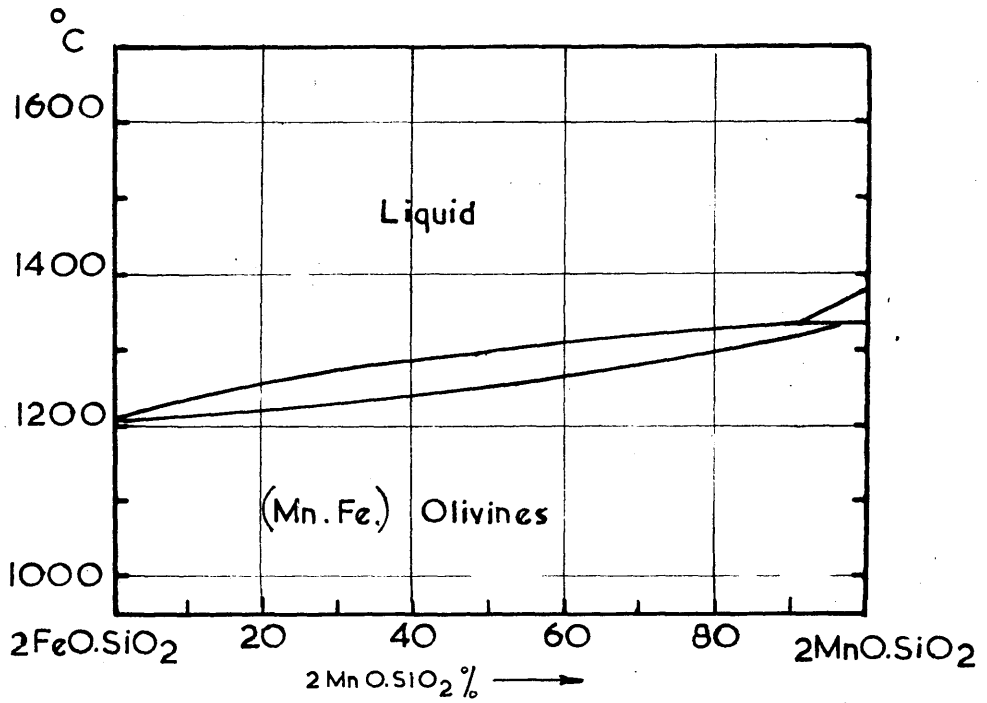
FIG.37 b. Tentative Diagram of System 2FeO.SiO$_2$–2MnO.SiO$_2$
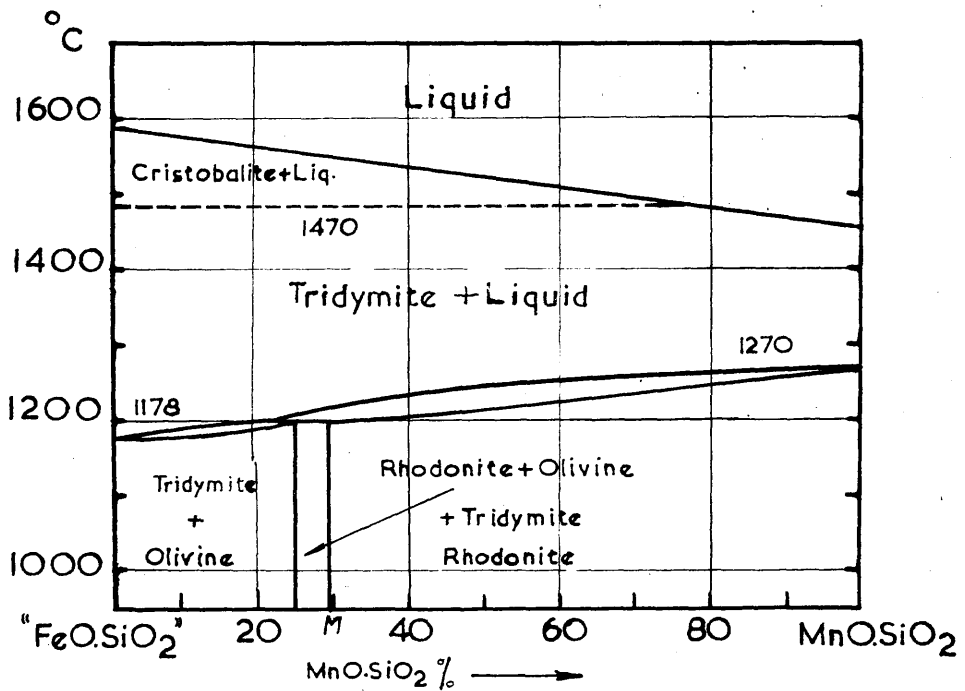
FIG.37 c. Tentative Diagram of System "FeOSiO$_2$"–MnOSiO$_2$

for the ortho silicate and metasilicate joins were also
constructed.   The orthosilicate join as given by White[40]
Fig.37b is not a true binary since tephroite melts incongruently.
knebalite was regarded as a solid solution and not a definite
compound.

The metasilicate join, Fig.37c, and the phase distribution
in the solid state beyond the orthosilicate composition are
based on the findings of Whiteley and Hallimond[28] who found
as mentioned before that rhodonite appeared in acid slags
when the MnO/FeO ration exceeded 27/73 approximately.   The
MnO/FeO ratio in the resulting rhodonite was 29/71.   The
first ratio was used to fix the point N while the latter ratio
fixed the point M.   Commenting on this, White said that no
great accuracy could be claimed since the iron rhodonites of
Whiteley and Hallimond contained CaO of the order of 5%.   Later
studies on these iron rhodonites by Perütz[58] have shown that
they differ structurally from natural rhodonites and resemble
instead the naturally occurring minerals pyroxmangite and
sobralite, (metasilicates of FeO, MnO and CaO).   On the other
hand Sundius[59] has reported an iron rhodonite isomorphous
with rhodonite.   It might be expected, therefore, that
rhodonite exists in two distinct modifications.

Maddocks[48] also prepared slags by melting the oxides
FeO, MnO and SiO_2 in molybdenum crucibles.   The differential
method was adopted for taking the heating and cooling curves
using a tungsten molybdenum couple and the data obtained from
the/
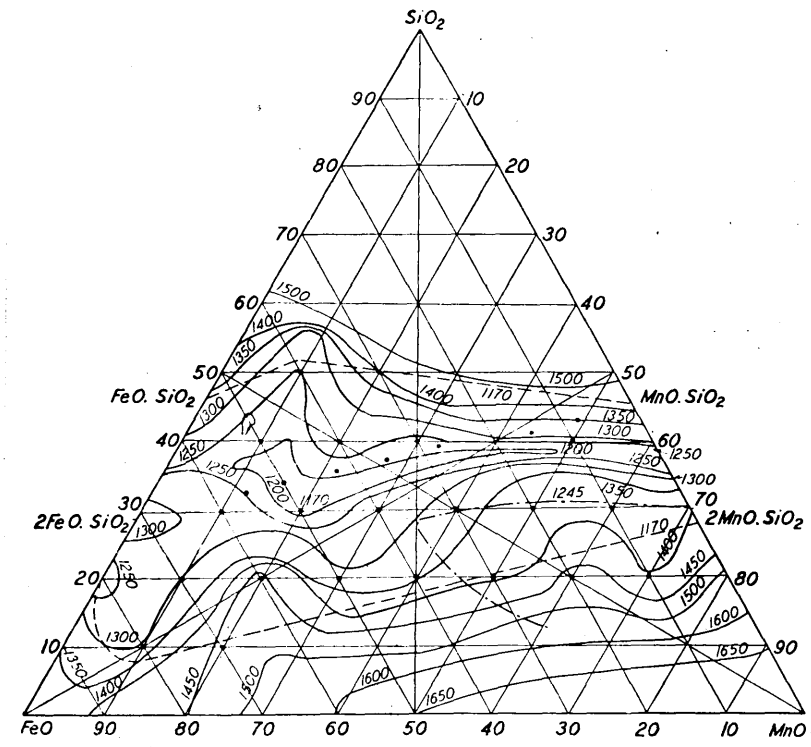
Fig. 38 — System FeO-MnO-SiO₂. (Maddocks.)
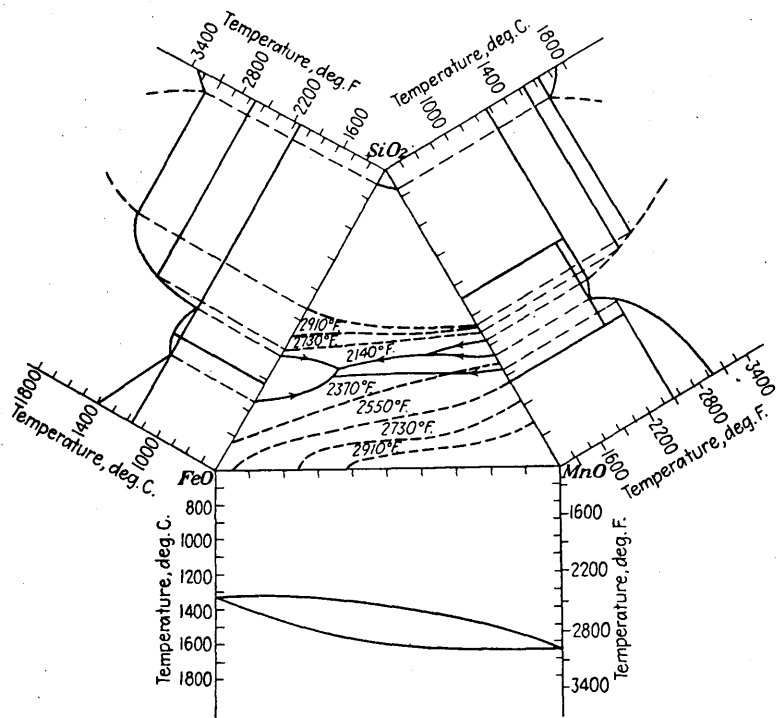
Fig. 39 — System FeO-MnO-SiO₂. (Wentrup.)

the thermal measurements were plotted as isothermal lines on the ternary triangle (Fig.38). His work indicated a ternary eutectic point at a composition of 50% FeO, 20% MnO and 30% SiO_2.

Maddocks determined the phases present by petrographic methods.

Wentrup [60] also has examined the FeO-MnO-SiO_2 system and his results are reproduced in Fig.39. This is very similar to the diagram of Hay, White and McIntosh, the main difference being that fayalite solid solutions and tephroite solid solutions are shown as having separate primary fields of separation. This results in a ternary eutectic between silica, fayalite rich solid solution and tephroite rich solid solution, the ternary eutectic liquid composition being 47% FeO, 20% MnO, and 33% SiO_2. No ternary compounds appear in the diagram of Wentrup..

Further discussion of the earlier work will be given after the experimental results obtained in the present investigation have been presented in the next chapter.

FIG. 40
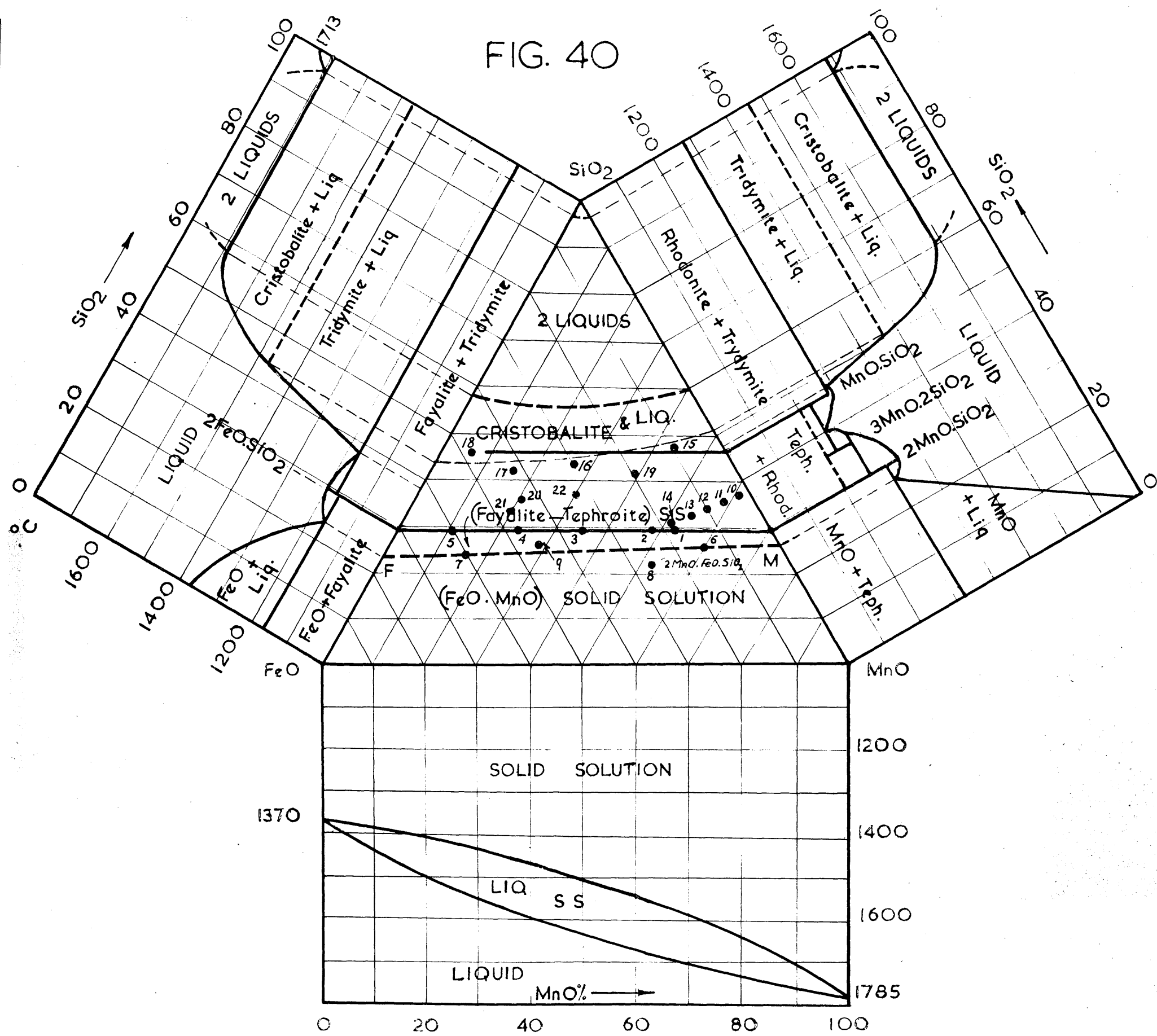
CHAPTER V.

Experimental Investigation of the
System FeO - MnO - SiO$_2$.

The previous chapter has shown that the ternary system
FeO-MnO-SiO$_2$ has never been satisfactorily explained and that
most of the published data has proved to be based on incorrect
binary systems.   It seems, therefore, very desirable that
this system should be re-examined, particularly as the results
would give the relationship between the melting points of
FeO-MnO-SiO$_2$ slags and their composition and so assist in the
location of regions of low melting point of compositions suit:
:able for deoxidation products.   The results might also
provide information on the constitution of solid slags, which,
by throwing light on the constitution of the corresponding
liquid slags, might help in studying slag-metal equilibria.

I.   Experimental Work.
i)   Preparation of Raw Material:

MnO and SiO$_2$ were prepared as described in Chapter III.
The method of preparation of FeO from ferrous oxalate is similar
except for details, to the method used to prepare MnO.   The
method has been described fully by Ibrahim[34].

ii)   Preparation and melting of the slag:

A charge of four grams was made up from the three oxides
FeO, MnO and SiO$_2$, according to the composition required.   The
slags/
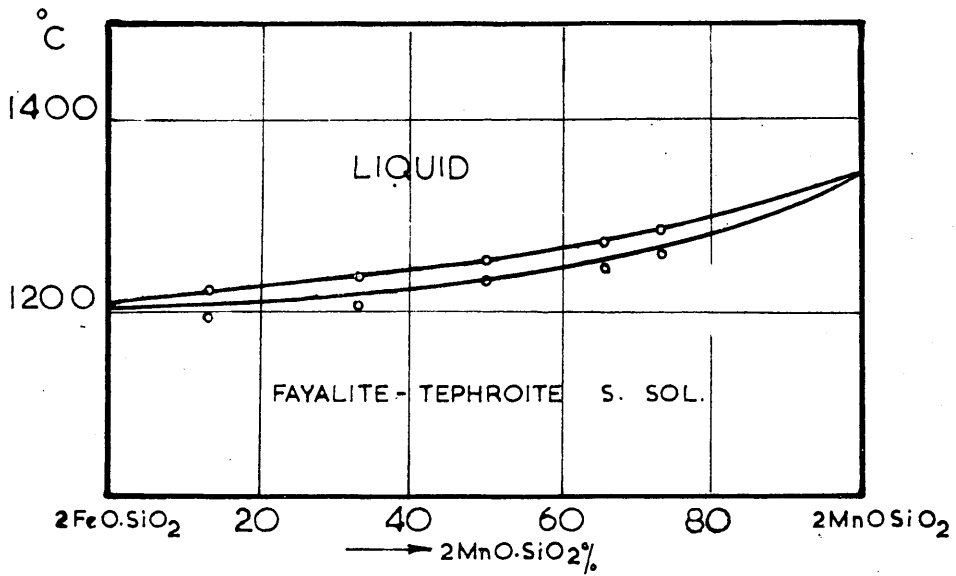
FIG.41. JOIN $2FeOSiO_2 - 2MnOSiO_2$
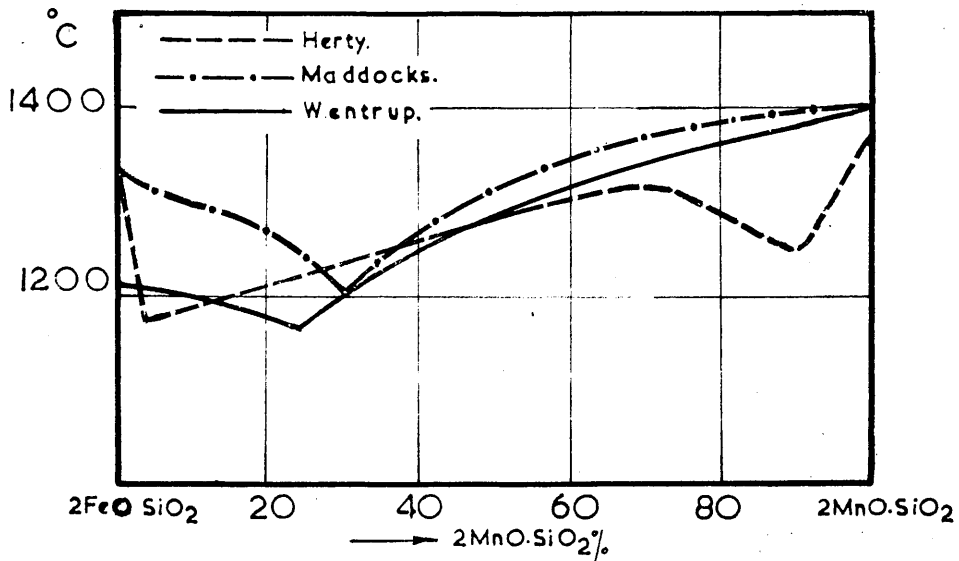
FIG.42.

slags were then prepared by melting in iron crucibles in a manner similar to that used in the preparation of $MnO-SiO_2$ slags, and a number analysed after melting to ensure that no serious change in composition had occurred.

Fayalite - Tephroite Join.

Since the $MnO-SiO_2$ diagram is similar to that of $CaO-SiO_2$ it might be expected that the $MnO-FeO-SiO_2$ system would bear certain resemblances to the $CaO-FeO-SiO_2$ system. This would suggest the possibility of the existence of the compound $FeO.MnO.SiO_2$ (analagous to $CaO.FeO.SiO_2$) giving rise to a double series of solid solutions, i.e., knebelite-fayalite and knebelite-tephroite.

Five slags were, therefore, prepared along the above join as shown in Fig.40. Their compositions and melting points are given in Table 8.

Table 8.

Slag No.	Composition as made up.			Melting Points.	
	FeO%	MnO%	SiO_2%	Starting	Finishing.
1	18.6	51.6	29.8	1260	1280
2	21.6	48.7	29.7	1239	1268
3	35.3	35.0	29.7	1230	1250
4	46.8	23.4	29.8	1200	1234
5	60.1	10.2	29.7	1187	1218

Slag /

Fig. 43 _ Slag No. 3 , "Knebelite" x 100

35.3% FeO , 35.0% MnO & 29.7% SiO₂.
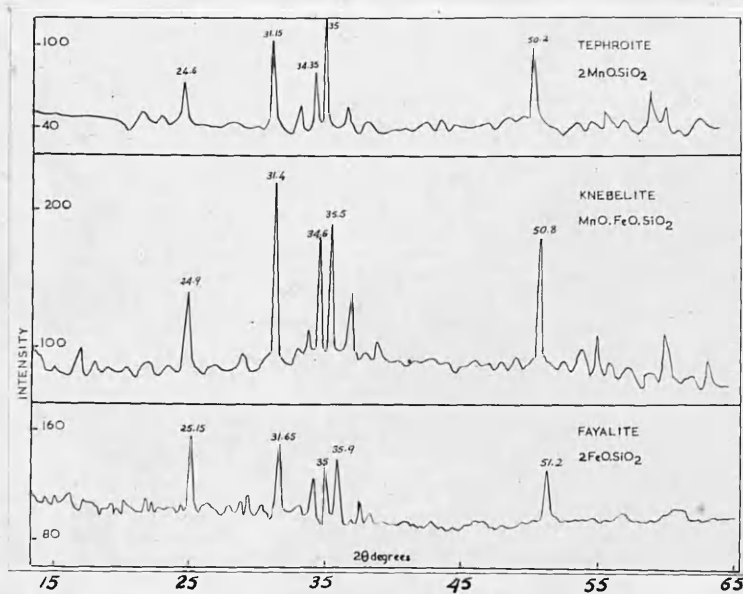
Fig. 44 .

Slag No.2 was analysed after melting. The results showed that it contained 21.8 per cent FeO, 48.7 per cent MnO and 29.5 per cent SiO_2, indicating a very slight deviation from the made up composition.

The colourof these slags changed gradually from the deep green colour of tephroite to the brownish black colour of fayalite. Under the microscope they showed only one phase. Some of them showed very small regions of oxide eutectic at the grain boundaries.

The melting points as plotted in Fig.41 indicate that there is a gradual fall in temperature of the liquidus and solidus curves across the diagram from tephroite to fayalite.

Slag No.3 contains equimolecular proportions of both orthosilicates and corresponds to the composition of the mineral knebelite $FeO.MnO.SiO_2$, the existence of which in synthetic slags has been the subject of much controversy. Under the microscope it also showed one phase, Fig.43, as did the rest of the series. Maddocks[48] maintained that it should be regarded as a compound since its optical pro: :perties were distinctly different from the general fayalite-tephroite solid solution. Fig.41 suggests that knebelite should not be regarded as a ternary compound but rather as a member of the fayalite-tephroite solid solution series.

Fig.44 compares the X-ray diffraction curves of the three compositions fayalite, knebelite and tephroite as obtained by the/

the Geiger counter X-ray spectrometer. The diffraction patterns for all three substances are very similar and probably correspond in all cases to orthorhombic crystals. Extensive calculations would be necessary to find out from the inten: :sities of the knebelite diffraction lines, whether the manganese and iron atoms were arranged in an ordered fashion, indicating an ordered solid solution which might be regarded as a ternary compound, or at random, indicating a disordered solid solution.

There is not sufficient evidence from the present X-ray and melting point data to consider knebelite as a ternary compound, although it is more difficult to determine the beginning and end of melting accurately when examining solid solution series and only a slight alteration of the obtained data could give a diagram of the type:-
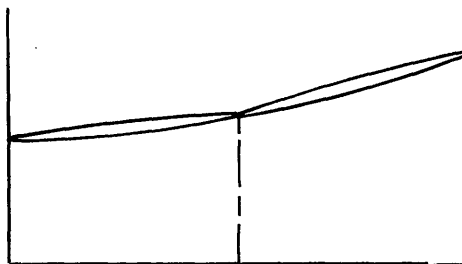
The diagram shown in Fig.41 is a true binary being only slightly different from the tentative diagram Fig.37b suggested by White[40] who was of the opinion that tephroite melted incongruently. There is, however, considerable difference between this diagram and those derived from the work of Herty and co-workers[56], Maddocks[47] and Wentrup[60].

Herty's/

Herty's work showed a maximum at approximately 71 per cent tephroite which he attributed to the probable existence of the ternary compound 2 MnO.FeO.SiO$_2$. Maddock's work showed a minimum on the fayalite-tephroite join at 30 per cent tephroite and a ternary eutectic point at a composition of 50 per cent, FeO, 20 per cent MnO and 30 per cent SiO$_2$, which falls but very slightly off the tephroite-fayalite join, very near to this minimum. A ternary eutectic at this point appears highly improbable. Wentrup's diagram also indicates a minimum on the tephroite-fayalite join at approximately 24 per cent tephroite. Their results are summarised and compared in Fig.42.

MnO – Tephroite, FeO-Fayalite Eutectic Trough.

Since the two solid solutions namely the MnO-FeO and 2MnO.SiO$_2$ – 2FeO.SiO$_2$ show a gradual temperature drop in the liquidus from the MnO to the FeO side of the diagram, a eutectic trough would, therefore, be expected to run across the diagram between the two solid solution series. The base of the eutectic trough is the line MF, Fig.40, joining the MnO-tephroite eutectic with the FeO-fayalite eutectic.

To verify this deduction, the following four slags were made as indicated in Fig.40. Their compositions and melting points are given in Table 9.
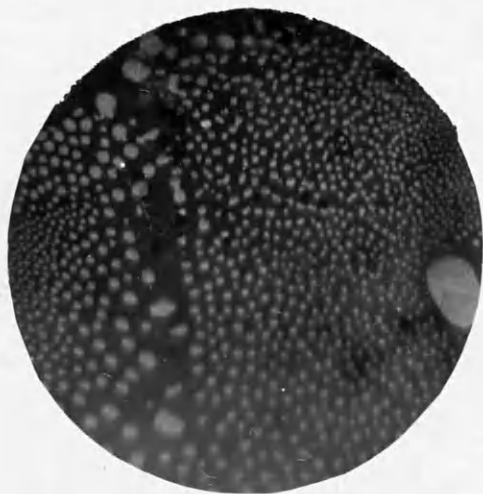
Table 9. /

Fig. 45. FeO- Fayalite eutectic x 400
78% FeO & 22% SiO$_2$
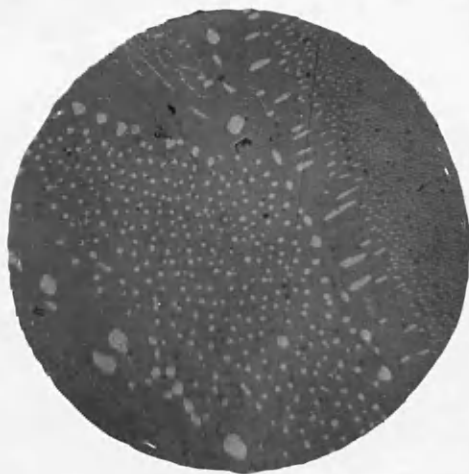
Fig. 46. Slag No. 6   x 400
14% FeO, 60% MnO & 26% SiO$_2$

Fig. 47. Slag No. 8   x 400
26.2% FeO, 51.8% MnO & 22% SiO$_2$

Fig. 48. Slag No. 9   x 400
45.1% FeO, 29.1% MnO & 25.8% SiO$_2$

Table 9.

Slag No.	Composition as made up.			Melting Points °C.	
	FeO%	MnO%	SiO$_2$%	Starting	Finishing.
6	14	60	26	1260	1275
7	60	16.6	23.4	1190	1197
8	26.2	51.8	22	1233	1245
9	45.1	29.1	25.8	1220	1230

Slags No.6 and 7 are on the line MF joining the two binary eutectics. Under the microscope they showed a completely eutectic structure which was very similar to that of the MnO-tephroite (Fig.14) and FeO-fayalite (Fig.45) eutectics. A photomicrograph of slag No.6 is shown in Fig.46; the two components of the eutectic structure are MnO-FeO (i.e., oxide) solid solution and $2MnO.SiO_2$-$2FeO.SiO_2$ (i.e., orthosilicate) solid solution.

Slag No.8 is Herty's[56] suggested ternary compound. Under the microscope it showed primary grains of oxide solid solution in a eutectic background of oxide and orthosilicate as shown in Fig.47. This does not appear compatible with the existence of the compound $2MnO.FeO.SiO_2$. The ternary eutectic suggested by Herty's diagram which has the composition 75 per cent FeO, 3 per cent MnO and 22 per cent SiO_2 falls slightly off the line MF joining the two binary eutectics and very near the FeO-fayalite eutectic which is composed of 78 per cent FeO and 22 per cent silica.

Slag No.9 has a composition between the line MF and the orthosilicate/

orthosilicate join.   Under the microscope it showed primary orthosilicate solid solution in a background of oxide-orthosilicate eutectic as shown in Fig.48.

The melting points of these slags show that there is a gradual decrease in temperature along the line MF from M to F and that from MF the liquidus surface will rise with increasing silica content to the liquidus of the tephroite-fayalite join, while decreasing silica will raise the liquidus surface more steeply towards the MnO-FeO liquidus and especially towards the MnO corner of the system.

The melting point determinations also showed that although the two slags No.6 and 7 are completely eutectic, yet melting took place over a range of temperature which is typical of a binary eutectic in a ternary system.

The structures and melting points of these four slags provide sufficient evidence for the existence of a eutectic trough between the two solid solution series FeO-MnO and $2FeO.SiO_2-2MnO.SiO_2$.

These results are in good agreement with the work of Hay, White and McIntosh[57] except when their eutectic trough JKL Fig.36, becomes a binary peritectic curve near the tephroite composition.

A number of slags were also prepared with compositions between the ortho- and meta- silicate joins in the ternary system $FeO-MnO-SiO_2$.   The main objects of this investigation were to locate the low melting slags which should be produced in deoxidation, and to check some of the earlier work.

Series I.

The slags of this series were prepared with compositions along the line joining the FeO corner to the point 62.5 per cent MnO, 37.5 per cent SiO_2 which is the eutectic point reported by White, Howat & Hay[24] in the MnO-SiO_2 system. The positions of these slags are marked on Fig.40 and their compositions are given in Table 10.

Table 10.

Slag No.	Composition as made up		
	FeO%	MnO%	SiO_2%
10	2.5	61.0	36.5
11	6.6	58.7	35.3
12	10.0	56.0	34.0
13	15.0	53.0	32.0
14	18.0	51.2	30.8
2	21.6	48.7	29.7

Slag No.2 on the orthosilicate join also fell on that line and is therefore included. The analyses and melting points of these slags are given in Table 11.

Table 11. /
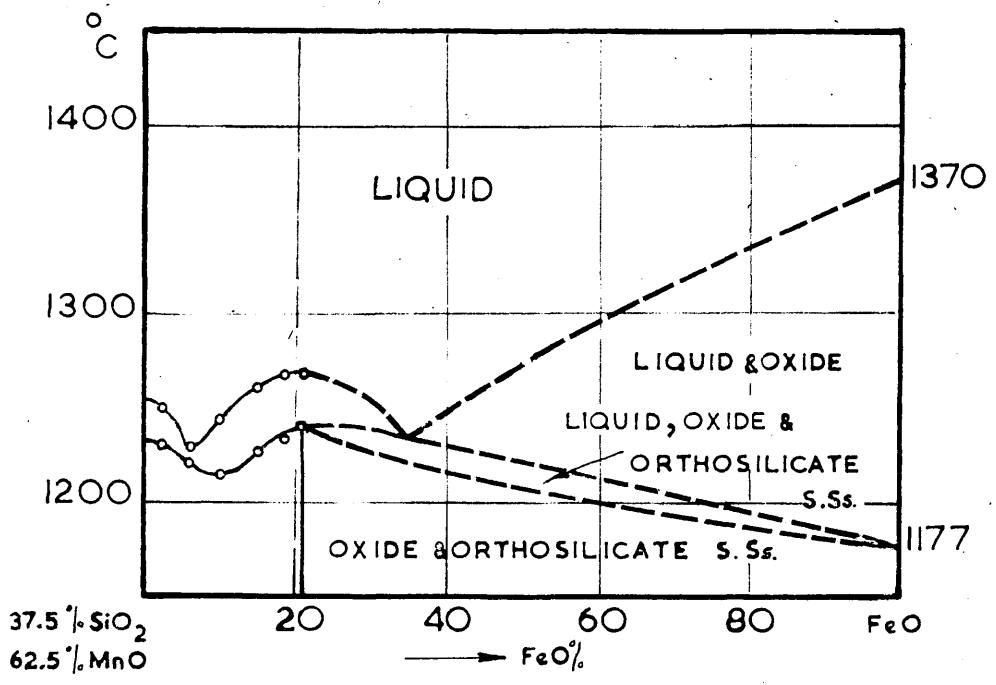
FIG. 49.

Table 11.

Slag No.	Analyses			Melting Points.	
	FeO%	MnO%	SiO$_2$%	Starting	Finishing.
10	2.6	61.0	36.4	1231	1242
11	6.2	58.8	35.0	1220	1227
12	10.0	55.9	34.1	1214	1244
13	15.2	52.9	31.9	1228	1260
14	18.7	51.9	29.4	1232	1268
2	21.8	48.7	29.5	1239	1268

It will be seen from the analyses that in general there is very slight variation from the made up compositions. The colour of these slags showed a gradual change from brownish grey to black, with increased FeO content. The slags nearer to the ortho-silicate join showed a very fine precipitation at the grain boundaries of the primary phase which might be a ternary eutectic, although it was not possible to establish this with certainty. Fig.50 shows the microstructure of slag No.13 after etching with a solution of 50 per cent HCl for a few seconds. An X-ray diffraction curve was obtained for this slag to determine the phases present. The only phase definitely identified as shown in Fig.57 was an orthosilicate solid solution of composition between "knebelite" and tephroite.

The melting points of these slags are plotted in Fig.49. The curve shows a marked dip in the liquidus at 6 per cent FeO and/

Fig. 50 _ Slag No. 13 etched in HCl.
x 100 (15.2% FeO, 52.9% MnO & 31.9% SiO₂)

Fig. 51 _ Slag No. 15 etched in HCl.
x 100 (10% FeO , 43.33% MnO & 46.66% SiO₂.)

Fig. 52 _ Slag No. 16 unetched x 40
30% FeO , 26.66% MnO & 43.33% SiO₂

Fig. 53. Slag No. 18 unetched x 100
49% FeO , 54% MnO & 45.6% SiO₂

and a gradual rise to the orthosilicate join.   The dotted
portion was deduced from the earlier results.

The liquidus of this join was expected, from the results
of previous workers, mainly Hay, Howat and McIntosh[57] and
White[40] to rise gradually towards the orthosilicate join.
The presence of this dip also suggests that there might be a
ternary eutectic in this region.

Series II.

With the discovery of the eutectic between rhodonite and
silica in the $MnO-SiO_2$ system, it was decided to investigate
whether a second eutectic trough existed in the ternary system
extending between the silica-rhodonite eutectic and the silica-
fayalite eutectic.   Three slags were prepared on the line
connecting the two binary eutectic points.   Their compositions
and melting points are given in Table 12.

Table 12.

Slag No.	Composition as made up.			Melting Points ^{o}C.	
	FeO%	MnO%	SiO_2%	Starting	Finishing.
15	10.0	43.33	46.66	1130	1255
16	30.0	26.66	43.33	1175	1185
17	42.0	17.00	41.00	below 1400	over 1400

Slag No.15 under the microscope showed a completely
eutectic structure as shown in Fig.51.   Visual examination
showed the pink colour characteristic of rhodonite and in general
the/

the structure is similar to that of the silica-rhodonite eutectic in the $MnO-SiO_2$ system.

Slag No.16 on visual examination, showed massive light coloured crystals with a greenish lustre and which were very different in appearance from rhodonite. Under the microscope these large crystals were again apparent but were separated by a very small proportion of darker material at the grain bound: :aries as shown in Fig.52. These crystals suggested the presence of a new phase. Unfortunately the X-ray diffraction curve of this slag, given in Fig.57 showed only the lines of the knebelite composition yet there is a considerable difference between the structure, colour and visual appearance of "knebelite" (Fig.43) and this slag. It appears that either the new phase has such a complex crystal structure that the resultant X-ray pattern is too weak to observe (in this case the lines obtained by X-rayswill be due to the dark material present at the grain boundaries) or the compound may dissociate in the solid state to orthosilicate (knebelite composition) and silica. The latter does not appear very probable.

These results indicate that rhodonite can take a limited amount of FeO in solid solution probably up to 10 per cent, and that more FeO will cause the appearance of a second phase probably the compound $MnO.FeO.2SiO_2$ analogous with the compound Hedenbergite, $CaO.FeO.2SiO_2$ in the system $CaO-FeO-SiO_2$ Consequently the solid solubility line of the metasilicate will not/

not be expected to extend so far into the ternary system as indicated by Whiteley and Hallimond[26] and accepted by later workers.   These conclusions are compatible with the work of Perutz[58] who showed that iron rhodonites differ structurally from natural rhodonites.   They are also in fairly good agree: :ment with the diagram of Wentrup who gave a small primary field of crystallisation for rhodonite.

Slag No.17 corresponds to the ternary eutectic reported by Whiteley and Hallimond[28] and accepted by Benedicks and Lofquist[21].   In the preparation of this composition by heating at 1400°C for half an hour, only partial melting occurred and it was noted that the slag was very viscous and tended to stick to the walls of the crucible.   The beginning of melting probably occurs below 1400°C but the final melting point appears to be considerably above 1400°C, and suggests that the composition of slag No.17 does not represent a ternary eutectic.

Miscellaneous Compositions:

Five slags were prepared mainly to check specific points in the diagram.   Their compositions and melting points are given in Table 13.

Table 13. /
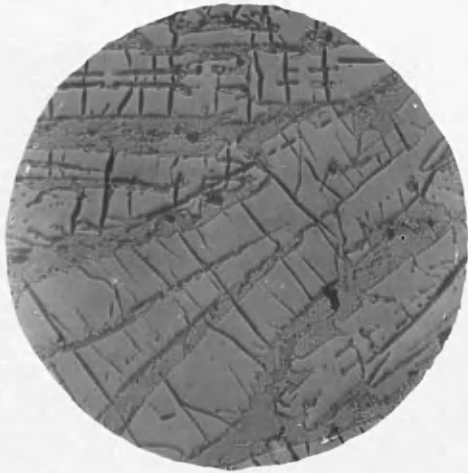
Fig. 54 - Slag No. 20 unetched ×100

42.9 % FeO ,21.2% MnO &35.9% SiO$_2$

Fig. 54a - Slag No. 20 etched in HCl ×400

42.9% FeO , 21.2% MnO & 35.9% SiO$_2$
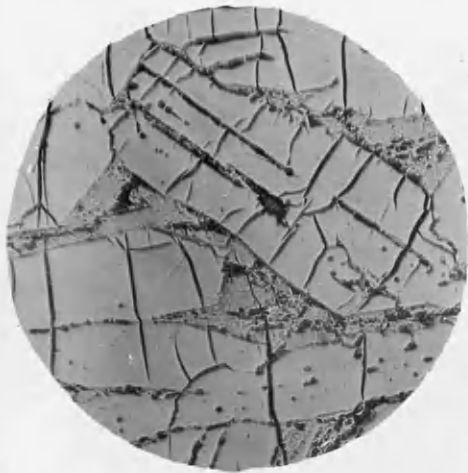
Fig. 55 - Slag No. 21 unetched ×400

47% FeO , 20% MnO & 33% SiO$_2$

Fig. 56 - Slag No. 22 unetched ×100

35.5 % FeO, 20% MnO & 33% SiO$_2$

Table 13.

Slag No.	Composition as made up.			Melting Points.	
	FeO%	MnO%	SiO_2%	Starting	Finishing.
18	49.0	5.4	45.5	melted at 1500	
19	19.3	39.2	41.5	not determined.	
20	42.9	21.2	35.9	1140	1175
21	47.0	20.0	33.0	1142	1220
22	35.5	30.0	37.5	1165	1175

Slag No.18 fell on the metasilicate join and contained 90 per cent "$FeO.SiO_2$" and 10 per cent $MnO.SiO_2$. Under the microscope as shown in Fig.53 it showed primary silica in a background of eutectic consisting of silica and orthosilicate solid solution. The microstructure of this slag is very similar to the composition "$FeO.SiO_2$" (Fig.8).

The two slags No.19 and 20 fell on the rhodonite-fayalite join. No.19 contained 28 per cent fayalite and 72 per cent rhodonite. On visual examination it showed a slag with the same large light coloured crystals with a greenish lustre as were seen in slag No.15 (Fig.52), but a little smaller. Under the microscope there was little but these large crystals to be seen, other than a very slight amount of a darker phase around the grain boundaries. No X-ray diffraction curve was taken for this slag but from the colour of these crystals, they look very different from rhodonite although the slag contained/
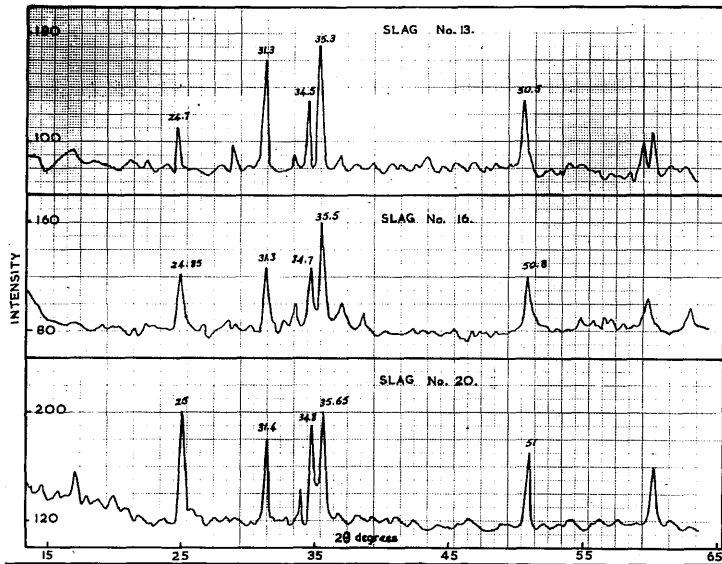
Fig. 57.

contained 72 per cent rhodonite. This agrees with the con:
:clusion drawn from the slags of Series II, that the primary
field of crystallisation of rhodonite in the ternary system
$FeO-MnO-SiO_2$ is small. Further investigations on the
fayalite-rhodonite join by Bell[61] have shown that X-ray diffraction
curves of samples containing 90 per cent rhodonite showed
mainly the lines of orthosilicate and that lines for rhodonite
only started appearing in samples containing 95 per cent
rhodonite.

Slag No.20 contained equimolecular proportions of
rhodonite and fayalite and corresponds to the formula
$2FeO.MnO.2SiO_2$. Under the microscope (Fig.53) it showed
primary crystals of orthosilicate solid solution and eutectic.
Fig.54a taken at a higher magnification shows the eutectic
more clearly. The X-ray diffraction curve of this slag,
Fig.57, showed lines which when compared with the diffraction
curves of fayalite, the knebelite composition and tephroite,
Fig.44, indicated that the composition of the orthosilicate
present in this slag was between fayalite and "knebelite".
The fact that this slag started melting at $1140^{o}C$ suggested
that a ternary eutectic may exist in this region of the diagram.

Slag No.21 corresponded to the ternary eutectic
suggested by Wentrup[60]. The structure of the slag does
not show a ternary eutectic; on the other hand it was
similar to slag No.10 with more fayalite-tephroite solid
solution/

solution and less eutectic as shown in Fig.55. It started melting at 1142°C again supporting the existence of a ternary eutectic.

Slag No.22 is on the eutectic trough F G H (Fig.36) suggested by Hay, White and McIntosh[57]. The structure of this slag shown in Fig.56 does not possess a completely eutectic structure. (It is, of course, possible for binary eutectics in ternary systems to have coarse structures quite different from the appearance of a binary eutectic in a binary system, due to the fact that freezing can occur over a range of temperature).   It showed large crystals of orthosilicate solid solution which appear to have taken part in a peritectic reaction.   The microstructure showed also another type of massive crystal, and a very fine structure at the grain boundaries which might be a ternary eutectic of the same composition as that of slags No.20 and 21.

Conclusions.

The examination of the slags mentioned above has not been sufficient to give conclusive results regarding the distribution of phases in the solid state or the nature of the liquidus surface between the meta- and ortho - silicate joins, yet it provides some fundamental information on which further investigation of that part of the diagram could be based.   The results may be summarised as follows:-

1.   The fayalite-tephroite join appears to behave as a true binary join.

2.   A/

2. A eutectic trough connects the $FeO-2FeO.SiO_2$ and $MnO-2MnO.SiO_2$ binary eutectic points.

3. All compositions examined in the region richer in FeO or MnO than the orthosilicate join showed only two phases, viz., oxide and orthosilicate solid solutions.

4. The primary field of crystallisation of rhodonite will be small and the solid solubility line of the meta: :silicate starting from the rhodonite composition will extend inside the ternary system to a much lower FeO percentage than that indicated by Whiteley and Hallimond[28] and hence accepted by subsequent investigators.

5. The existence of a ternary eutectic is probable, as is suggested by certain of the microstructures and especially that of No.20. This slag started melting at 1140°C., approximately 40°C lower than the silica-fayalite eutectic in the $FeO-SiO_2$ system.

6. X-ray examination was unable to establish with certainty the existence of stable ternary compounds in the $FeO-MnO-SiO_2$ system. Due probably to the low order of crystal symmetry of these silicates, only lines of orthosilicate solid solution were obtained in most of the slags, although the micro: :structures gave clear indication of the presence of at least one new type of phase. It would seem that/

that petrographic examination of such slags might be
superior to X-ray analysis for identifying the phases
present in the solid slags.   It was not possible to
use this method of identification in the present work.

7.   Slags No.15 and 17 showed that the silica liquidus
surface starts rising near the $FeO-SiO_2$ system at a
lower percentage of silica than near the $MnO-SiO_2$
system.   This is also to be expected from the binary
systems.

8.   In general there is a very fluid slag region existing
approximately between the two lines connecting the two
points 41 per cent silica and 38 per cent silica in
the $MnO-SiO_2$ system with the two points 38 per cent
silica and 35 per cent silica in the $FeO-SiO_2$ system.
Slags within this region are almost completely fluid
at 1200°C.

It would appear preferable to produce slags or inclusions
within this range of composition during deoxidation with
manganese-silicon deoxidisers, since these would be very fluid
at steel making temperatures, coalesce easily into larger
globules and be rapidly removed from the molten metal.

The steelmaker should, therefore, aim to add deoxidisers
of the correct Mn/Si ratio and in the correct amount to
produce inclusions with compositions within this range.   This
is further discussed in a later chapter.

CHAPTER VI.

Theory of Slag-Metal Equilibria.

Of fundamental importance in considering slag-metal equilibria is a knowledge of the activity of the reactants and products in the phases taking part in the reaction. The work of Chipman [6][62] has done much to elucidate the variation of activity with composition in dilute metallic solutions, e.g., carbon and oxygen in steel as discussed in Chapter 1. In the case of slags, conditions are much more complex and earlier workers found that the total weight or molar concentrations when substituted in the mass action expression did not give a true constant. The determination of the activity of the different constituents is more difficult because our knowledge of the structure of slags in the liquid state is far less satisfactory than in the solid. The methods employed in assessing activities in slags can be summarised as follows:-

1. The assumption of electroneutral oxides and compounds in the slags.

2. The assumption of complete ionisation of slags.

3. Data derived from experimental results.

4. Thermodynamic calculations.

The Structure of liquid slags:

Before discussing these methods, it is of interest to consider our knowledge of the structure of liquid slags which are mainly silicates.
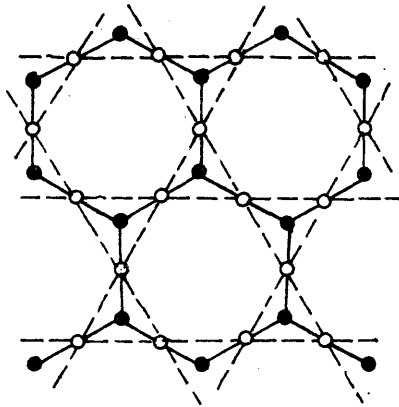
Richardson/
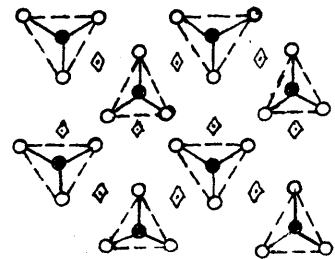
Solid silica

Solid fayalite
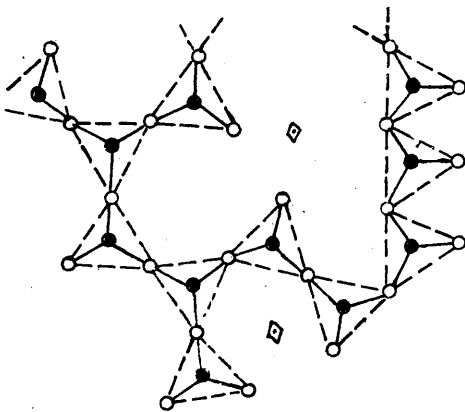
Liquid silica containing small amounts of iron oxide.
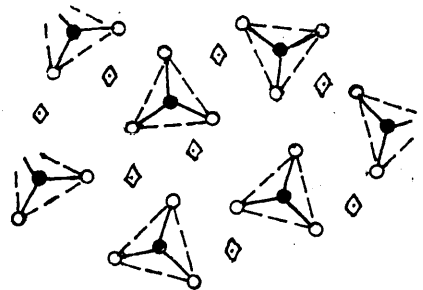
Liquid fayalite

- Silicon atom
- o Oxygen atom
- ◊ Iron atom or ion

FIG. 58. Schematic representation of solid and liquid slags. (after Richardson.)

Richardson, Jeffes and Withers[63] in their survey of the

thermodynamics of compounds between oxides have shown that the

entropies of fusion of silicates are not unduly high so that no

major changes in the structure are to be expected on melting,

e.g. the entropy of fusion of Na_2SiO_3 is 9.2 as compared with

values of 6.7 and 6.5 for NaCl and Na NO_3. This shows that the

changes taking place on the fusion of silicates differ little

from those which normally accompany the melting of typical salts.

One would, therefore, expect the liquid structure to resemble

the solid, lacking, of course, the long-range order of crystall:

:ine materials. Fig.58 proposed by Richardson[64] illustrates

the structure of solid and liquid silica and fayalite.

The structure of liquid silicates can also be inferred by

analogy with similar systems such as glass, whose structure is

well understood due to the work of Zachariasan[65] and Warren[66].

Confirmatory information is available from measurements of sur:

:face tension, viscosity and electrical conductivity of slag

systems.

(a.)Surface tension measurements:

The work of King[67] on the surface tension of slags has

shown unexpectedly, an increase in the surface tension of certain

slags with temperature. To explain why rhodonite has a positive

temperature coefficient, he suggested that the original chain

structure broke down with increase in temperature to give a

structure containing discrete SiO_4 tetrahedra characterised by

tephroite, and silica rich groupings. Thus more unsatisfied

bonds/

bonds on the liquid surface are produced, therefore the surface energy increases. If this effect is larger than the decrease produced by thermal expansion then the overall temperature coefficient will be positive. The breakdown of rhodonite can be expressed by the following equation:-

$$2(MnO.SiO_2) \rightleftharpoons 2MnO.SiO_2 + SiO_2$$

or on the ionic basis:

$$2n(Mn)^{2+} + 2(nSiO_3)^{2n-} \rightleftharpoons 2n(Mn)^{2+} + n(SiO_4)^{4-} + n(SiO_2)$$
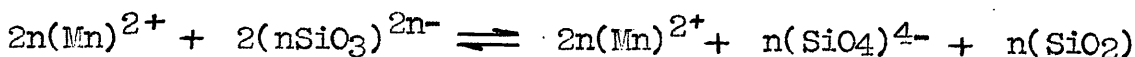
This is not the only possible reaction; an alternative would be:

$$2n(Mn)^{2+} + 2(nSiO_3)^{2n-} \rightleftharpoons 2n(Mn)^{2+} + (\frac{n}{2} Si_2O_5)^{2n-} + (\frac{n}{2}Si_2O_7)^{6n-}$$
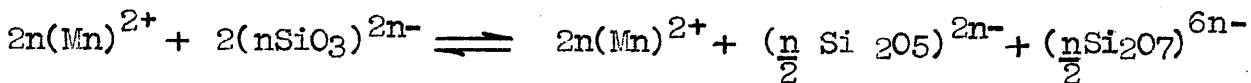
but there is no direct evidence of any tendency towards the formation of these groupings.

Tephroite also showed a slight increase of surface tension with temperature. Since the structure formed on melting teph: :roite contains only discrete SiO_4 tetrahedra, any further break: :down must result in the production of free oxygen ions and either silica or intermediate groupings between silica and SiO_4 tetra: :hedra, e.g.,

$$2n(Mn)^{2+} + n(SiO_4)^{4-} \rightleftharpoons n\{2(Mn)^{2+} + 2O^{2-}\} + nSiO_2$$
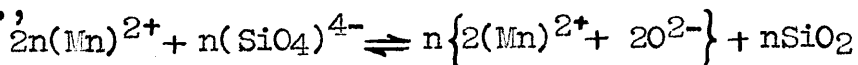
It is possible that the attraction of the manganese ion for the oxygen ion is sufficiently strong to favour the above reaction. On this basis one would expect the stability of silicates in the liquid state to decrease as the radius of the metal ion decreases. Therefore in slags containing Mn, Fe and Mg silicates, their stabilities will be in that order. The above equation also shows that the SiO_4 tetrahedra can be regarded/

regarded as a source of oxygen ions in the slag.

(b.) Viscosity Measurements:

The work of Towers and Kay[68] has shown that rhodonite exhibits anomolous viscosity which is indicated by the fact that its apparent viscosity decreases with increased rate of shear molten rhodonite, thus behaving as a non- Newtonian liquid. This was attributed to the tendency for the chain structure of rhodon: :ite to break down under shear into an island structure character: :istic of tephroite, with associated silica groupings, thus replacing the complex chain structure by the simple island type, with a resultant decrease in viscosity. This agrees with the work of King[67] and in addition suggests that the breakdown can be effected mechanically as well as thermally. This must mean that the energy change involved is very small and that rhodonite may be considered highly unstable. This is also expected from the $MnO-SiO_2$ diagram given in Chapter III, where the liquidus curve at the rhodonite composition is very flat. The order of stability of the three main binary compounds in the ternary system $FeO-MnO-SiO_2$ according to the shape of the liquidus curves will be as follows:-

Tephroite $2MnO.SiO_2$,   Fayalite $2FeO.SiO_2$, and Rhodonite $MnO.SiO_2$

decreasing stability.

The viscosity measurements of Losana[69] and more recently Urbain[70] suggest the occurrence of the compounds $2FeO.SiO_2$ and $2MnO.SiO_2$ in liquid slags.

(c.) Electrical /

(c) Electrical Conductivity measurements.

The findings of Bockris and his co-workers[50] on the
electrical conductivity of silicate melts have shown that in the
$CaO-SiO_2$ and $MnO-SiO_2$ systems, the degree of dissociation into
ions is substantial but in the $Al_2O_3-SiO_2$ system it is small.
Guggenheim[71] pointed out that slags are relatively poor
conductors of electricity and therefore can contain but few ions.
This suggests that slags are by no means completely ionised in
the sense inferred by Bockris and his co-workers. Moreover,
dissociation of these slags into ions might be due to the influ:
:ence of the applied electromotive force and it might be that
such dissociation would not take place without the help of this
applied external force. Accordingly the equations illustrating
the breakdown of these silicates should be expressed, e.g., in
the case of rhodonite:-

$$2n \ Mn.SiO_3 \rightleftharpoons 2n(Mn)^{2+} + 2(nSiO_3)^{2n-}$$

$$\rightleftharpoons 2n(Mn)^{2+} + n(SiO_4)^{4-} + n(SiO_2) \rightleftharpoons nMn_2.SiO_4 + nSiO_2$$
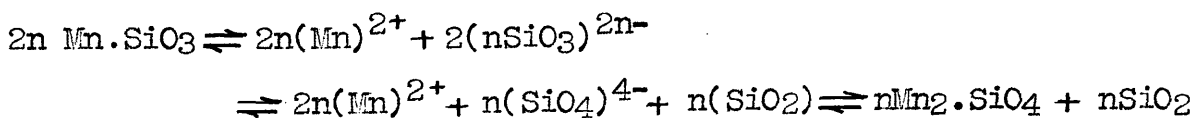
Guggenheim[71] also stated that so far as slag-metal
equilibria are concerned it is irrelevant whether any atom
or groups of atom carries a net charge or not and that it is more
reasonable and in most cases strictly more accurate to express
the equilibrium in terms of atoms or group of atoms.

Carter[72] also mentioned that molten $MnO-SiO_2$ mixtures
of composition near that of rhodonite $MnO.SiO_2$ on quenching give
rise to a pink glass which can by further annealing give pink
crystalline rhodonite. Glasses obtained by quenching molten

mixtures/

mixtures of composition approaching that of tephroite $2MnO.SiO_2$

show the green colour of manganous oxide, whilst in the crystall:

:ine state tephroite is almost colourless and manganous oxide is

green.   If the pink colour of molten rhodonite is to be attribu:

:ten to the presence of manganous ions according to Bockris and

co-workers[50]   then it must be inferred that all the manganese

cannot be present as manganese ions in melts richer in MnO than

$MnO.SiO_2$.

Methods Used in assessing Activities.
(a) The assumption of electroneutral compounds:

One of the earliest attempts to assess the activity by

assuming the presence of certain compounds was made by Colclough[73]

who tried to group the oxides found in basic slags into stable

combinations.   He concluded that CaO combined primarily with

P_2O_5 and SiO_2 to form $4CaO.P_2O_5$ and $2CaO.SiO_2$ respectively while

excess CaO combined with Fe_2O_3 to form calcium ferrites.   On the

other hand Krings and Schackmann[74]   concluded that it was the

metasilicates of CaO, MnO and FeO that occur in liquid slags,

their stabilities decreasing in that order.

Schenck[75] developed this further by assuming that slags

are composed of free oxides and oxides combined in the form of

compounds whose dissociations are governed by the Law of Mass

Action.   For instance the formation and decomposition of

fayalite according to the equation

$$2FeO + SiO_2 \rightleftharpoons 2FeO.SiO_2$$

is governed by the expression $K = \dfrac{(FeO)^2(SiO_2)}{(2FeO.SiO_2)}$

where K is the dissociation constant of the compound, and
(FeO)/

(FeO) and (SiO) represent the "free" concentration of these oxides in the slag.

He then developed his "balanced equations" from which he predicted slag-metal equilibria knowing total slag compositions and temperature.

Chipman preferred a method in which by selecting the right compound the activity coefficients in slags can be reduced to unity. Thus Taylor and Chipman[76] proposed a double molecule of dicalcium silicate in liquid slags, dissociating according to the equation $4CaO.2SiO_2 \rightleftharpoons 2CaO.2SiO_2 + 2CaO$.

They also assumed that fayalite $2FeO.SiO_2$ was almost completely dissociated at $1600^{\circ}C$ to enable them to explain the observed activity of FeO in $FeO-SiO_2$ slags. It should be stated, however, that the ideal behaviour of FeO in $FeO-SiO_2$ slags does not necessarily mean that fayalite is completely dissociated as will be discussed later.

Similar assumptions were put forward by different investi: :gators, notably White[77], Carter[12], Körber and Oelsen[78] and Darken and Larsen[79]. Recent work on slag-metal equilibria is full of such assumptions which have proved to be very useful in interpreting slag-metal equilibria. Experimental support for this theory is found in the work of Losana[69] and Urbain[70] as mentioned before.

(b.) Ionic Theory of slag-metal Equilibria.

Herasymenko[80] was the first to develop a theory of slag-metal/

metal equilibria based on the complete ionisation of slags.
Temkin[81] developed a similar theory and with Samarin and Schwarz:
:mann[82] applied it to sulphur distribution between metal and
slag.   It is unlikely, however, that the theory in this simple
form can be applied to all slag-metal equilibria.   Thus in apply:
:ing the theory of completely ionised slags to slag-metal equil:
:ibria, Herasymenko and Speight[83] found it necessary to introduce
an empirical factor in calculations based on this theory, e.g. in
the equilibrium

$$\underline{Fe} \quad \underline{O} \rightleftharpoons Fe^{++} + O^{--}$$

they found that the equilibrium ratio for this reaction given by

$$k = \frac{(Fe^{++})(O^{--})}{[O]}$$

was not constant, but depended on the content of (O^{--}). Plotting
log k against log (O^{--}) at a practically constant temperature,
a straight line was obtained, represented by the equation

$$\log k = \frac{3}{2} \log (O^{--}) + \log 3$$

$$\text{or} \quad k = \frac{(Fe^{++})(O^{--})}{[O]} = A (O^{--})^{3/2}$$

where A is an empirical constant.   This equation was used to
calculate the oxygen content of the metal from the slag analysis.
Similar correction factors were found necessary in dealing with
certain other slag-metal reactions, and in general, the activity
of slag reactants was not equal to the ionic fraction, but
depended on slag composition.   These arbitrary correction
factors detract from the value of the theory of completely

ionised/

ionised slags and its use as a means of estimating slag activities.

(c) Activities determined experimentally:

White[77] calculated the activity of iron oxide from slag-gas equilibria involving oxygen pressure measurements over the melt. He also studied the effect of lime and silica additions on the activity of iron oxide melts. It was found that lime increased the activity of FeO in the slag while silica decreased it. This method was developed further in a paper by Murray and White[55].

The determination of activity from experimental results is also illustrated by the work of Chang and Derge[84]. They calcul: :ated the activity of silica in $CaO-SiO_2$ and $CaO-Al_2O_3-SiO_2$ slags from electromotive force determinations using the following expression

$$E - E_o = \frac{RT}{nF} \ln \acute{a}_{SiO_2}$$

where E = cell electromotive force.

E_o = standard cell electromotive force.

n = number of electrons involved in cell reaction.

$\acute{a}_{SiO_2}$ = activity of SiO_2 in slag.

(d) Activities from thermodynamics calculation:

It is also possible to determine activities from thermal equilibrium diagrams. The solidification curve of a component can give information on its activity, particularly if it crystall: :ises in the pure state and not as a solid solution. Thus, the activity/

activity of silica in silica saturated melts is unity when referr:
:ed to solid silica as the standard state.   The activity of a
melt saturated with silica at absolute temperature T referred to
supercooled liquid silica at the same temperature as the standard
state, is given by the expression

$$\log a_{SiO_2} = \frac{L}{4.575} \times \left(\frac{1}{T_m} - \frac{1}{T}\right)$$

Where a_{SiO_2} = activity of silica in the saturated solution.

   L   =   latent heat of fusion of pure silica

   T_m =   absolute temperature of melting point of silica.

   The activity of the solution at temperatures higher than the
saturation temperature can only be calculated when the partial
molar heat of solution $\bar{L}$ is known.   An approximate value for the
activity can be calculated if the binary solution is assumed to
be "regular" (in the sense used by Hildebrand [85]) and use made
of the relation

$$R T \ln \gamma_1 = b N_2^2$$

where γ_1 = activity coefficient of component (1)

   N_2 = molar fraction of component (2)

   b = constant

and the further assumption made that b is independent of temper:
:ature.   Chipman [62] has successfully used this method to deter:
:mine the activity of iron in liquid iron-iron sulphide solutions.

   For a given binary silicate composition

$$b N^2 = \text{constant} = RT \ln \gamma_{SiO_2}$$

This/

This method has been used in Chapter IX to calculate the activity
of silica in MnO-SiO$_2$ and FeO-SiO$_2$ solutions.

(86)

Rey used a similar method to determine the activity of
silica at 1600°C in a number of binary silicate systems with
reference to solid silica as the standard state.   He used the
equation

$$\log (a^1)_T = \frac{T - T_c}{T} \times (\log N - \frac{L}{4.575 T_m})$$

to determine the activity $(a^1)_T$ at a temperature T

where T_m =   melting point of silica

T_c =   saturation temperature

N   =   molar fraction of silica

L   =   latent heat of fusion of pure silica.

Discussion of the Manganese Reaction:

The reaction between molten iron containing manganese and
molten ferrous oxide - manganous oxide mixtures can be represent:
:ed by the equation

$$FeO \ (slag) + \underline{Mn} \ \rightleftharpoons \ MnO(slag) + \underline{Fe}$$
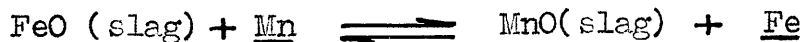
The equilibrium constant of this reaction has been denoted by
KMn and is given by

$$K_{Mn} = \frac{(a_{MnO})}{(a_{FeO})[a_{Mn}]}$$

The two oxides MnO and FeO behave ideally with respect to
each other in the liquid state and in simple MnO-FeO slags the
activity coefficient for both oxides is unity and their activity
is equal to their molar concentration.   Manganese is usually
present in small amounts in the liquid iron and according to

Henry's/

Henry's law the activity is proportional to the concentration which may be expressed in any convenient unit since at suffic: :iently great dilution each concentration unit bears a fixed ratio to every other.

For the slag, molar concentrations should be used only, but since the atomic weight of manganese differs only very little from that of iron, it is permissible to calculate with weight percentages.   The equilibrium constant may then be expressed as follows:-

$$K_{Mn} = \frac{(\% \ MnO \ )}{(\% FeO) \ [\% \ Mn]}$$

The presence of other basic oxides such as MgO and CaO has no effect on the activities of FeO and MnO, which remain equal to their concentration.   Acidic oxides such as SiO_2 and P_2O_5 affect the activity of FeO and MnO differently and when total concentrations by weight of the two oxides are substituted in the mass action expression, varying values are obtained for K_{Mn} when expressed in the above form.

It is, therefore, essential to distinguish between the true equilibrium constant K_{Mn} where activies are substituted in the mass active expression and the equilibrium ratio "KMn" for which total concentrations of FeO and MnO are substituted in the mass action expression

$$"K_{Mn}" = \frac{(\Sigma \ MnO)}{(\Sigma \ FeO) \ [Mn]}$$

Under simple FeO-MnO slags KMn = "KMn"

The/

The true equilibrium constant K_{Mn} has been determined by a number of investigators. Among the early workers were Oberhoffer and Schenck [87] and Tammann and Oelson [88]. Their results suffer from the failure to appreciate the speed of the reaction where the equilibrium shifts quickly with temperature if the metal and slag are cooled slowly together. Among the other investigators are Herty [89], Korber and Oelson [90] and Krings and Schackmann [91] whose results have suffered from other inaccuracies such as dependence upon optical temperature measure: :ments and exposure to atmospheric oxidation.

The new data on K_{Mn} for FeO-MnO slags relatively free from silica published recently by Chipman, Gero and Winkler [92] are appreciably higher than those of Korber and Oelsen [90] and are in general somewhat above those of other investigators. The equation of the isochore was given by

$$\log K_{Mn} = \frac{+6440}{T} - 2.95$$

They also calculated the equation of the isochore from published thermodynamical data as

$$\log K_{Mn} = \frac{+6440}{T} - 2.82$$

which agrees well with their experimental results. In both equations the slag composition is expressed in molar fractions.

Korber and Oelsen [78] also studied the equilibrium of iron under iron-manganese silicate slags saturated with silica. They found that the slags contained approximately 50 per cent silica by weight which was independent of the FeO/MnO ratio or the temperature. This is what would be expected from the nature of/

of the silica liquidus surface at 1600°C in the FeO-MnO-SiO$_2$ system. Their results in this field are the best quantitative data to date.

The results of Korber and Oelsen[78][90] Chipman, Gero and Winkler[92] are given in Table 14, where slag composition is expressed in weight percentage.

Table 14.

Temp. °C.	Korber and Oelsen.		C, G. & W.
	"K$_{Mn}$"(SiO$_2$ Sat.Slags)	K$_{Mn}$	K$_{Mn}$
1550	15.5	2.5	3.77
1600	12.0	2.0	3.00
1650	9.0	1.7	2.46

CHAPTER VII.

Slag-Metal Experiments.

The Rotating Crucible Furnace.

The equilibrium of iron under MnO-FeO slags and silica-saturated FeO-MnO-SiO$_2$ slags has been studied by several invest::igators as discussed in the previous Chapter.

In the present investigation it was decided to study the equilibrium of iron under iron manganese silicate slags which were not saturated with silica and which fell mainly between the orthosilicate join 2MnO.SiO$_2$- 2FeO.SiO$_2$ and the FeO-MnO side of the ternary system FeO-MnO-SiO$_2$. It has been shown in Chapter V that the phases present in the solidified melts of this part of the diagram are MnO-FeO and 2MnO-SiO$_2$ - 2FeO.SiO$_2$ solid solutions.

The work of Taylor and Chipman [76] on the study of the activity of FeO in slags of the system (CaO,MgO) - SiO$_2$ - FeO, and the solubility of oxygen in liquid iron under pure iron oxide slags suggested that a rotating crucible furnace might be useful in the investigation of deoxidation equilibria.

The most important advantage of the rotating crucible furnace would appear to be that it enables investigatons to be conducted on slag-metal equilibria with the minimum contam::ination of the slag by the crucible material. Since this work was started two papers have recently been published by Hilty and Crafts, the first concerning deoxidation by aluminium [93] and /

DIMS IN INCHES

SCALE 1:4.

GLASS WINDOW

COOLING COIL

SHUTTER BAFFLE PLATE

SCREW

RUBBER PACKING

LEVER

REFRACTORY COVER

COPPER COIL

BAKELITE SUPPORT

SILICA SLEEVE

IRON BASE

18

BALL BEARING

BALL BEARING & SUPPORT

DRIVING PULLEY

MOTOR

NITROGEN INLET

NITROGEN OUTLET

N$_2$ DISTRIBUTOR

MAGNESIA CRUCIBLE

FUSED ALUMINA

RUBBER SEAL

STEEL SHAFT

24

16

24
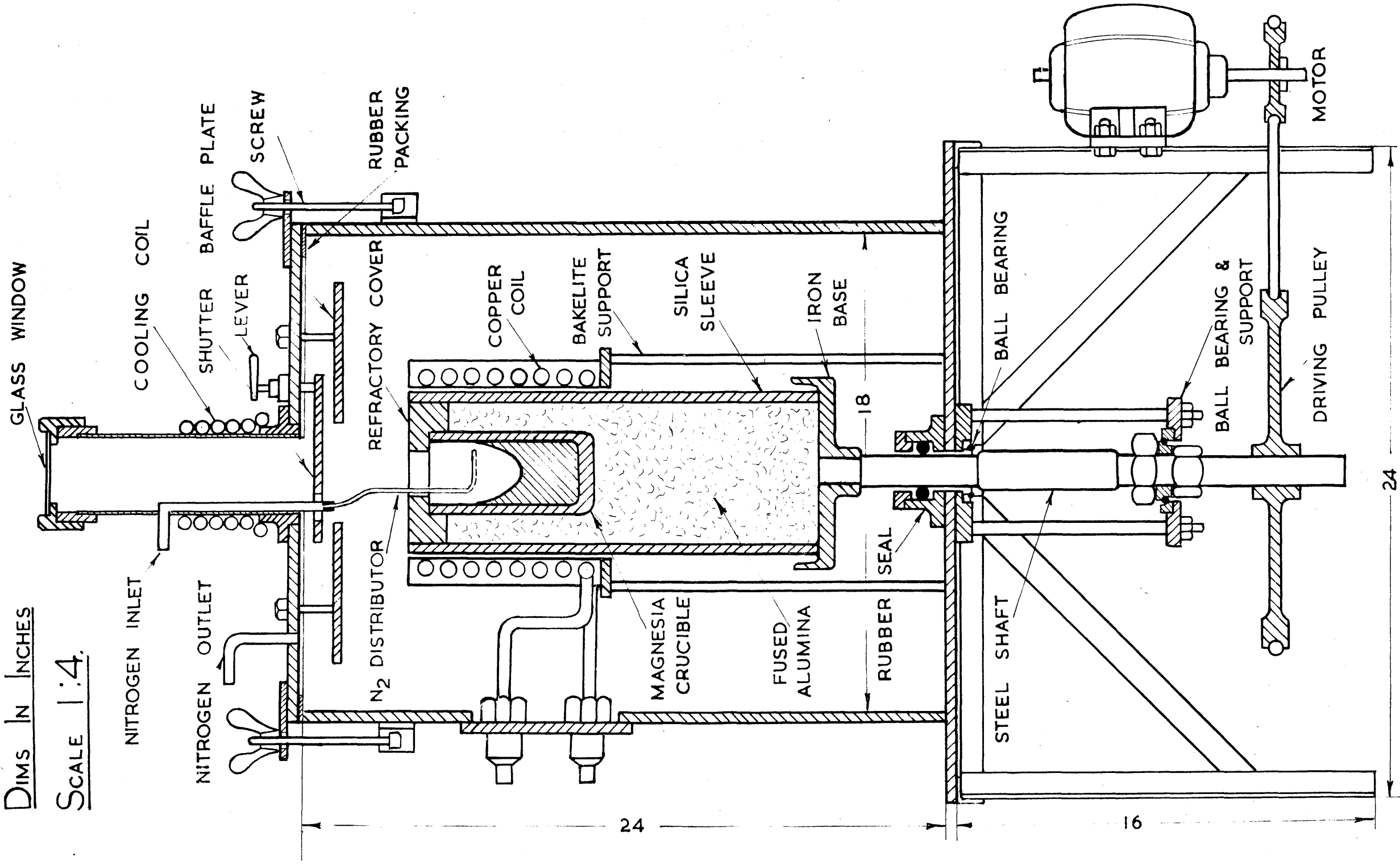
FIG.59. THE ROTATING CRUCIBLE FURNACE

and the second deoxidation with manganese-silicon mixtures [94].
In both cases a rotating crucible furnace was used for the slag-
metal reactions.

Apparatus:

Fig.59, is a detailed drawing of the furnace used in this
investigation.   In many respects it is similar to that of Taylor
and Chipman [76] which is a modification of those developed by Barrett
Holbrook and Wood [95].

The furnace consists of a rotating steel shaft supported
on ball bearings and carrying an iron base on which a silica sleeve
is cemented .   A magnesia crucible is placed centrally inside the
silica sleeve and insulated from it with fused alumina.   The
crucible should be well placed in the field of the induction coil to
get the maximum efficiency from the high frequency generator.   The
set used was a Philips type F45/3 with a maximum power input of 20
Kilo-Watts and operating frequency of 400 Kilo-Cycles per second.
The generator was a valve driven one, with one spare oscillator
valve and two spare rectifying valves fitted to provide for rapid
resumption of work when any valve reaches the end of its life.

The rotating sleeve and crucible were enclosed in a refract:
:ory box 16" x 16" x 24" made of "Syndanio"(asbestos) board to control
the atmosphere.   This was made gas tight by fitting a rubber "Gaco"
seal round the rotating shaft at the bottom while the furnace top
was provided with a narrow strip of rubber along the edges and
pressed on the box walls by 12 screws, three on each side.   A
baffle/

baffle plate was fitted to the furnace top to protect it from the heat coming off the crucible whilst the shutter protects the glass window. The shutter could be moved from its central position by operating the lever, to allow for metal and slag additions, sampling, temperature measurement and observation of the melt.

A nitrogen atmosphere was effectively maintained over the melt by a circular copper distributor tube kept inside the crucible where the nitrogen flows from a number of holes drilled on the circular main.

The crucible was rotated by means of a D.C. motor, connect: :ed in series with a resistance, at any rate between 180 and 600 r.p.m.

Experimental Procedure:

In all melts the metallic charge consisted of 800-1000 gms of Armco iron containing 0.02 per cent carbon, 0.03 per cent manganese and traces of silicon. Manganese and silicon addit: :ions consisted of either pure manganese metal electrolytically prepared (99.9 per cent Mn) and the purest available silicon (98 per cent Si , 0.76 per cent Mn, 0.8 per cent Fe, with traces of Al, Ca and Ti) or manganese-silicon alloys prepared from these components. Three alloys were prepared in which the Mn : Si ratios were approximately 3 : 1, 4 : 1 and 5 : 1. Slag additions consisted of the purest available silica sand, oxides of iron such as FeO and Fe_2O_3 and oxides of manganese such as MnO and MnO_2. In contact with molten iron, higher oxides are largely converted to FeO and MnO.

In the early experiments, the metallic and slag mixtures were charged in the crucible, the furnace top put in place and tightened with the screws. The furnace was flushed first with a heavy stream of nitrogen for half an hour; the power was then switched on and the temperature slowly raised so that melting took place in 3 - 4 hours. This technique was adopted to avoid undue thermal shock on the crucible. When melting started the crucible was rotated.

It was noticed that the iron manganese silicate slags would not remain in the bottom of the rotating cup but crept up its walls towards the rim leaving the bulk of the metal uncovered. Thus prevention of attack of the crucible by the slag was not attained.

Hilty and Crafts[94] in an attempt to secure a check on the value of K_{Mn} published recently by Chipman, Gero and Winkler[92] found that manganese oxide/slags were of the same nature as those described above. They crept up the walls of the rotating cru:cible towards the rim where they could not be sampled. They made an effort to keep some slag on the surface of the cup by increasing the slag volume but the slag volume necessary was so large that the slag became chilled on the top surface and could not be considered representative of true equilibrium conditions. The results they obtained with high slag volumes were discarded and the attempt to determine the equilibrium constant K_{Mn} was abandoned.

The work of Hilty and Crafts[93] on deoxidation with aluminium/
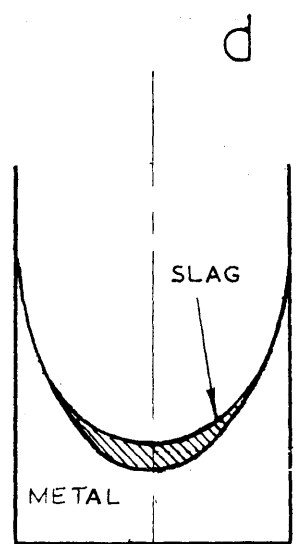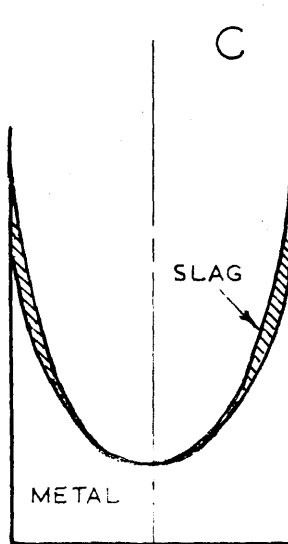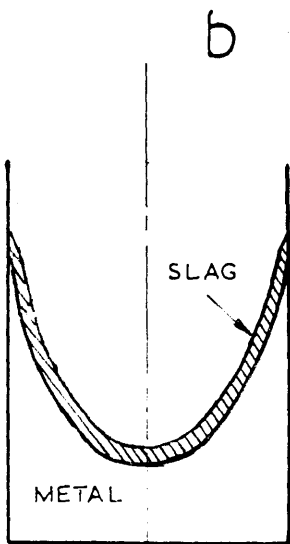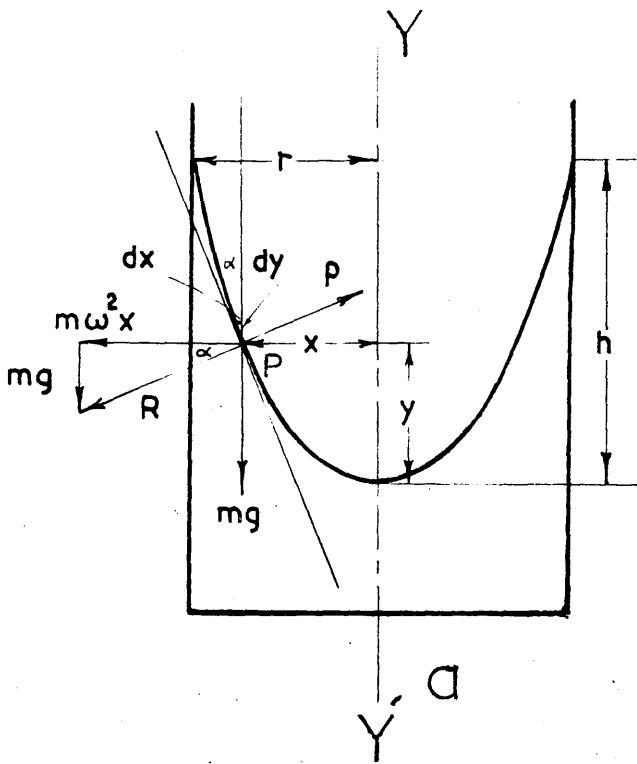
FIG. 60.

aluminium also indicated that slag sampling in the rotating furi:
:nace was not very successful and that very few slags samples
were of sufficient size or sufficiently free from contamination
with finely divided particles of metal to warrant chemical anal:
:ysis.

To explain this behaviour of slags in the rotating crucible
furnace, the theory of the furnace was examined more closely.

Theory of the Rotating Furnace:

Suppose we have a cylinder of radius r containing a liquid
and revolving about its axis Y - Y with an angular velocity ω
(Fig.60a). Consider the equilibrium of the point P on the free surface
of the liquid and let mg be the weight of a very small portion
of the liquid at P.   The forces acting on the liquid at P are:

(1)   The weight mg acting vertically downwards.

(2)   The centrifugal force acting horizontally $m\omega^2 x$.

(3)   The fluid pressure p which must be perpendicular to
the free surface of the fluid and which must balance
the resultant R of mg and $m\omega^2 x$

$$\tan \alpha = \frac{mg}{m\omega^2 x} = \frac{g}{\omega^2 x}$$

$$\tan \alpha = \frac{dx}{dy}$$

$$\frac{dx}{dy} = \frac{g}{\omega^2 x}$$

$$\omega^2 x \, dx = g \, dy$$

$$\int \omega^2 x \, dx = \int g \, dy$$

$$\frac{\omega^2 x^2}{2} = gy + c$$

when/

when $x = 0$, $y = 0$ $c = 0$

therefore $\frac{\omega^2 x^2}{2} = gy$ and $y = \frac{\omega^2 x^2}{2g}$

This is the equation of a perabola. If h is the height of the cup the radius r of the cylinder

$$h = \frac{\omega^2 r^2}{2g} = \frac{v^2}{2g}$$

This means that the height of the cup is independent of the density.

In deriving the above expression no account was taken of the other operating factors such as surface tension and contact angles. If we have two immiscible liquids rotating in a cylin: :der, a third factor will be operating, viz:- the interfacial tension between the two liquids. Neglecting all these factors we get the ideal case where the two liquids form two paraboloids of revolution which are displaced along the axis of rotation as shown in Fig.60b and the slag will still touch the crucible walls.

The rotating crucible furnace would be expected to fail in its function of preventing slag-crucible contact if the metal does not wet the crucible, i.e., has a high contact angle against the crucible, while the slag has a low contact angle against the metal and low interfacial tension which will result in the spreading of the slag over the metal and the subsequent contact with the crucible walls. Such conditions will be aggravated if the slag has a low contact angle against the crucible as shown in Fig.60c.

Thus for the rotating crucible furnace to work, the metal should/

should wet the crucible, i.e., have a low contact angle against
the crucible while the slag should have a high contact angle
against the metal and high interfacial tension.   These two
factors will prevent the slag from spreading over the metal.
Instead it will keep down in the rotating cup as shown in Fig.
60d.   Such conditions will also be favoured by a low slag
volume.

     This explains in a qualitative way the failure of the
rotating furnace in the case of certain slags and indicates that
it will only be successful when the metal has a low contact
angle against the crucible (wets the crucible) while the slag
has a high contact angle against the metal (does not wet the
metal).   A high interfacial tension should also exist between
the metal and the slag.

     An effort was made to keep the slag down by applying
a strong jet of nitrogen directed on the slag which collects
around the upper rim of the rotating metallic cup.   This was not
successful and the experimental procedure was modified as follows.

     The metal was first melted and then the crucible rotated
for half an hour to close the pores of the crucible around the
slag line with iron oxide.   The latter may have come from the
metal via partition, or may have resulted by reaction of the metal
with MgO to form FeO and magnesium.   This procedure appeared to
slow down subsequent slag attack.   The rotation was then stopped
and slag and metal additions were made when the metal regained
its horizontal level. ·   The additions were introduced through
a/
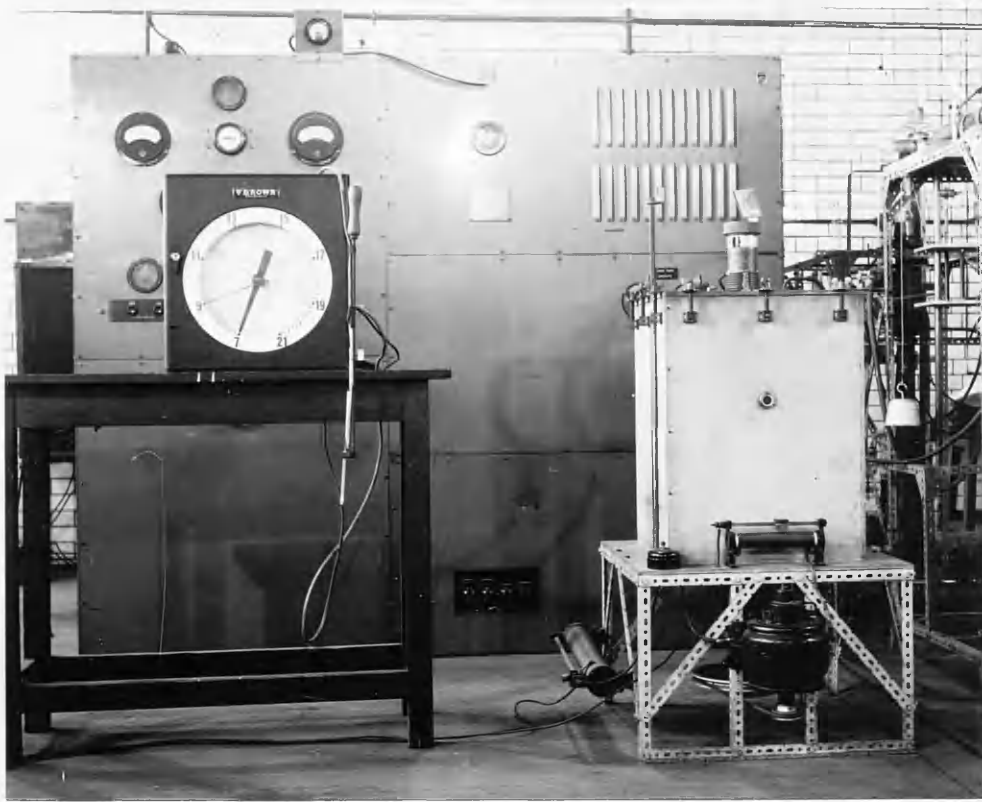
Fig. 61- The Rotating Crucible Furnace and the Honeywell- Brown
Electronic Temperature Recorder.

Fig. 62.

a refractory tube passing from the top right down to the crucible.
Before removing the glass window to introduce the tube, it was
found necessary to increase the nitrogen stream to maintain enough
positive pressure inside the furnace to prevent any inward diffus:
:ion of air which might upset the equilibrium between the slag and
the metal. When the slag was completely molten, the temperature
was kept steady for half an hour which, according to Korber and
Oelsen [78][90] and Winkler and Chipman [96] is quite sufficient to
establish equilibrium between metal and slag.

Temperature Measurement.

The temperature was measured by the immersion method using
a platinum-platinum 13 per cent rhodium thermocouple protected
with a silica sheath.

The temperature was automatically recorded by a Honeywell-
Brown Electronic temperature recorder. A photograph of the
rotating crucible furnace and the Honeywell-Brown Electronic
recorded is shown in Fig.61.

Sampling:

Slag samples obtained by dipping an iron rod into the slag
were invariably contaminated with metal especially when the slag
layer was very thin. Consequently the charge was allowed to
solidify inside the crucible and samples were taken from the solid
metal and slag. It was found when operating at comparatively
low temperatures (in the region of $1550^{\circ}C$) that the melt was
completely solidified within 10-15 seconds after switching off
the /

the power.   The crucible was taken out of the furnace when it was cold enough for handling.   A slag layer of thickness vary::ing between 3 and 5 millimeters was easily separated from the ingot and analysed for FeO, MnO, SiO_2 and MgO.   The metallic ingot was then cut diametrically into two halves.   From roughly corresponding portions of these two halves, samples were taken for

(a) vacuum fusion analysis for total oxygen.

(b) chemical analysis for manganese and silicon.

No significant change in the equilibrium conditions would be expected on cooling with such a high rate of cooling .   This is supported by the results given in Chapter IX where melt No.8 is mainly under an FeO-MnO slag, the silica content of the slag being only 1.69 per cent.   The value of K_{Mn} calculated for this melt equals 3.12 at 1550°C which is a reasonable average between 2.5 as given by Korber and Oelsen[90] and 3.77 as determined recently by Chipman, Gero and Winkler[92] .   This value of 3.12 may be slightly high as if any reaction did occur during cooling, the "equilibrium" would correspond to a lower temperature than 1550°C, and it is known that K_{Mn} falls with rise of temperature.

This method of sampling is not so reliable for melts made at temperatures far removed from the melting point of iron as changes in composition of slag and metal during cooling might be more serious and would result in too high values for K_{Mn}. The majority of the melts in this investigation were carried out at 1550°C.

In /

In the author's opinion this method for sampling at 1550°C
and under a high rate of cooling is superior to that of Taylor
and Chipman [76] (suction of molton metal into a copper mould) in
which there is the possibility of mechanical entrapment of slag
particles in the metal sample during suction. There is also the
possibility of oxidation of the hot metal by the air present in
the sampler, although this may be avoided by sweeping out the
sampler with nitrogen. The latter reason might explain why the
results of Hilty and Crafts [93] on aluminium deoxidation using
the Taylor sampler show oxygen concentrations in the liquid iron
about three times greater than the values of Wentrup and Hieber [97]
and 10-20 times the value calculated from thermodynamic data.

Crucibles:

In the early experiments the crucible was made within
the silica sleeve by firing a graphite former held centrally and
resting on magnesia powder (-60 +150 mesh) in the silica sleeve.
Further magnesia was added to fill in the space between the silica
sleeve and the former; this was then thoroughly tamped down.
The graphite former was then fired to 2000°C for 10 minutes and
then immediately lifted from the magnesia. It was thought that
the crucible so formed could be used directly without being
disturbed from the silica sleeve but it was noticed that the hard
sintered body of the crucible was surrounded with a lightly
sintered layer containing a considerable amount of carbon (Fig.62)
and the crucible had to be removed from the silica sleeve, the
carbon scraped off and the crucible fired again to burn the
carbon /

carbon in case it might diffuse through the crucible and contam:
:inate the iron.

The same **phenomenon** was reported recently by Dancy [98]
who explained the carbon deposition by the fact that magnesia
is reduced by carbon at above 1890°C as calculated from the data
of Richardson and Jeffes [46] . The magnesium and carbon monoxide
formed both from this rea**ct**ion and from the atmospheric oxidation
of the heated graphite diffuse through the surrounding magnesia
until a zone of about 1890°C is reached. Below this temperat:
:ure carbon monoxide is reduced by magnesium vapour to give
magnesia and deposits carbon.

It was noticed in the present investigation that carbon
deposition will take place at temperatures as low as 1400°C
which suggests that there may be no need to reduce magnesia to
cause the deposition but that it may be due to magnesia acting
as a cat**a**lyst for carbon deposition in the reaction

$$2 \; CO \; \rightleftharpoons \; C + CO_2$$
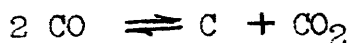
The magnesia crucibles used were finally moulded in the
following manner. A ver small amount of water glass solution
was added to fused magnesia powder. Some of the magnesia paste
was then put in the mould to form the bottom layer of the crucible
and a wooden f**o**rmer held centrally over this layer of magnesia
inside the mould. More magnesia was pressed into the space
between the former and the mould and finally the former was
withdrawn leaving the crucible to dry slowly over two days.
The crucible was then taken out of the mould and fired at
about/

about 1500°C.   The firing schedule took about 10 hours.

The crucibles so produced were found to have a good resistance to thermal shock, although there was an appreciable amount of magnesia pick up by slag as will be shown in Chapter IX.

Approximately 25 runs were made but only 9 of these were successful.   The remainder failed mainly due to the creeping of the slag towards the rim of the cup of metal formed by rotation and its absorption by the crucible material.   A few failed due to a breakdown in the crucible during the conduction of the experiment.   Table 15 gives details of the slag and metal charges of the 9 successful runs.

Table 15.

Run No.	Metal Charge (gms).					Slag Additions (gms).				
	Armco Iron.	Mn.	Si.	Mn-Si alloy. Wt.	ratio.	SiO_2	Fe_2O_3	MnO	Mn_2O_3	MnO_2
1	800	10	5	–	–	15	30	–	–	30
2	700	–	5	10	3:1	20	30	–	10	–
3	1050	–	–	15	5:1	30	25	–	65	–
4	1000	–	–	12	3:1	50	–	15	70	–
5	1040	6	–	10	4:1	60	–	20	70	–
6	1000	–	–	–	–	30	90	–	–	–
7	840	–	–	10	3:1	30	60	–	100	–
8	740	8	2	–	–	–	80	–	40	–
9	870	–	3	10	4:1	85	10	15	60	–

Chemical Analysis of Metal and Slag:
a - Slag Analysis.

The slags, which were soluble in HCl, were ground finely in an agate mortar and analysed for MnO, FeO, SiO_2 and MgO, as follows:-

MnO/

MnO: This was determined by the sodium bismuthate method.

FeO: The total iron content of the slag was determined by the usual titration with dichromate using diphenylamine as an indicator. The value so obtained was converted to FeO.

SiO$_2$: This was determined in the usual way by dehydration of silicic acid to insoluble silica from the hydrochloric acid solution. The residue was ignited and treated with hydrofluoric acid in a platinum dish to obtain the content of silica.

MgO: This was determined, after the removal of silica, iron and manganese, by precipitation as Mg NH4 PO4 and ignition to Mg$_2$ P$_2$O$_7$ at 1000°C according to the method described by Smith[99].

b - Metal Analysis:

Manganese, silicon and oxygen were determined in all metal samples.

Manganese was determined by the bismuthate method.

Silicon in the metal was converted to SiO$_2$ using the standard method of analysis.

Oxygen was determined by the vacuum fusion method as described in Chapter VIII.

CHAPTER VIII.

The Determination of Oxygen.

The methods employed for the determination of oxides and oxygen in ferrous materials may be divided into two groups.

    (a)   Residue Methods.
    (b)   Reduction Methods.

Residue Methods:

In principle, these methods depend on attacking the metal with some reagents which dissolves the iron and the alloying ele: :ments, but does not attack the non metallic inclusions. The best known methods are:

    1.   The nitric acid method.

    2.   The hydrochloric acid method.

    3.   The electrolytic method.

    4.   The chlorine method.

    5.   The alcoholic iodine method.

The iodine method seems to be the most promising of the residue methods. The application of this method is limited by the insol: :ubility of certain of the alloying elements or their compounds. Iron and manganese carbides are decomposed by iodine, but Cr, V and W carbides are more or less insoluble.

Sulphides may be attacked by the iodine solution to some extent but they are not completely dissolved. Difficulties have been reported in dealing with aluminium killed steels and some to which aluminium has been added, mainly the medium and high carbon type./

type.   The difficulty is due to the retention of undecomposed
aluminium carbide or nitride in the oxide residue thus giving
high results.

The iodine method gives low results for rimming steels.
This might be due to the fact that MnO and FeO in the steel are
not combined with SiO_2 and thus more readily attacked by the iodine
solution.

In the chlorine method, some attack of the silica and oxides
of iron and aluminium occurs.

In all these methods, subsequent analysis of the insoluble
residue permits the determination of the individual oxides present
such as FeO, MnO, SiO_2 and Al_2O_3 and the calculation of the oxygen
content of the steel.

Reduction Methods:

These methods depend upon the reducing action of carbon or
hydrogen at elevated temperatures on the oxygen containing con:
(100)
:stituents.   With the exception of the development by Reeve
of the fractional vacuum fusion method, by which the distribution
of oxygen in a steel among the various oxides FeO, MnO, SiO_2 and
Al_2O_3 can be determined, the reduction methods do not attempt to
identify the individual oxides and compounds but yield only the
total oxygen content of the steel.   This group includes:

1.   The hydrogen reduction method which depends upon the
     reduction of oxides in the sample by means of purified
     hydrogen at elevated temperatures.   The amount of water
     vapour/

vapour in the hydrogen leaving the furnace indicates the amount of oxides reduced.   It is generally believed that FeO and MnO are completely reduced under these conditions.   This method is not very reliable for steels deoxidised with silicon and aluminium.

2.   The vacuum fusion method.

3.   The fractional vacuum fusion method.

Vacuum Fusion Method:

Principle: The method depends fundamentally on the affinity of carbon for oxygen and its ability to decompose oxides at high temperatures with the formation of carbon monoxide accord: :ing to the following equations.

$$FeO + C \rightleftharpoons Fe + CO$$

$$MnO + C \rightleftharpoons Mn + CO$$

$$Al_2O_3 + 3C \rightleftharpoons 2Al + 3CO$$

$$SiO_2 + 2C \rightleftharpoons Si + 2CO$$
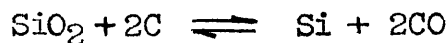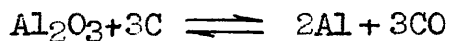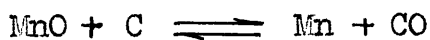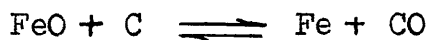
If total reduction is required it is necessary to carry out the determination at high temperatures and also to remove the gaseous products of the reaction (mainly carbon monoxide) as rapidly and completely as possible.

The oxide most difficult to reduce is Al_2O_3, the standard free energy change for the reaction:

$$Al_2O_3 + 3C \rightleftharpoons 2Al + 3CO$$
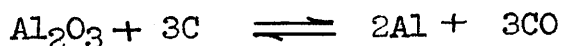
being given by

$$\Delta G^o = +306,200 \quad -129.30 \, T$$

Hence/

Hence for 1550° C, $K = p^3CO = 3.126 \times 10^{-9}$ corresponding to an equilibrium pressure of CO of 1.11 mm Hg.

In the actual reduction, the aluminium is not produced as the pure metal but as a very dilute solution of aluminium in molten iron in which its activity would be much less than unity. The numerical value of the activity would depend on the relative amounts of alumina originally present, and iron and no figure can be assigned to it. The effect of this dilution would be to increase very considerably the equilibrium pressure of carbon monoxide.

Since the working pressure in the furnace tube is of the order of 1×10^{-5} mm Hg, the reaction should go to completion and the accuracy of the method depends on the efficiency of the pumping system in transferring the gaseous products to the gas collecting side of the apparatus.

The introduction of the modern vacuum fusion method for the determination of oxygen, hydrogen and nitrogen is usually ascribed to Oberhoffer and his co-workers [101]. Although early workers used resistance heaters, high frequency induction heat: :ing, first introduced by Jordan and Eckman [102] is now univer: :sally employed.

Thompson, Vacher and Bright [113] in their report on the co-operative study of the methods used for the determination of oxygen in steels recorded the results obtained by the vacuum fusion apparatus of 25 laboratories comprising more than 2000 analytical determinations on 8 different steels. The results showed/

showed that the vacuum fusion method yields accurate results for the oxygen content of plain carbon steels, either aluminium-killed, silicon killed or of the rimming type.   The iodine method, according to their report, yields accurate results for some types of killed steels and low results for other steels. Sloman (104)(105)(106)(107) of the National Physical Labor: :atories, has given a fairly comprehensive description of the vacuum fusion method.

It is of interest to review the difficulties and the different sources of error encountered by previous investigators when using vacuum fusion apparatus.   These were avoided as much as practicable in building our unit.

1. <u>The Blank</u>:   One of the major considerations in the operation of the apparatus is that its blank at the operating temperatures should be as low as possible.   To get a low blank it is desirable to have:

a. The apparatus vacuum tight.
b. High degassing temperature.
c. High purity graphite for crucible making and insulation.   The graphite should be chosen according to the ash content which should be as small as possible (less than 0.1 per cent).
d. All the mercury used should be redistilled for high vacuum work.

The average blank of the apparatus was found to be of the order of 0.2 ml/hr containing 33% CO.   This may be compared with the rate of gas (mainly CO) evolution obtained during a determination, which varied from approximately 3 - 20 ml. per hour.

A /

A blank determination was carried out every time the apparatus was assembled.

2. Interference due to Manganese.

The presence of 0.5 per cent or more manganese in a steel to be analysed constitutes a potential source of error in the apparatus, either as a result of the presence of manganese vapour in the furnace chamber or its subsequent condensation on the furnace walls. This manganese film absorbs some of the gases evolved leading to low recoveries of oxygen. To avoid manganese interference it is essential to have:

a. Rapid melting. This is accomplished by high frequency heating.

b. Complete removal of the evolved gases from the reduction chamber before any appreciable manganese vapour is formed. This depends very largely on the efficiency of the pumping system and the proper choice of a diffusion pump with the highest possible backing pressure.

c. When dealing with steel of high manganese content, it is advisable to use fresh crucibles for each determination or to resort to dilution of the samples with manganese free iron.

d. Frequent cleaning of the furnace chamber.

e. It has also been found by Thanheiser and Brauns (108) that recoveries of oxygen were poorer when the furnace tube was water jacketed than when it was less drastically cooled by means of a copper coil.

3. Spattering:

This is probably one of the principle causes of erratic results. It was found that steels with large oxygen contents have the greatest tendency to spatter. This may result in

either/
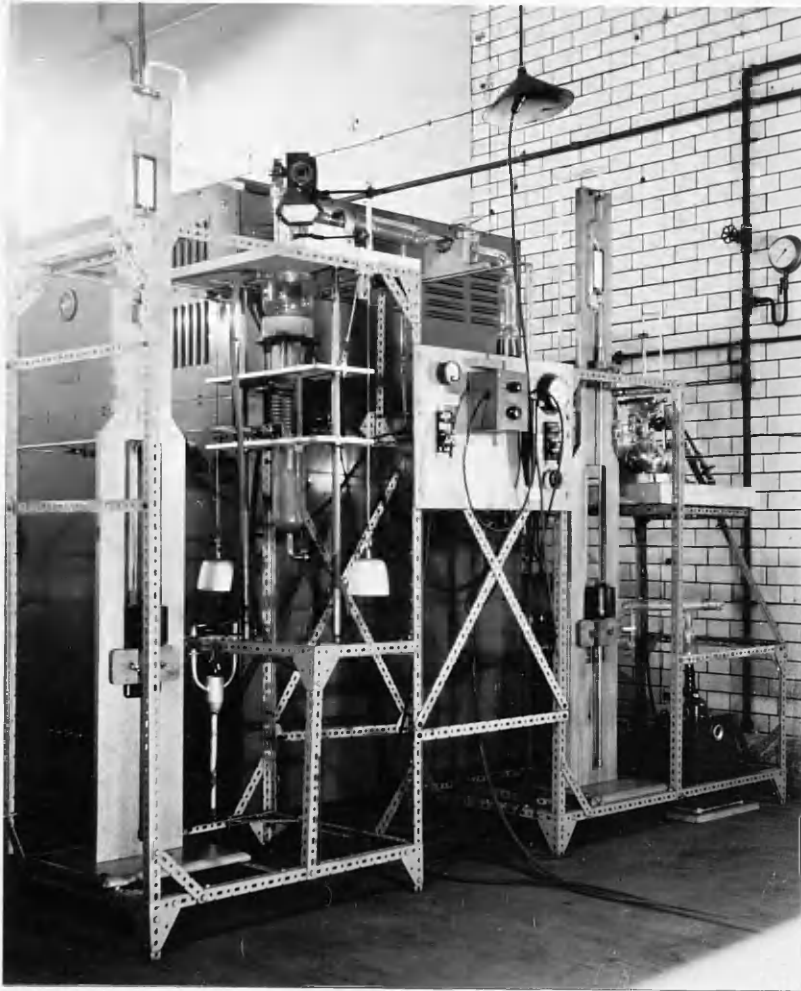
Fig. 63 _ The Vacuum Fusion Furnace.

either high or low values for oxygen. If the spattered globules
of molten metal come in contact with the silica furnace tube,
reaction between the molten metal (containing carbon dissolved
from the crucible) and silica might result in the formation of
carbon monoxide giving high values for oxygen. On the other
hand if the portion thrown out from the crucible solidifies before
falling on the furnace tube the oxygen of that portion of the
sample is lost unless it falls back in the crucible. To prevent
spattering the crucible should be closed once the sample has been
dropped in and allowance only made for gases to pass.

4. The Size of Inclusions:

Thompson and Holm [(109)] reported difficulty with certain
samples containing Al_2O_3 particles of greater size than the normal
particularly when the melt contained high percentages of mangan:
:ese or other "volatile" metals. The particles floated to the
top of the vacuum fusion melt where their reduction took place
too slowly to be complete. Similar difficulty was also
encountered when large, globular SiO_2 inclusions were present.
Certain steels fall into a borderline class with respect to
inclusion size. These steels give accurate results by the
total vacuum fusion method but give low results by fractional
vacuum fusion, the reason being that in the latter method, the
melt is held for a rather long time at $1060 - 1320^{\circ}C$, during
which the more refractory oxides such as Al_2O_3 and SiO_2 float
to the top of the melt and agglomerate forming masses difficult
to reduce.

SIDE ARM F SIDE ARM E TAP I

TOEPLER PUMP R

SIDE ARM C

TRANSPARENT
SILICA TUBE B

2

ELECTRO
MAGNET

TRANSLUCENT
SILICA TUBE A

7

3

Hg DIFFUSION
PUMP

INDUCTION
COIL

4

Hg

PYREX GLASS
WATER JACKET

BURETTE

5   6

SLIDING   PLATFORM

McLeod GAUGE M
0.1 — 0.00001 Mms Hg

P_2O_5 TRAP T

8

McLeod GAUGE N
10 — 0.01 Mms Hg

Drain

HYVAC MECH. OIL PUMP
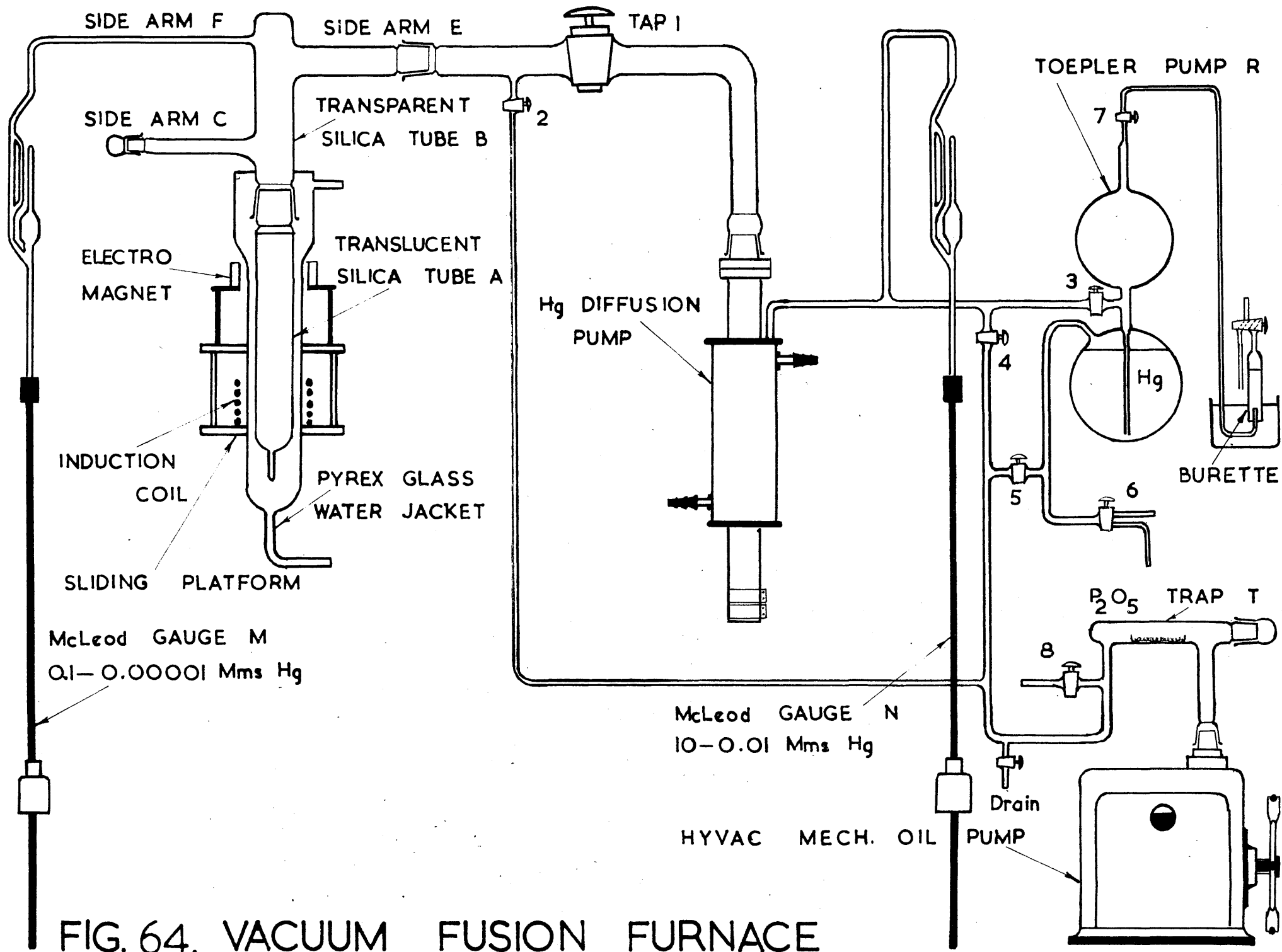
FIG. 64. VACUUM FUSION FURNACE

5. High Silicon Steel:

Sloman[107] has discussed some of the difficulties encount:
:ered in analysing high silicon steels.   Silicon being a
graphitiser causes graphite to precipitate in the melt and thus
tends to give rise to a mushy semi-solid mass in which bubbles
of gas are trapped.   In addition silicon seems to soak into
the graphite causing it to swell and crack possibly due to the
formation of silicon carbide.   Mallett[110] stated that this
condition could be avoided by dropping the samples into an empty
crucible or by analysing samples in such an order that the per
cent of silicon in the melt is never increased.

The Construction of the Apparatus:

The apparatus as shown in Fig.63 and 64 consisted mainly
of two parts:

(i)   The reduction chamber where the samples are melted and
      oxides reduced.

(ii) The gas collecting side where the gases resulting from
      the reduction are collected and transferred to the
      burette for analysis.   The two parts are separated
      by a pyrex glass stop cock No.1 (one inch bore), the
      biggest available when the apparatus was constructed.

A detailed drawing of the reduction chamber is given in
Fig.65.   The McLeod gauge which is connected to the side arm
F reads from 1×10^{-5} to 1×10^{-2} mm of Hg.

The crucible, lid and support were made of graphite.
After a crucible had been used it was not possible to remove
the metallic contentc from it.   It was, therefore, found
expedient to use a small crucible inside the main one.   Only
the/

SIDE ARM F

SIDE ARM E

TRANSPARENT
SILICA TUBE B

SIDE ARM C

STEEL SAMPLES

TRANSLUCENT
SILICA TUBE A

ELECTRO MAGNET

ADJUSTABLE BASE

GRAPHITE
CRUCIBLE

GRAPHITE
POWDER
−200 mesh

INDUCTION
COIL

SLIDING PLATFORM

PYREX GLASS
WATER JACKET

SCALE 1:5
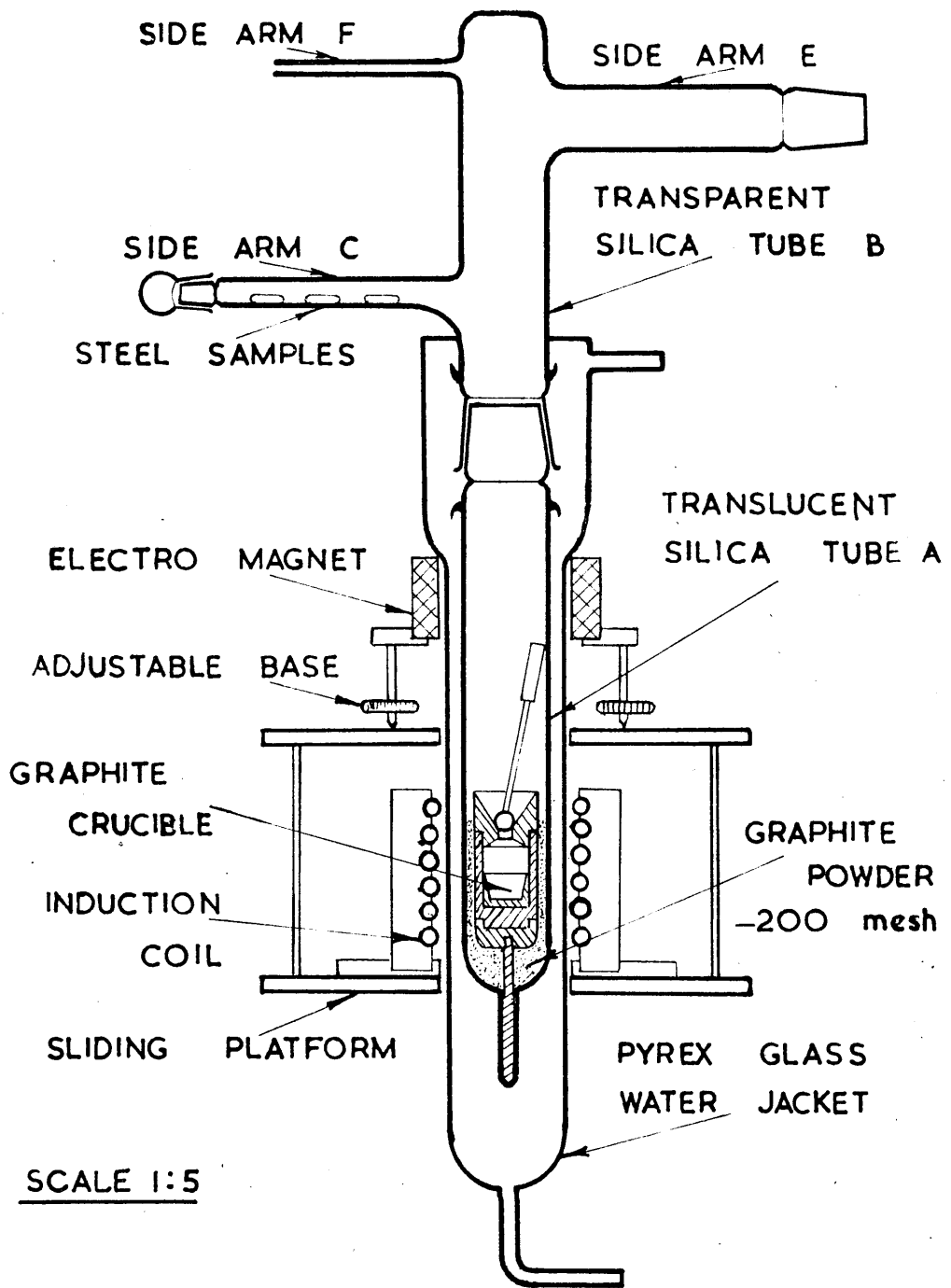
FIG. 65. THE REDUCTION

CHAMBER.

the inner crucible had to be thrown away thus effecting consid:
:erable economy since the main crucible could be used several
times.   To avoid spattering, the crucible was covered with a
graphite sphere provided with a series of shallow grooves.   A
graphite rod with a piece of soft iron tube at the top was
screwed to the sphere.   The soft iron tube enabled the sphere to
be lifted by an electromagnet before dropping the sample.   The
crucible and accessories are shown in Fig.66.

The furnace tube A was cooled externally by means of a
water jacket supported on a double deck sliding platform.   On
the lower deck was the induction coil for heating the crucible.
On the upper deck an electromagnet in the form of a horizontally
wound solenoid was supported outside the waterjacket.   The
dimensions of the magnet were obtained by the following calcula:
:tion.

$$\text{Weight to be lifted} = 30 \text{ gms.}$$

$$\text{The diameter of the magnet, } 2r = 9 \text{ cm.}$$

$$\text{For a short coil the magnetic field } H = \frac{2 \pi AT}{10r}$$

$A =$ current (amps)   and $T =$ No. of turns.

$$\text{Pull of the magnet} = \frac{H^2 \times a(\text{area})}{8\pi}$$

$$= 30 \times 981 \text{ dynes.}$$

$$30 \times 981 = \frac{H^2 \times \pi \times (4.5)^2}{8\pi}$$

$$\text{Hence} \quad H = 109$$

$$\text{and} \quad AT = \frac{H \times 10r}{2} = 780$$

i.e. /

Dims In Mms
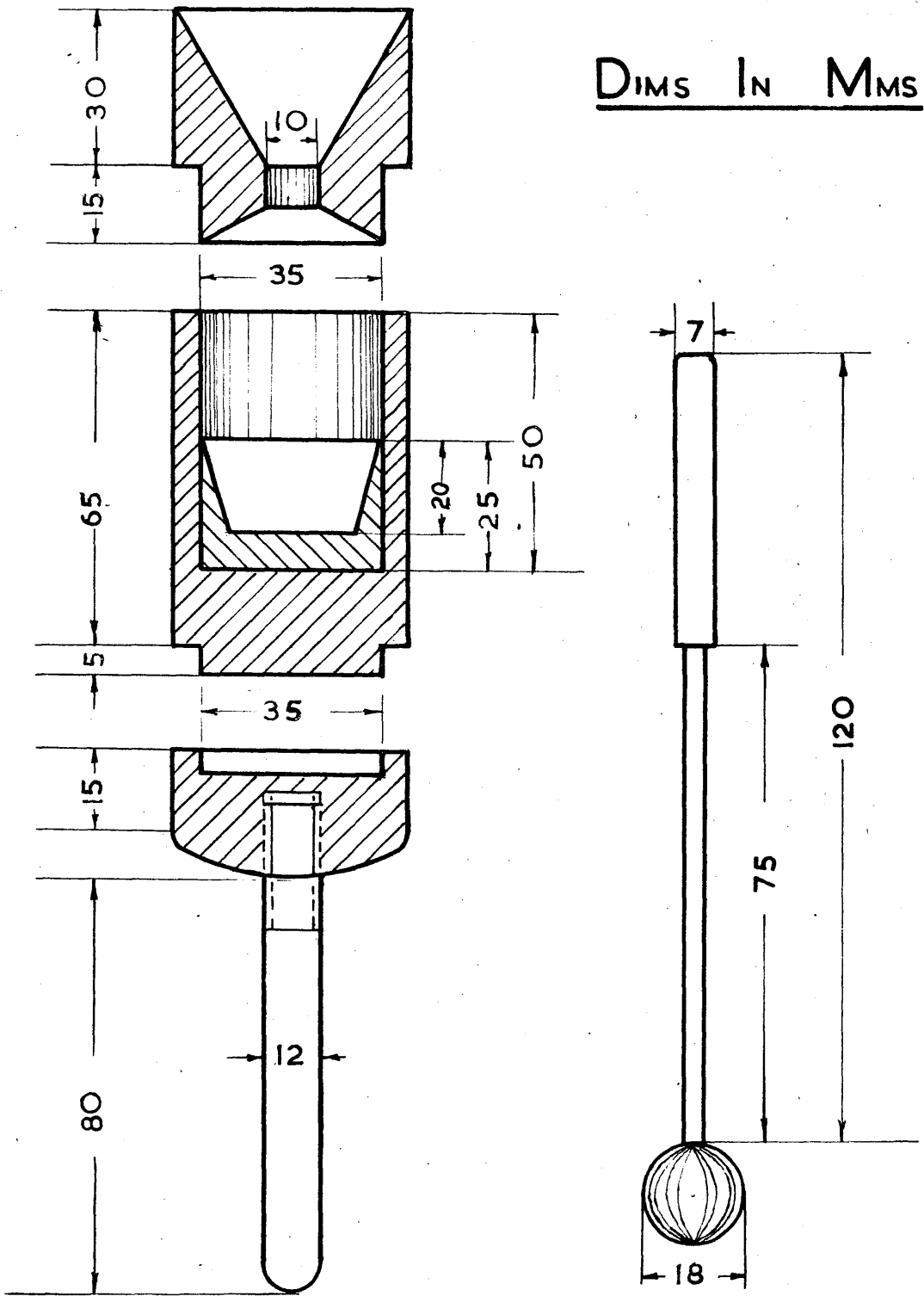
FIG.66. DETAILS OF CRUCIBLE

i.e., using a current of one amp. the minimum number of turns
= 780.   The electromagnet was made with 1000 turns of insulated
copper wire.

The gas collecting side was similar to that of Sloman (104)
except for the diffusion pump.   Sloman   used a Gaede four-stage
mercury diffusion pump which can maintain its efficiency against
backing pressures up to 40 mm Hg.   These pumps were not avail:
:able and an Edwards Two-stage mercury diffusion pump type 7 was
used, this being the only available substitute for the Gaede pump.
The highest permissible backing pressure for this pump is 4 mm Hg
                        pressure
This low backing/has caused much trouble in operating the appar:
:atus, especially with alloys of high oxygen content, when it
was found that the pump was not capable of handling the first
rush of gas after the sample had been dropped in the crucible at
1550°C., the working temperature.   This resulted in blowing
off of the crucible lid with the subsequent fall of the insulat:
:ing graphite powder inside the crucible , and the apparatus
had to be shut down and the determination abandoned.   This
difficulty was overcome by lowering the temperature of the
crucible to 700°C before dropping the sample, followed by rais:
:ing the temperature slowly to the working temperature to avoid
sudden melting of the sample, thus allowing the gas to generate
gradually.

It was also noticed that the diffusion pump stopped
pumping when the pressure on the gas collecting side (i.e., the
backing pressure) exceeded 1.5 mm Hg.   This immediately
caused/

caused a build up of pressure in the reduction chamber which could affect the progress of the reactions in the crucible. (This shows the importance of a high backing pressure for the diffusion pump). Such conditions necessitated an excessive number of operations of the Toepler pump and the degassing of one sample might take an hour. For these reasons the apparatus was standardised, using samples of known oxygen content provided by the National Physical Laboratories and the Gases and Non-Metallic Sub-Committee of the British Iron and Steel Research Association.

Operation of the Apparatus:

1. Preparation of the Samples:

These were prepared in the form of cylinders having round: :ed ends, 0.5 to 1 cm in diameter, and 1 to 2.5 cm long. They weighed from 5 to 10 grams depending on the oxygen content. Immediately after turning to shape, they were stamped for identi: :fication, cleaned in benzene and acetone, dried and weighed and finally stored in a desiccator until required. The samples were then introduced into the side arm C, which was closed by a ground glass cap.

2. The furnace tube A was assembled as shown in Fig.65, fitted to tube B by means of a ground joint, the two tubes being held together by springs. The sliding platform was raised into position carrying the water jacket, the induction coil and the electromagnet.

3. The /

3. The apparatus was evacuated by means of the mechanical pump, all taps being open except 2, 6, 7 and 8. The diffusion pump was then switched on and the crucible heated slowly up to 300°C and then fairly rapidly to 2000°C, the degassing temperature. Temperature measurement was carried out with a Foster disappear: :ing filament optical pyrometer. It was not possible to degas at temperatures higher than 2000°C. owing to the formation of a graphite film on the sides of the silica furnace tube. This was also reported by Hurst and Riley[111]. The degassing period was normally between 3 and 4 hours, its completion being indicated by steady readings on gauges M and N.

4. The temperature was then dropped to 1550°C (the work: :ing temperature) and the blank collected for an hour, with tap 4 closed and 3 open. After transferring the gas to the collect: :ing burette, tap 4 was opened to remove any gases left in the system to the atmosphere and the apparatus was ready to receive the first sample, tap 4 being closed again and 3 opened.

5. The samples were dropped by a magnet with the spherical graphite cover lifted. The crucible was covered immediately and pumping continued until the sample was completely degassed. The criterion for this was that the pressure on gauge M should fall to its value during the collection of the blank. The number of Toepler pump strokes required to transfer the gas produced by the samples varied between 3 and 15 according to the oxygen content. During degassing of the samples, the reading of gauge N should be watched, the Toepler pump being operated immediately the pressure on/
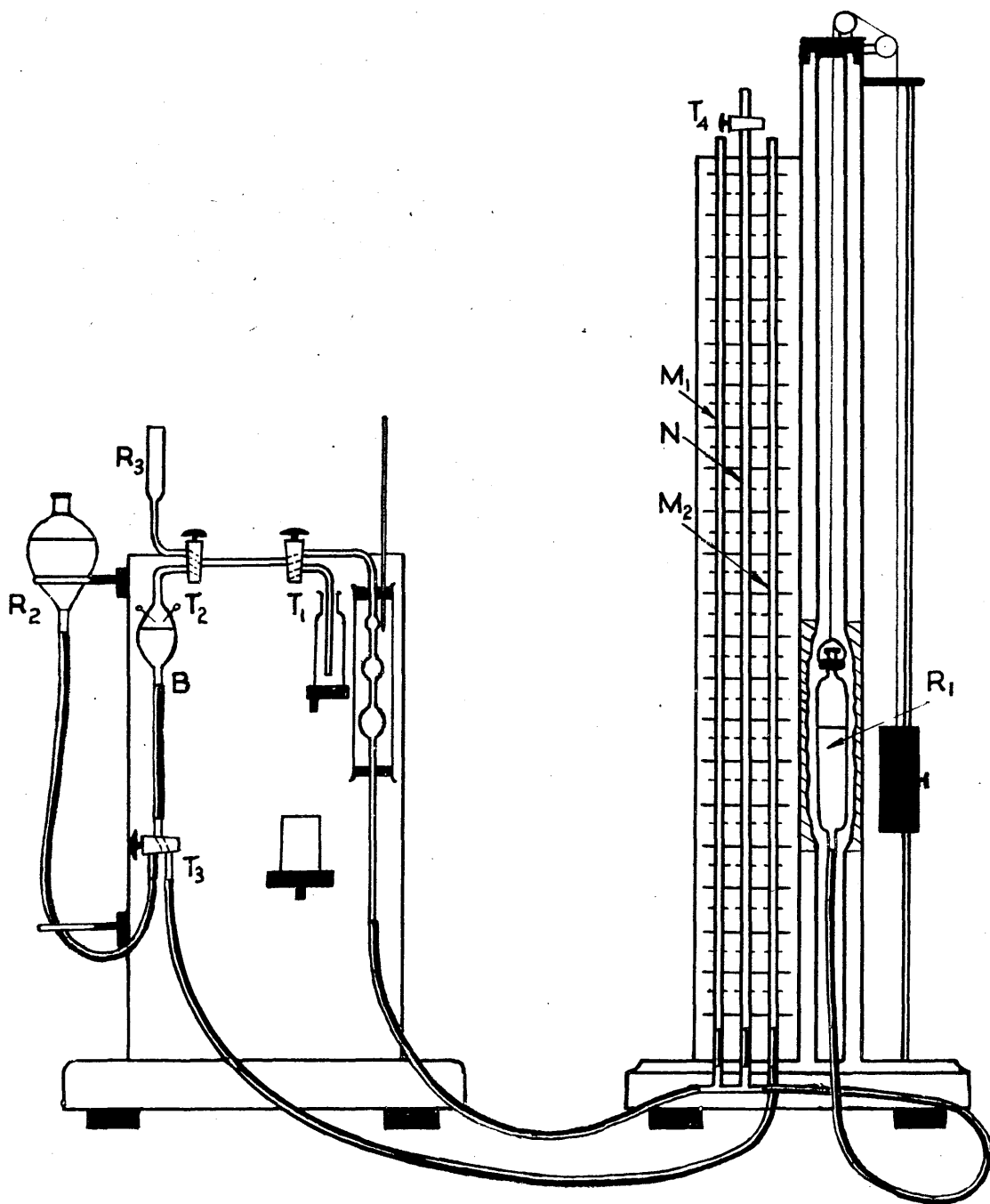
FIG. 67. GAS ANALYSIS APPARATUS

on N exceeds 1.5 mm.   After the last stroke of the Toepler pump the pressure of gauge N was recorded and used to calculate the amount of gas left in the system external to the Toepler pump.

6.   When all the samples had been reduced, tap 1 was closed, the furnace tube was allowed to cool down and the diffusion pump was switched off.   Taps 3, 4 and 5 were closed, the mechanical pump switched off and tap 8 immediately opened, otherwise the oil from the pump would fill the system.   The gas collecting side should always be kept under vacuum. ' Air was admitted to the reduction chamber only through tap 2.   The furnace tube was then dismantled, emptied, cleaned and the graphite powder sieved as it tended to coalesce.   The whole was then ready for re-assembly with a new inner crucible.

Gas Analysis:

(112)

The gas was analysed for CO_2, O_2 and CO using Ambler's gas analysis apparatus shown in Fig.67.   This is capable of handling gas samples between 1 and 15 m.l.

CO_2 was absorbed by 33% KOH, and oxygen by an alkaline pyrogallol solution prepared by mixing 40 per cent KOH solution with 25 per cent aqueous pyrogallol solution in the ratio of 4 : 1.

Ammoniacal cuprous chloride solution was used for absorbing CO.   This was prepared by adding 75 gms of white cuprous chloride to a solution of 15 gm NH_4Cl in 80 m.l. of

water/

water and then adding sufficient concentrated ammonia until solution was completed. The solution was stored in a stoppered bottle in contact with metallic copper.

Calculation of the volume external to the Toepler pump:

Consider the amount of gas occupying the volume external to the Toepler pump, comprising the space between the taps 3 and 4 and the 2nd stage of the diffusion pump and including the volume of the gas in gauge N. Let this volume be V and the pressure on gauge N be P_1. If the Toepler pump has been "evacuated", when tap 3 is opened the pressure on gauge N will drop to P_2 and then according to Boyle's law we have

$$VP_1 = P_2 (V + 700)$$

700 is the volume of the Toepler pump in m.l. An actual test gave the figures.

$$P_1 = 0.9 \text{ mm}$$

$$P_2 = 0.2 \text{ mm}$$

Hence $\quad V = 200 \text{ m.l.}$

Table 16.

Sample No.	Supplied by	Oxygen content.		y/x
		Actual Analy.(x)	Present Result(y)	
9273-2P	N.P.L.	0.012	0.0090	.75
			0.0093	.775
			0.0091	.76
1753-MB	N.P.L.	0.020	0.0140	.7
			0.0141	.705
8652-4	B.I.S.R.A.	0.0145	0.0098	.68
784-4	B.I.S.R.A.	0.0105	0.0076	.72

The/

The results obtained with the standard samples mentioned
earlier are shown in Table 16.   They show good reproducibility
although the oxygen values are appreciably lower than the actual
values.   The results show that the values obtained by our
apparatus are about 0.73 times the actual values.   This
empirical factor was used to correct the oxygen contents in the
actual slag-metal experiments.

The low results obtained are probably due to the ineffic:
:iency of our pumping system.

Example of actual determination.

Oxygen determination in Run No.5.

Weight of sample.	=	7.9627 gms.
Time required for degassing sample.	=	30 mins
Reading on gauge N after last stroke of Toepler Pump.	=	0.2 mm.Hg.
Volume of blank.	=	0.24 ml/hr.
Percentage CO. in the blank.	=	32 per cent.
Volume of gas obtained from sample.	=	8.2 m.l.
Percentage oxygen in gas.	=	0 per cent.
Percentage CO_2 " "	=	0 " "
Percentage CO * "	=	76 .* "
Volume of gas at 1 atm. pressure external to Toepler Pump.	=	V

where $200 \times 0.2 = V \times 760$

$$\therefore V \qquad = \qquad 0.057 \ m.l.$$

Corrected volume of gas.	=	8.26 "

CO /

CO in gas	8.26×0.76	$=$	6.28 m.l.
CO in blank	$\frac{1}{2} \times 0.24 \times 0.32$	$=$	0.038 "
CO from sample.		$=$	6.24 "
1 m.l. CO		$=$	0.000715 gms.O_2
O_2 in sample	0.000715×6.24	$=$	0.00446 gms.
Percentage O_2	$\frac{0.00446}{7.9627} \times 100$	$=$	0.056 per cent.
Corrected value	$\frac{0.056}{0.73}$	$=$	0.077 per cent.
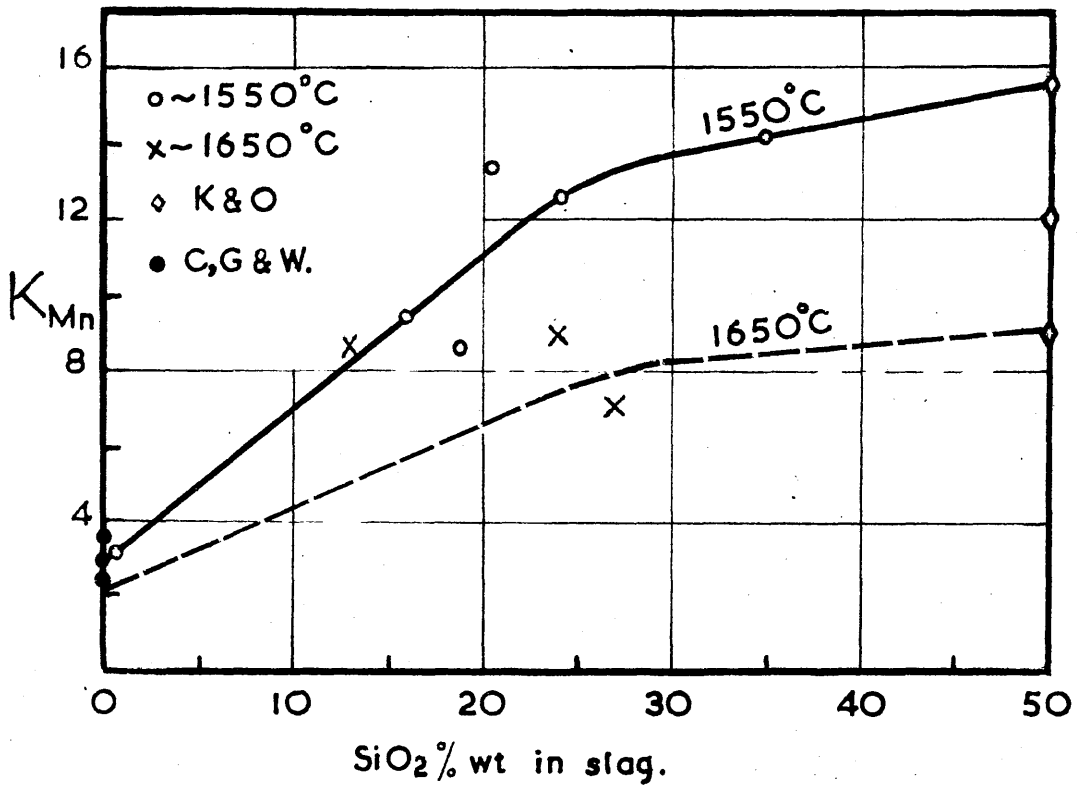
FIG. 68

CHAPTER IX.

Results and Discussions.

The experimental results obtained from the slag-metal experiments are given in Table 17.

Table 17.

Run No.	Temp. °C.	Steel Analy.			Slag Analysis, wt.%				$K_{Mn} = \dfrac{(\Sigma \ MnO)}{(\Sigma FeO)[Mn]}$
		Mn%	Si%	O%	FeO	MnO	SiO_2	MgO	
1	1650	0.05		0.105	55.5	24.2	13.04	6.8	8.8
2	1670	0.035		0.096	51.0	16.7	24.5	7.2	9.3
3	1550	0.05		0.071	44.0	29.8	20.9	5.3	13.5
4	1550	0.12	below 0.005	0.042	27.2	42.0	23.8	7.3	12.9
5	1640	0.22		0.056	24.3	42.2	27.2	7.9	7.3
6	1550	0.005		0.0985	75.1	3.6	16.3	5.5	9.6
7	1562	0.08		0.051	42.8	28.4	19.9	8.1	8.4
8	1550	0.1		0.11	73.5	23.0	1.7	2.1	3.12
9	1558	0.056		0.056	31.8	25.8	35.8	6.7	14.4

In Fig.68, K_{Mn} is plotted against the silica content of the slag as given in Table 17. The values of K_{Mn} obtained by Chipman, Gero and Winkler[92] for FeO-MnO slags containing 1 - 4 per cent silica, and by Korber and Oelsen[78] for silica saturated slags as given in Table 14, Chapter 6 are also indicated. Fig.68 shows that K_{Mn} increases with the addition of silica. This is in agreement with the experimental results of Krings and Schackmann[91] and the values of K_{Mn} calculated by Murray and White[55].

Most of the increase in K_{Mn} takes place between O and 30 per cent silica, and no appreciable increase occurs with further addition of silica. If we consider the ternary system $FeO-MnO-SiO_2$ it will be seen that 30 per cent silica almost coincides /

coincides with the orthosilicate join ($2MnO.SiO_2$ - $2FeO.SiO_2$) which means that at 30 per cent silica all the oxygen of FeO and MnO should be incorporated in SiO_4 tetrahedra; any further increase of silica cannot therefore affect the amount of "free" FeO and MnO in the slag. One cannot, however, infer that the activities of FeO and MnO in orthosilicate slags are zero, and the small increase in the value of K_{Mn} between 30 and 50 per cent silica is due to the fact that a_{MnO} is lowered to a greater extent than a_{FeO}. This is also the reason why K_{Mn} increases between 0 and 30 per cent silica and is caused by the greater stability of SiO_4 tetrahedra in the presence of manganese ions as compared with their stability in the presence of ferrous ions.

On the electroneutral oxides and compounds theory, this effect of an increase of K_{Mn} from 30 to 50 per cent silica would be represented as due to the effect of an excess of silica on the equilibria:-

$$2 \, MnO.SiO_2 \rightleftharpoons 2MnO + SiO_2$$
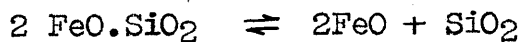
$$2 \, FeO.SiO_2 \rightleftharpoons 2FeO + SiO_2$$

thus slightly decreasing the amounts of "free" FeO and MnO. As the dissociation constant of $2MnO.SiO_2$ is usually taken as being much lower than that of $2FeO.SiO_2$ (i.e., $2MnO.SiO_2$ is more stable than $2FeO.SiO_2$) the effect of a given increase of SiO_2 is to cause a proportionately greater decrease of free MnO than free FeO.

The above effect of SiO_2 on K_{Mn} is also supported by the findings of Darken and Larsen [79] in their examination of the

manganese/
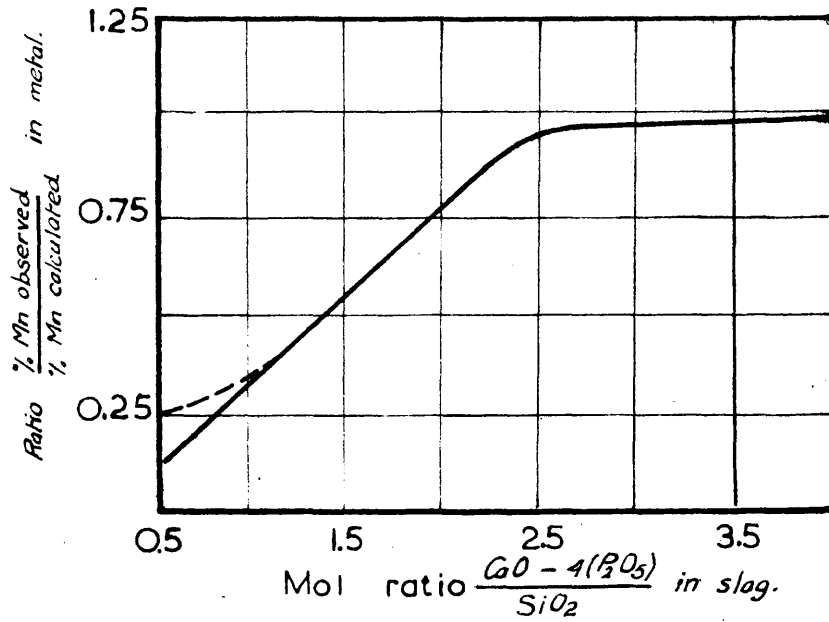
FIG. 69
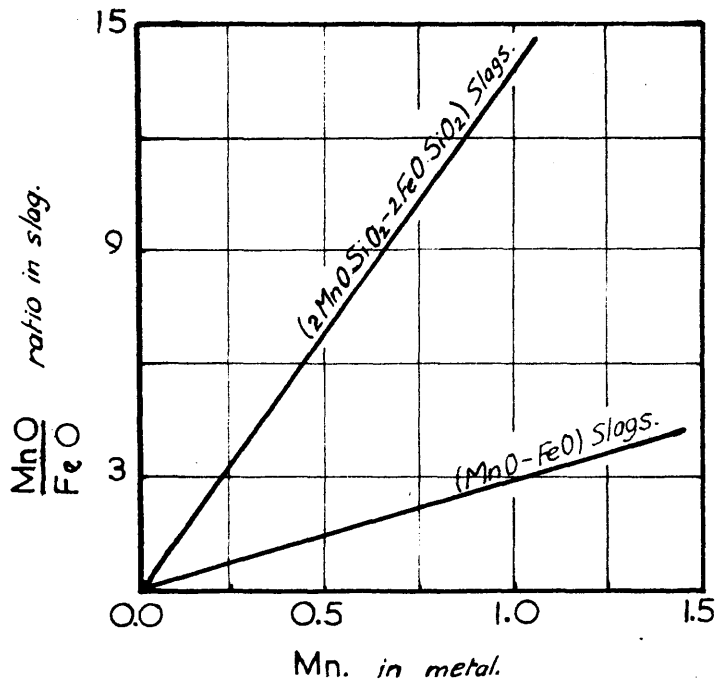
FIG. 70

manganese reaction in the basic open hearth furnace. They
calculated the manganese content of steel under basic open
hearth slags from the formula

$$[\%Mn] = \frac{(\Sigma MnO)}{(\Sigma FeO)} \times \frac{1}{K_{Mn}}$$

Where (ΣMnO) and (ΣFeO) are the total analytical contents of
the two oxides in the slag and K_{Mn} is the equilibrium constant
under FeO-MnO slags. Ratios of observed values of manganese to
calculate values were then plotted against the basicity of the
slag defined by the molar ratio V where,

$$V = \frac{CaO - 4(P_2O_5)}{SiO_2}$$

as shown in Fig.69.

The results indicate that, at basicities greater than
about 2.4, there is little evidence of combined manganese oxide
or iron oxide in the slag. All the silica (and phosphorus
pentoxide) appear to be combined with lime over this range of
basicities, and a constant value of K_{Mn}, corresponding to the
FeO-MnO slags, would be expected. With lower basicities
(i.e. increased silica contents) the results indicate that the
activity of manganese oxide is lowered to a greater extent than
that of iron oxide by silicate formation. This is in good
agreement with the results obtained in the present work,
illustrated in Fig.70. This shows the amount of manganese
in the metal in equilibrium with FeO-MnO slags and ortho-
silicate slags. For a certain manganese content in the metal,
a higher $\frac{(\Sigma MnO)}{(\Sigma FeO)}$ ratio is needed with orthosilicate slags, in
which/

which MnO is largely combined as silicate, than with pure FeO-MnO slags. The above infers, therefore, that the orthosilicate of manganese is more stable than that of iron, which supports the MnO-SiO$_2$ diagram advanced in Chapter III, rather than the previously accepted diagram.

The present work indicates that manganese silicate formation increases K$_{Mn}$ approximately four-fold, and that silica additions greater than 30 per cent have little further effect on K$_{Mn}$. One would therefore expect silica additions beyond V = 2.4 to cause an approximately four-fold decrease in the ratio of observed values of manganese to calculated values in Fig.69, and that further addition of silica would have little effect . The course of the curve in Fig.69 is, therefore, probably as indicated by the dotted line. The results of Darken and Larsen also fit quite well with this dotted line. Similar results to those of Darken and Larsen[79] were obtained by Tammann and Oelsen[113].

The amount of magnesia pick up by the slag from the crucible varied between 2 - 8 per cent. It was feared that this magnesia might form magnesium silicate, but the results obtained show that magnesia appears to have no effect and acts only as an inert diluent. This is in harmony with the fact that the magnesium has the smallest ionic diameter of the three metals present (Mn, Fe, Mg.) and is least able to contribute to the formation of stable SiO$_4$ tetrahedra in the liquid state. It was even suggested by Huggins[114] that magnesium ions replace part/

part of the silicon ion in the complex silicate anions.   This
also agrees with the results obtained by King[67] for surface tension
of molten magnesium silicate slags.

These results can be explained by the free oxide theory
and the assumption of certain compounds, e.g. $2MnO.SiO_2$, in the
slag.   They can also be explained by the ionic theory of slag-
metal equilibria advanced by Herasymenko[80] which is based on
the complete ionic dissociation of liquid slags, and excludes
the presence of electroneutral molecules.   According to this
theory, manganese and iron are present in the slag exclusively
as the divalent ions Mn and Fe , and the reaction

$$FeO + \underline{Mn} \rightleftharpoons MnO + \underline{Fe}$$
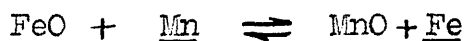
is written $$Fe^{++} + \underline{Mn} \rightleftharpoons Mn^{++} + \underline{Fe}$$

where $$K_{Mn} = \frac{(Mn^{++})}{(Fe^{++})\,[Mn]}$$

This means that the manganese equilibrium between iron and iron
manganese silicate slags depends only on the concentrations of
(Fe^{++}) and (Mn^{++}) and not on the nature of the anions.   This is
supported by Korber and Oelsen[78] who proved experimentally that
the manganese equilibrium remains practically unchanged when
silicate ions are replaced by phosphate ions.   The theory in
this simple form does not explain the variations observed in
K_{Mn} for acid and basic slags and to account for these variations
Herasymenko and Speight[83] have suggested that the activity of
ferrous ions depends on the concentration of oxygen ions, and
that the activity of manganous ions is influenced by the concen:
:tration of calcium ions.

Thus/
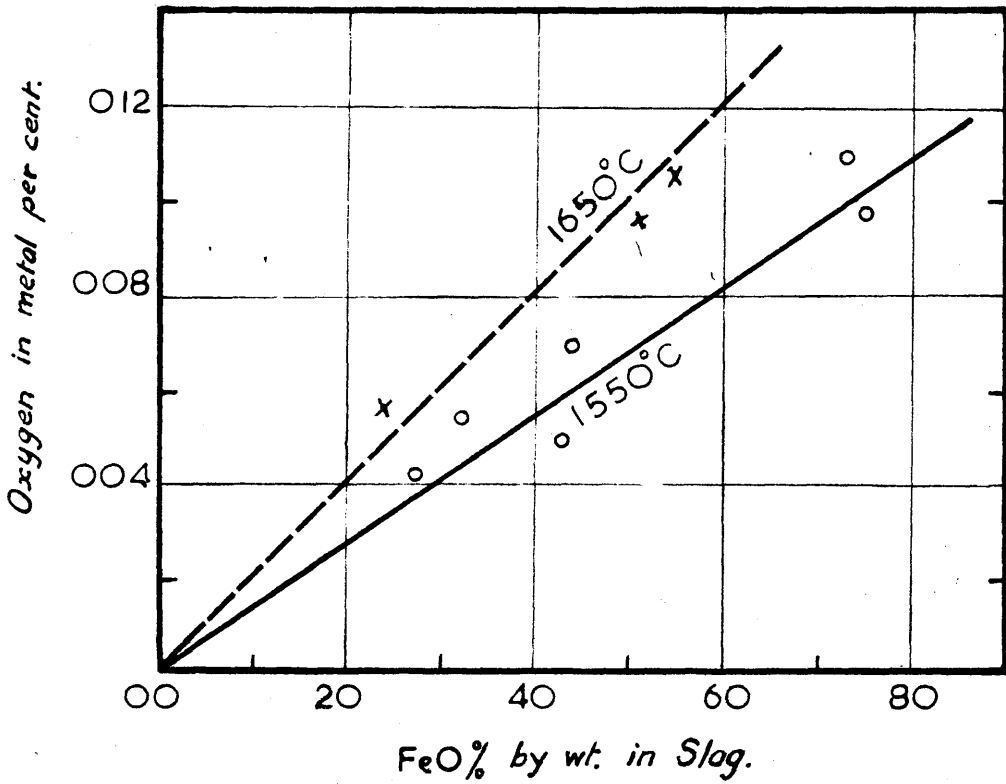
FIG. 71

Thus although the theory which regards slags as consis:
:ting of unionised oxides and compounds appears to be in direct
contrast with the ionic theory, yet both can be made to explain
steelmaking data and the results obtained in this investigation.

Another aspect of the application of the ionic theory
to slags has been presented by Zintl and Marawietz[115] who suggest:
:ed that the most probably type of silicate anions existing in
acid slags seem to be the orthosilicate anion, SiO_4^{-4}. Excess
silica over the amount necessary to satisfy electrochemically
the cations present in the slag is completely dissociated
according to the equation

$$2 SiO_2 \rightleftharpoons Si^{4+} + SiO_4^{-4}$$
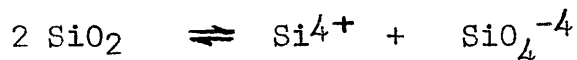
Chang and Derge[24] also found that their experimental results
on electromotive force determinations on $CaO-SiO_2$ and
$CaO-Al_2O_3-SiO_2$ slags could be best explained by assuming the
presence of Si^{4+} and SiO_4^{-4} ions.

In Fig.71 the total oxygen content of the metal as
determined by vacuum fusion is plotted against the total FeO
content of the slag. Although the number of points is small they
suggest that the oxygen content of the metal is proportional to
the FeO content of the slag, which would mean that FeO behaves
ideally in $FeO-MnO-SiO_2$ slags containing less silica than the
orthosilicate composition (acid slag compositions were not
investigated). Chipman and Taylor[76] showed that in the system
$FeO-SiO_2$, the solution is ideal for FeO at 1600°C, so that its
activity is equal to its molar concentration and inferred that
any compound between FeO and SiO_2 was completely dissociated.
Since FeO - MnO slags also behave ideally with
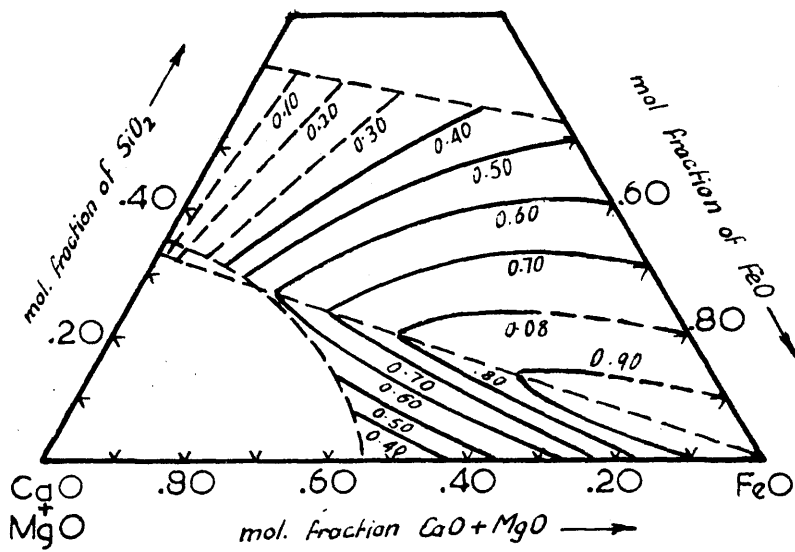
FIG. 72 a
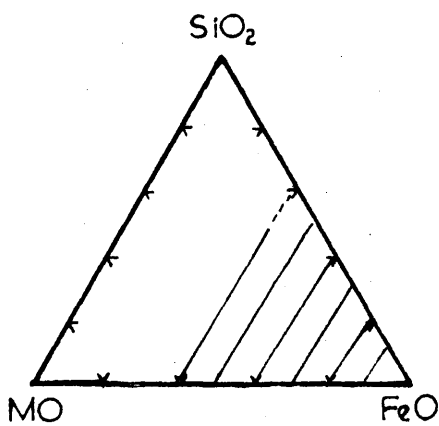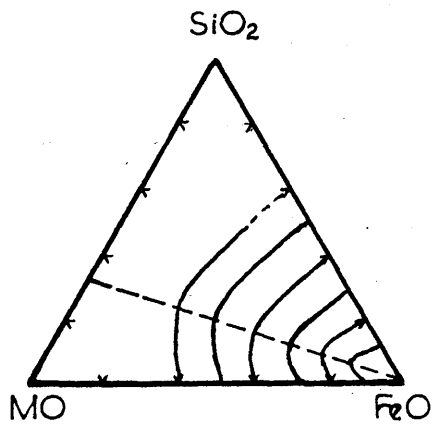
FIG.72 b

FIG.72 c

with respect to FeO one might expect that $FeO-MnO-SiO_2$ slags would also be ideal, as suggested by the relationship in Fig. 71, although a certain amount of caution must be exercised in making such predictions for a ternary system from a knowledge of the activities in the binary systems.   Thus the determina: :tions of Taylor and Chipman[76] of the activity of FeO in $CaO(MgO)-FeO-SiO_2$ slags illustrated in Fig.72a, indicate that although in the $FeO-SiO_2$ system the activity of FeO equals its molar fraction, and the same applies approximately to the $CaO-FeO$ system, the activity of FeO in the ternary system can be considerably different from its molar fraction.   This is mainly due to the fact that CaO and SiO_2 cannot be considered as separate components, but show a strong tendency to form $Ca_2.SiO_4$.   In a system $MO-FeO-SiO_2$ in which MO showed no such tendency to silicate formation one would expect ideal behaviour as shown by Fig.72b.   In the $FeO-MnO-SiO_2$ system, MnO shows a tendency to silicate formation which is not asmarked as that of CaO, and one would expect behaviour intermediate between that of the ideal case and that shown by the $CaO(MgO)-FeO-SiO_2$ system, as shown in Fig.72c.   The experimental points appear to indicate ideal behaviour, but unfortunately the limited number of deter: :minations is not sufficient to detect the deviation from ideality expected.

In Table 18, the slag compositions are recalculated on a molar fraction basis and the oxygen contents of the steel are corrected according to the empirical factor given in Chapter VIII, namely 0.73.

Table 18./
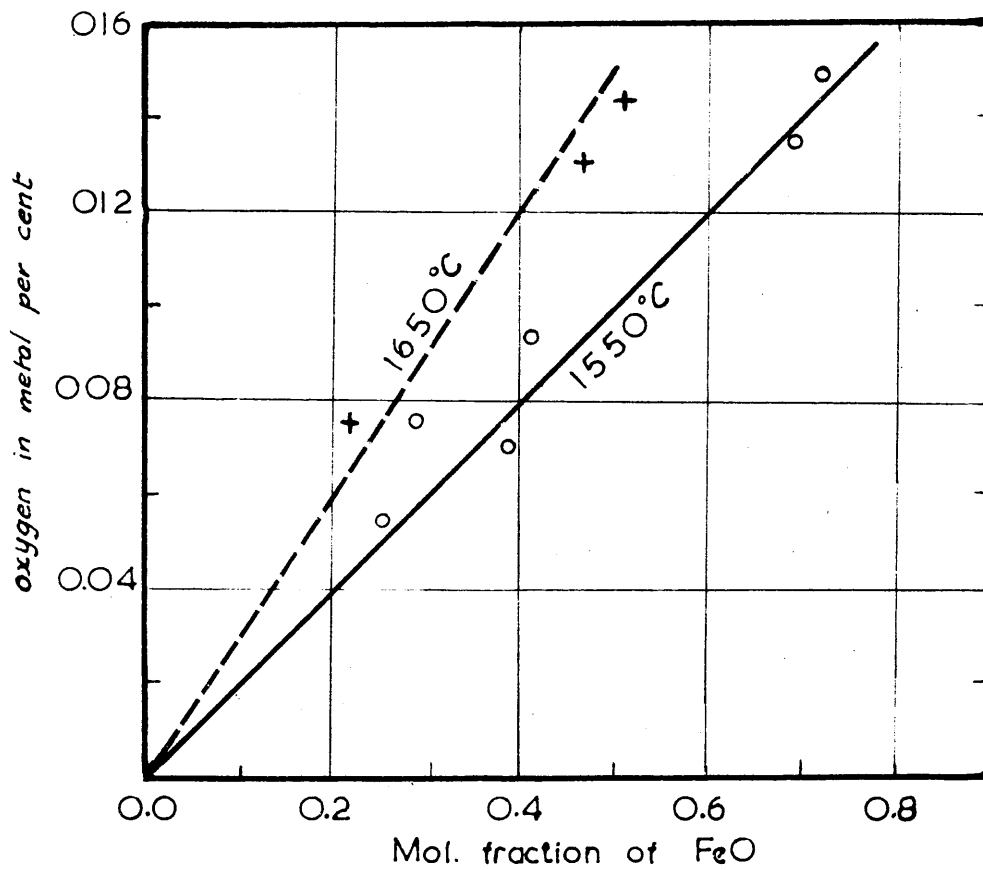
FIG. 73

FIG. 74 a.
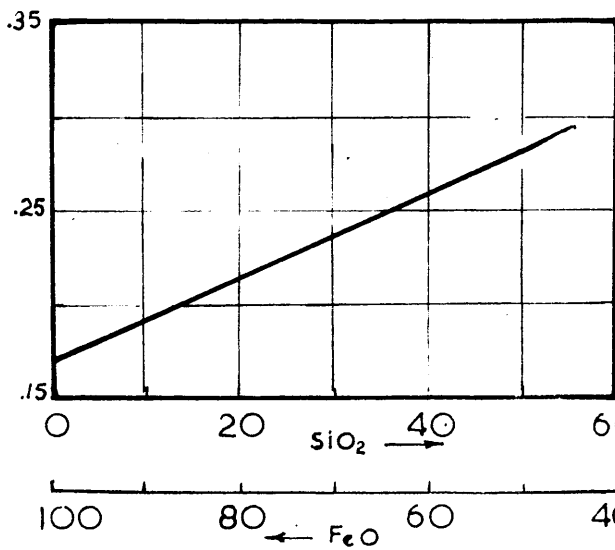
FIG. 74 b.
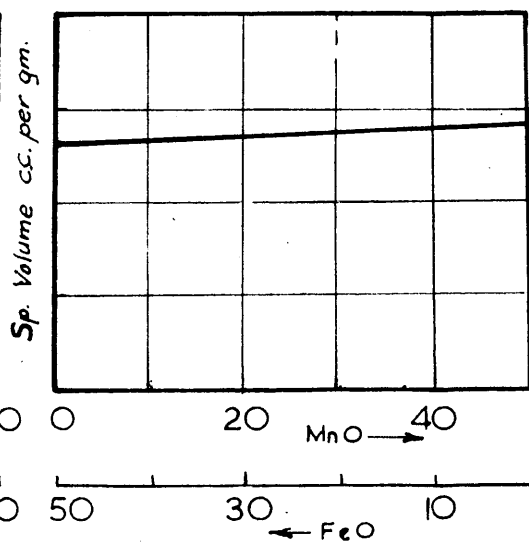
Table 18.

Run	Temp. °C.	Slag Analysis in Mol.fraction.				[o] % by weight.
		FeO	MnO	SiO_2	MgO.	
1	1650	0.516	0.228	0.143	0.112	0.144
2	1670	0.464	0.153	0.266	0.116	0.130
3	1550	0.405	0.288	0.299	0.087	0.097
4	1550	0.251	0.380	0.254	0.115	0.057
5	1640	0.217	0.376	0.284	0.123	0.077
6	1550	0.695	0.338	0.180	0.091	0.135
7	1562	0.390	0.262	0.216	0.131	0.070
8	1550	0.718	0.228	0.019	0.352	0.150
9	1558	0.283	0.232	0.379	0.105	0.077

In Fig.73, the oxygen content of the steel is plotted against the molar fraction of FeO in the slag. The lines give a distribution ratio $\frac{[o]}{(FeO)} = 0.20$ at $1550^{\circ}C$, and 0.30 at $1650^{\circ}C$. where $[o]$ is in percentage by weight and (FeO) is molar fraction in slag.

Korber and Oelson gave a distribution ratio $\frac{[o]}{(wt.\% \ FeO)} = 0.0026$ for FeO-MnO slags [90] and 0.0017 for silica saturated FeO-MnO-SiO_2 slags [78], both at $1550^{\circ}C$. This shows that the distribution ratio is lowered by more than a third in acid slags compared with simple FeO-MnO slags. This might be taken to infer that in silicate melts, FeO is partially combined as iron silicate. This inference loses its significance if the specific volume of the two types of slag are considered. Korber and Oelsen pointed out that the distribution theorem of Nernst strictly applies to concentrations expressed as gm mol. per unit volume. In the FeO-SiO_2 system the specific volume of the saturated silicate is almost /

almost double that of FeO (at 20°C) as shown in Fig.74a. Since

the atomic weights of Fe and Mn are almost equal, then the

specific volume of silica-saturated FeO-MnO-SiO₂ slags should

not change appreciably with varying FeO/MnO ratio. As the

specific volume of FeO-MnO slags does not vary much, as shown in

Fig.74b, there should be no necessity to take specific volume

into account in considering FeO-MnO slags.

Assuming that the specific volume relationships given in

Fig. 74a and Fig. 74b also apply to liquid slags, Korber and

Oelsen corrected their distribution coefficients for silica-

saturated slags to take into account the specific volume effect

and found that the value so obtained agreed with that observed

in FeO-MnO slags.

Table 19 compares the values obtained for the distribution

ratio $\frac{[O]}{(FeO)}$ at 1550°C. and 1650°C. by the different investi:

:gators. For the results of Korber and Oelsen, allowance was

made for the conversion from percentage by weight of (FeO) to

molar fractions.

Table 19.

$\frac{[O]}{(FeO)}$		Investigator.
1550°C	1650°C	
0.20	0.30	Present work.
0.185	0.28	Taylor and Chipman[76] for FeO-SiO₂ slags and pure FeO slags.
		Chipman, Gero and Winkler[92] for FeO-MnO slags
0.19	0.29	Korber and Oelsen[78] for silica-saturated FeO-MnO-SiO₂ slags.
0.26	0.39	Korber and Oelsen[90] for FeO-MnO slags.

The/

The results obtained in the present investigation are slightly higher than those of Chipman and his co-workers and those of Korber and Oelsen for silica-saturated $FeO-MnO-SiO_2$ slags but they are considerably lower than those of Korber and Oelsen for FeO-MnO slags.

Table 19 also shows that the volume effect was not notice: :able in the work of Chipman and others and that in $FeO-SiO_2$ slags containing up to 50 per cent silica the activity of FeO remained equal to its molar fraction irrespective of changes in the specific volume. In the present work no significant effect of specific volume was noticed.

It is probable, therefore, that the results of Korber and Oelsen for FeO-MnO slags are high. It may also be questioned whether the specific volume changes can be applied to the liquid state since they were only measured at $20^{\circ}C$.

Activity of MnO and SiO$_2$ in FeO-MnO-SiO$_2$ Slags at 1550°C.

a. Activity of MnO.

Assuming that FeO behaves ideally in $FeO-MnO-SiO_2$ slags then the change in K_{Mn} caused by the addition of silica may be attributed to a change in the activity of MnO, if it is also assumed that liquid Fe-Mn solutions behave ideally. If the true equilibrium constant for the manganese reaction is taken as the value of K_{Mn} in simple FeO-MnO- slags, viz., 3.0 at 1550°C then
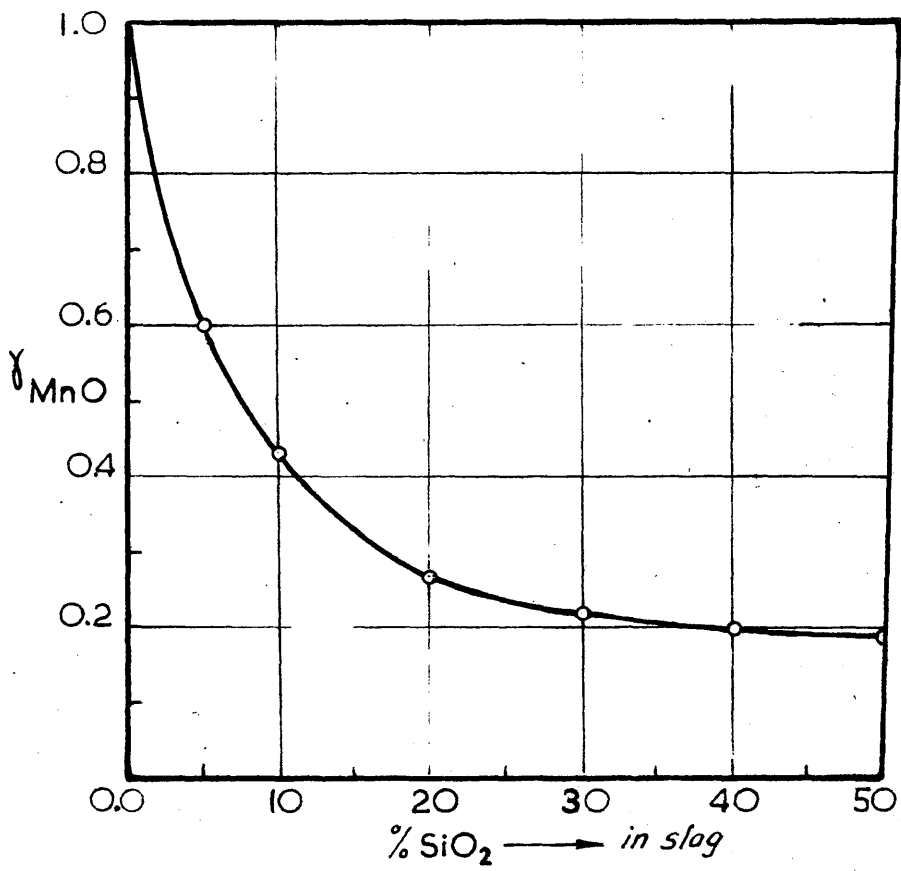
FIG. 75
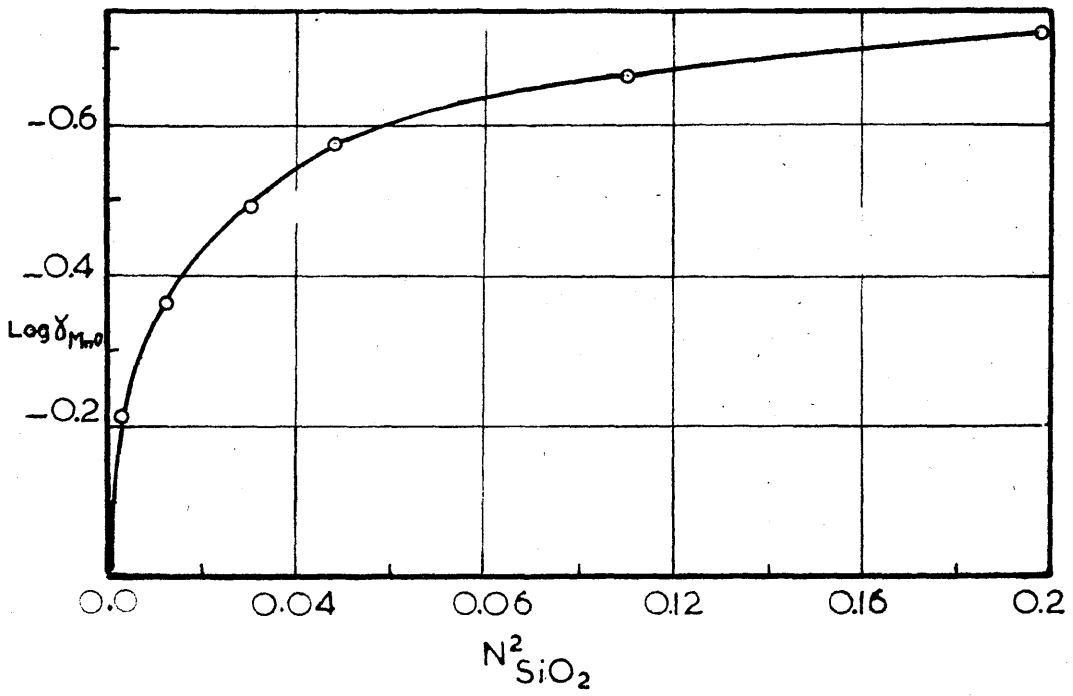
FIG. 76

then

$$3.0 = \frac{(a_{MnO})}{(a_{FeO})[Mn]} = \frac{\gamma_{MnO}(\Sigma MnO)}{(\Sigma FeO)[Mn]}$$

where γ_{MnO} is the activity coefficient of MnO in the slag

and $\dfrac{(\Sigma MnO)}{(\Sigma FeO)} = $ (approx.) $\dfrac{N_{MnO}}{N_{FeO}}$. It follows that the

activity coefficient of MnO in a slag of given SiO_2 content

will be equal to

$$\gamma_{MnO} = \frac{3.0}{K_{Mn}}$$

where K_{Mn} is the value taken from Fig.68 for that particular

silica content of the slag. The values so obtained for MnO

are given in Table 20.

Table 20.

% SiO$_2$ in Slag.	K$_{Mn}$	γ_{MnO}	MnO - SiO$_2$ System.			
			N$_{MnO}$	a$_{MnO}$	log γ MnO	N^{2}SiO$_2$
0	3.0	1	1	1	0	0
5	5.0	0.60	0.943	0.565	-0.22	0.003
10	7.0	0.43	0.89	0.383	-0.365	0.012
15	9.1	0.33	0.83	0.273	-0.48	0.030
20	11.2	0.27	0.78	0.21	-0.57	0.048
30	13.8	0.22	0.67	0.15	-0.66	0.109
40	14.9	0.20	0.56	0.11	-0.70	0.194
50	15.5	0.19	0.46	0.09	-0.72	0.292

The activity coefficient of manganese oxide is plotted against

the silica content of the slag in Fig.75. For the system

MnO-SiO$_2$ the activity of MnO shows a marked negative deviation

from Raoult's law, due to compound formation. In Fig.76 MnO

is plotted against N^{2}SiO$_2$ for the system MnO-SiO$_2$. The curve

obtained indicates that the solution is regular with respect to

MnO over only a small range of slag composition (approximately

0-6 per cent silica). Chipman[62] has described this type of

behaviour/
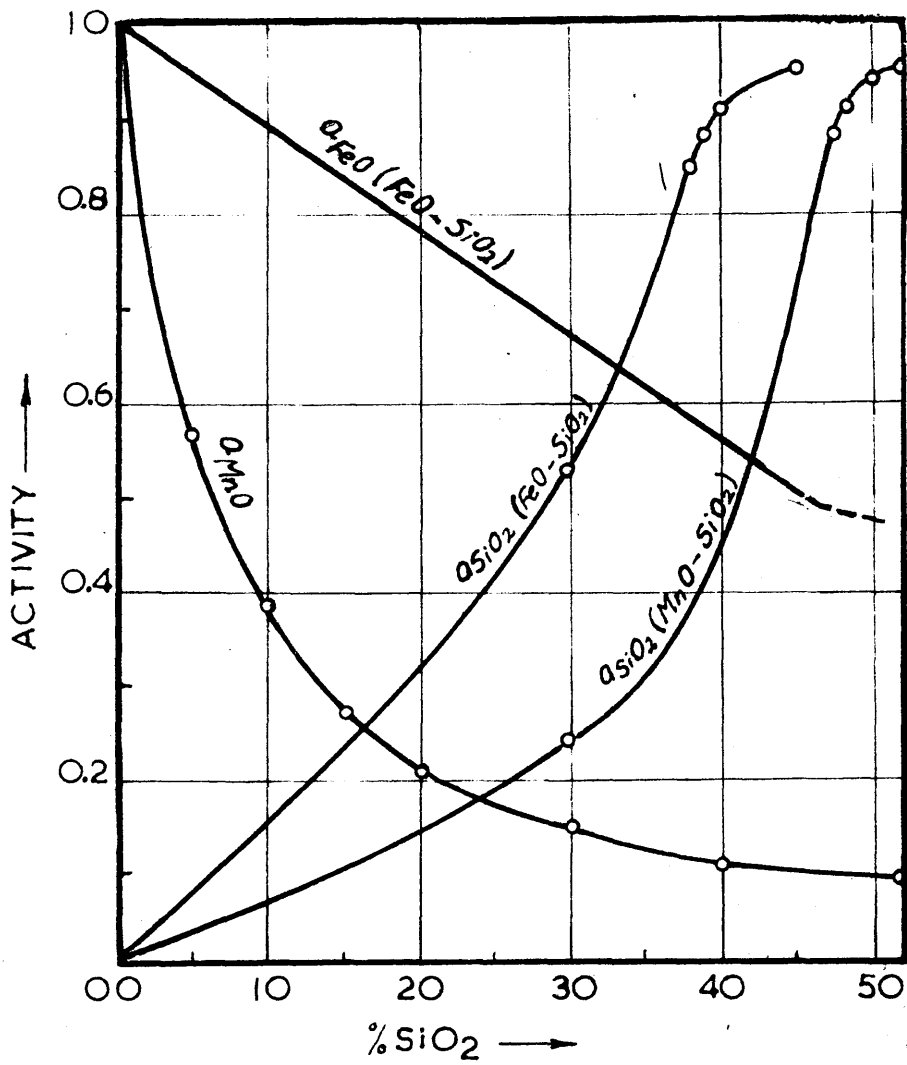
FIG. 77

behaviour as "semi-regular".

b. Activity of Silica.

The activity of SiO_2 in $FeO-MnO-SiO_2$ slags cannot be deduced directly but can be calculated from a knowledge of the silica liquidus curve of the $MnO-SiO_2$ and $FeO-SiO_2$ systems, by the method described in Chapter VI.

The results obtained referred to pure supercooled liquid silica as the standard state are given in Table 21.

Table 21.

Temperature $= 1550^{\circ}C.$

%SiO_2	N_{SiO_2}	a_{SiO_2}	%SiO_2	N_{SiO_2}	a_{SiO_2}
MnO-SiO_2 system.			FeO-SiO_2 system.		
52	0.56	0.95	45	0.49	0.95
50	0.54	0.94	40	0.44	0.91
48	0.52	0.92	39	0.43	0.88
47	0.51	0.88	38	0.42	0.85
29.9	0.33	0.24	29.7	0.33	0.54

The activity of silica at the orthosilicate composition in the MnO-SiO_2 system ($N_{SiO_2} = 0.33$) was obtained from a know: :ledge of the activity of MnO at different compositions by applying the Gibbs-Duhem equation :-

$$\log \gamma_1 = -\int_0^{N_2} \frac{N_2}{N_1} d \log \gamma_2$$

$\dfrac{N_{MnO}}{N_{SiO_2}}$ was plotted against $\log \gamma_{MnO}$ and $\log \gamma_{SiO_2}$ at 29.9% SiO_2

$(\dfrac{N_{MnO}}{N_{SiO_2}} = 2)$ evaluated graphically

These results are shown in Fig.77, which also shows the variation in a_{MnO} with silica content.

For the fayalite composition in the $FeO-SiO_2$ system, the value given by Richardson[64] for a_{SiO_2} was used after a slight correction for temperature . The activities of MnO and SiO_2 in the $MnO-SiO_2$ system and FeO and SiO_2 in the $FeO-SiO_2$ system, were then calculated and are shown in Fig.77.

On the assumption that the slags behave as ideal mixtures of electroneutral oxides and compounds, the activities of MnO and SiO_2 in molten tephroite would be attributed to the dissoc:
:iation of tephroite

$$2 \; MnO.SiO_2 \; = \; 2 \; MnO + SiO_2$$
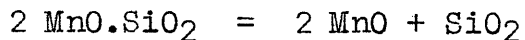
and the activity of SiO_2 in molten tephroite would be equal to 0.07 (i.e., one half that of MnO). This neglects the tendency to positive deviation from Raoult's law in the system and the true value would be expected to be higher. On the other hand the value (0.24) given in Table 21 may be high because of the inaccuracies involved in applying the Gibbs-Duhem equation to a system in which a miscibility gap appears, as well as compound formation.

Calculation of lines of iso-concentration of [Mn] and [Si] at 1550°C under $FeO-MnO-SiO_2$.

a. [Mn] lines:

The manganese concentration in the metal in equilibrium with any $FeO-MnO-SiO_2$ slag containing up to 50 per cent SiO_2 has been calculated from the equation

$$[\% \; Mn] \; = \; \frac{\gamma_{MnO} \; (\Sigma \; MnO)}{3.0 \; (\Sigma \; FeO)}$$

where MnO is taken from Fig.75 at the corresponding silica content /

content, and (ΣMnO) and (ΣFeO) are the percentages by weight of total MnO and FeO in the slags. The results obtained for FeO-MnO-SiO$_2$ slags of varying compositions are given in Table 22.

Table 22.

[Mn]	0%SiO$_2$ MnO%	10%SiO$_2$ MnO%	20%SiO$_2$ MnO%	30%SiO$_2$ MnO%	40%SiO$_2$ MnO%	50%SiO$_2$ MnO%
2.5	88.2	85.0	77.2	68.1	58.5	48.7
1	75.0	78.5	73.4	65.3	56.3	47.0
0.6	64.3	72.0	69.5	62.6	54.0	45.1
0.4	54.5	65.6	65.2	59.4	51.4	43.1
0.25	41.2	56.3	58.6	54.5	47.4	39.8
0.15	28.6	46.8	49.8	47.1	41.6	35.0
0.1	23.1	36.5	41.9	41.0	36	30.4
0.06	15.3	25.8	31.8	32.0	28.4	24.1
0.03	8.3	15.0	20.3	20.7	18.0	15.8
0.01	2.9	5.5	8.0	8.6	8.0	6.6
0.005	1.5	2.5	4.2	4.6	6.5	3.5

b. **Si lines:**

Silicon iso-concentration lines for FeO-MnO-SiO$_2$ slags were calculated after interpolating the silica activity from the two silica activity curves of Fig.77.

Korber and Oelsen [78] found that for silica-saturated slags containing about 50 per cent silica the equilibrium constant for the reaction

$$2\ \underline{Fe}\ +\ SiO_2\ \rightleftharpoons\ 2\ FeO\ +\ \underline{Si}$$
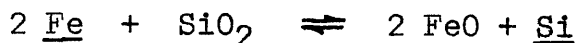
could be expressed by

$$K^1{}_{Si}\ =\ (FeO)^2\ [\underline{Si}]$$

and was equal to 4.5 at 1550°C.

Actually $K^1{}_{Si}\ =\ \dfrac{(a_{FeO})^2\ [\underline{Si}]}{(a_{SiO_2})}$

and/

and the above expression for K^1_{Si} assumes that:-

a)   the activity of FeO equals its percentage by weight

b)   dilute solutions of silicon in iron behave ideally
      (Chipman[62] has shown that this is not the case but
      in the concentration range covered in this work the
      effect of the slight increase in activity coefficient
      (1.0 to 1.01) as the silicon concentration increases
      may be neglected).

c)   the activity of SiO_2 is unity.   As the slags are saturated
      with SiO_2, this is true if the activities are referred
      to solid SiO_2 atthe same temperature as the standard
      state.

   If supercooled liquid silica is used as the standard
state, the value of $^aSiO_2$ = 0.95 at 1550°C (calculated as
described on page 78) may be used for silica-saturated slags,
and the above expression re-written as

$$K_{Si} = \frac{(^aFeO)^2 \, [\%Si]}{(^aSiO_2)} = \frac{4.5}{0.95} = 4.72$$

Again assuming that these slags behave ideally with respect
to FeO,

$$[\%Si] = 4.72 \times \frac{^aSiO_2}{(^{\cdot}FeO)^2}$$

Hence, knowing the activity of SiO_2 in the slag, the silicon
concentration in the metal in equilibrium with any FeO-MnO-SiO_2
slag up to about 50 per cent SiO_2 may be calculated.   The
results obtained are given in Table 23.

Table 23. /

FIG. 78.
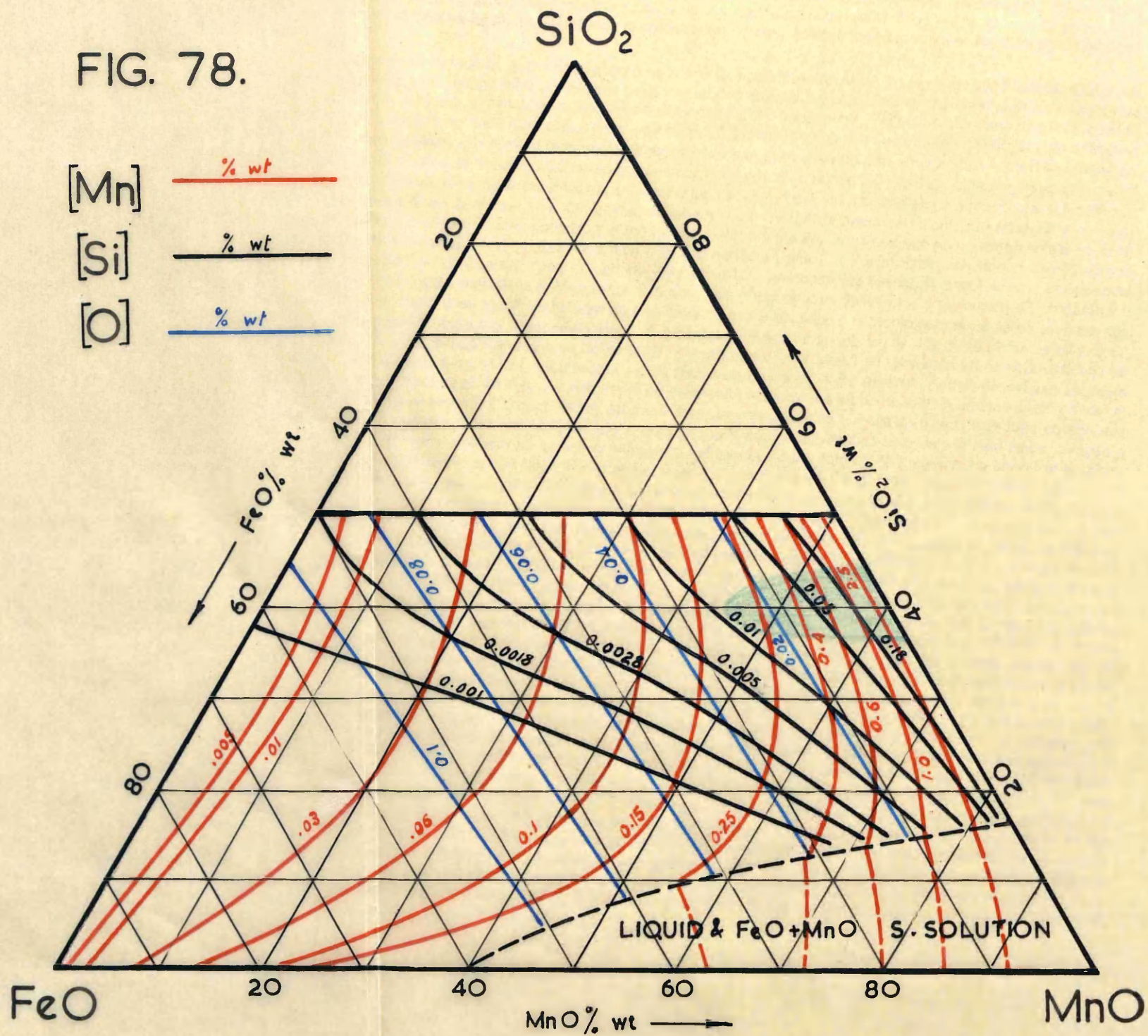
Table 23.

Si	50%SiO$_2$	45%SiO$_2$	40%SiO$_2$	35%SiO$_2$	30%SiO$_2$	20%SiO$_2$
	FeO%	FeO%	FeO%	FeO%	FeO%	FeO%
0.18	5.0	4.6	3.8	3.1	2.5	1.8
0.05	9.5	8.3	7.4	5.9	4.9	3.4
0.01	21.2	19.7	17.3	13.9	11.7	8.0
0.005	30.0	28.9	25.7	20.7	16.7	11.0
0.0028	40.0	38.9	35.6	28.4	24.1	16.0
0.0018	50.0	48.9	46.9	40.0	30.0	21.0
0.001	-	-	-	56.0	43.0	30.0

The results given in Tables 22 and 23 are plotted in Fig.78, which shows the iso-concentration lines of Si and Mn under FeO-MnO-SiO$_2$ slags.

If the activity coefficient of FeO in FeO-MnO-SiO$_2$ slags is taken as unity, the iso-concentration lines of oxygen in the metal will run almost parallel to the MnO-SiO$_2$ side of the ternary diagram, as shown. (The diagram shows slag compositions as weight, not molar, percentages). It may be, however, that they are more truly represented by the curves shown in Fig.72c.

Fig.78 explains why the silicon contents of the steels under the slags examined and reported in Table 17 are beyond the accuracy of normal chemical analyses. Fig.78 indicates [Si] less than 0.005 per cent for these slags and Chipman[6] stated that the analytical error with silicon or oxygen contents below 0.006 per cent is likely to be large.

Fig.79 compares some of the recently published data of Hilty and Crafts[94] on deoxidation with silicon and manganese alloys with those calculated from the present work at 1550°C. The latter data are presented in Table 24. Fig.79 shows that the/
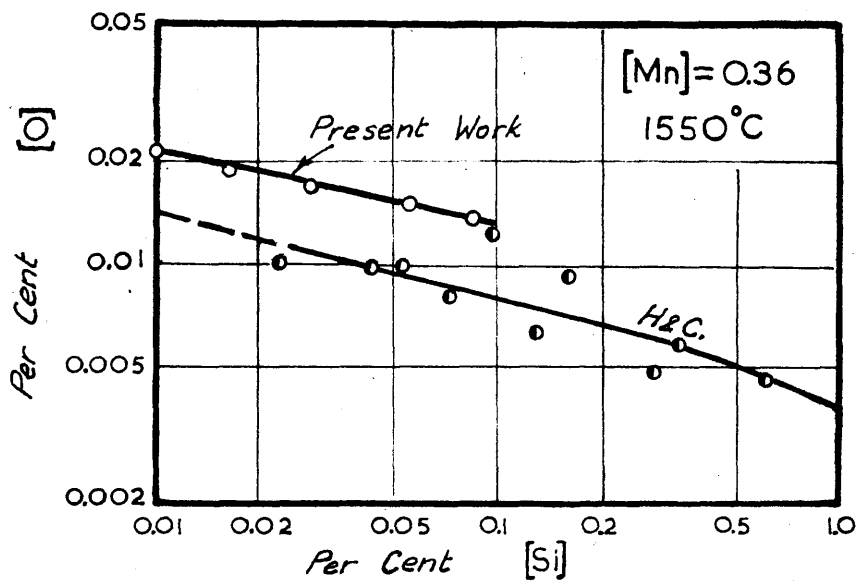
FIG. 79.

the oxygen contents of Hilty and Crafts are considerably lower
than those obtained in the present work.

Table 24.

Metal Analysis (weight per cent).			Slag Analysis (weight per cent).		
[Mn]	[Si]	[O]	(FeO)	(MnO)	(SiO$_2$)
0.36	0.078	0.0140	7.6	42.4	50
0.36	0.055	0.0157	8.5	46.5	45
0.36	0.031	0.0176	9.4	50.6	40
0.36	0.017	0.0190	10.5	54.5	35
0.36	0.010	0.0216	11.7	58.3	30

For any given manganese content in iron, the highest silicon
content is obtained with a silica-saturated FeO-MnO-SiO$_2$ slag
which is in equilibrium with that manganese content. According
to Table 24, percentages of silicon higher than 0.078 per cent
cannot exist with 0.36 per cent manganese under equilibrium
conditions. Fig.79 shows silicon contents up to 1 per cent
in equilibrium with 0.36 per cent manganese. Hilty and Crafts
also reported silicon contents up to 1 per cent in iron contain:
:ing 0.04 per cent manganese. Such a manganese content can
only be in equilibrium with silicon contents up to a maximum
of 0.005 per cent. Therefore, it seems doubtful whether Hilty
and Crafts obtained true equilibrium conditions. This probably
also applies to the work of Hilty and Crafts on deoxidation
with aluminium, as their deoxidation products contained iron
oxide and hercynite (FeO.Al$_2$O$_3$), under conditions where Al$_2$O$_3$
would be expected to be the equilibrium product.

The /

The amount and composition of deoxidiser required to accomplish varying degrees of deoxidation.

The melting point determinations carried out on FeO-MnO-SiO$_2$ slags, and reported in Chapter V, have shown that very low melting slags occur at approximately 38-40 per cent SiO$_2$ irrespective of FeO/MnO ratio.   Most of these slags are liquid at 1200°C.   Superheated to steelmaking temperatures, inclusions of these compositions should have a very low viscosity (e.g.,

62.5 per cent MnO, 37.5 per cent SiO$_2$, = 6.5 poise at 1600°C) and should easily coalesce to form larger inclusions.

The above results can be used to calculate the amount of deoxidiser needed to produce an inclusion of this type, and to bring the oxygen content of iron down to any required level. To illustrate this the following example is given:-

EXAMPLE: It is required to remove 80 per cent of the oxygen from 1000 gm. iron containing 0.04 per cent oxygen at 1550°C (but containing no silicon or manganese).

A slag or inclusion composition within the fluid range mentioned above, and indicated in Fig.78, should be aimed at.

After deoxidation the iron will contain 0.008 per cent oxygen.   The oxygen content of iron saturated with oxygen at 1550°C is 0.20 per cent.   It follows that iron containing 0.008 per cent oxygen would be in equilibrium with a slag containing about 4 per cent FeO.   If a silica content of 40 per cent is aimed at, the composition of the inclusion will be:-

56 per cent MnO, 40 per cent SiO$_2$, and 4 per cent FeO.

Using/

Using the following three equations it is possible to calculate the amount of deoxidiser required.

Total oxygen in iron = [O] after deoxidation + oxygen in slag.

Total Mn added = [Mn] after deoxidation + manganese in slag.

Total Si added = [Si] after deoxidation + silicon in slag.

Let x = weight of manganese added (gm.)

y = weight of silicon added (gm.)

z = weight of slag produced (gm.)

Then

$$Mn = \frac{\gamma_{MnO} (MnO)}{3.0 \ (FeO)} = \frac{0.20 \times 56}{3.0 \times 4} = 0.93$$

$$Si = \frac{K_{Si} \ a_{SiO_2}}{(FeO)^2} = \frac{4.72 \times 0.46}{16} = 0.135$$

Oxygen balance.

$$\frac{0.04}{100} \times 1000 = \frac{0.008}{100} \times 1000 + 0.4xZx\frac{32}{60} + 0.56xZx\frac{16}{72} + 0.04xZx\frac{16}{72}$$

$$0.32 = 0.348Z$$

$$Z = 0.92 \ gm.$$

Manganese balance.

$$x = \frac{0.93 \times 1000}{100} + 0.92 \times 0.56 \times \frac{55}{71}$$

$$= 9.3 + 0.40 = 9.70 \ gm.$$

Silicon balance.

$$y = \frac{0.135}{100} \times 1000 + 0.92 \times 0.4 \times \frac{28}{60}$$

$$= 1.35 + 0.17 = 1.52 \ gm.$$

$x + y$ = weight of deoxidiser = 11.22 gm.

$$\frac{Mn}{Si} \text{ ratio in deoxidiser} = \frac{9.7}{1.52} = 6.38$$

FIG. **80.**

Percentage deoxidiser added

Initial [0] = 0.04%

Initial [0] = 0.2%

Percentage oxegen removed
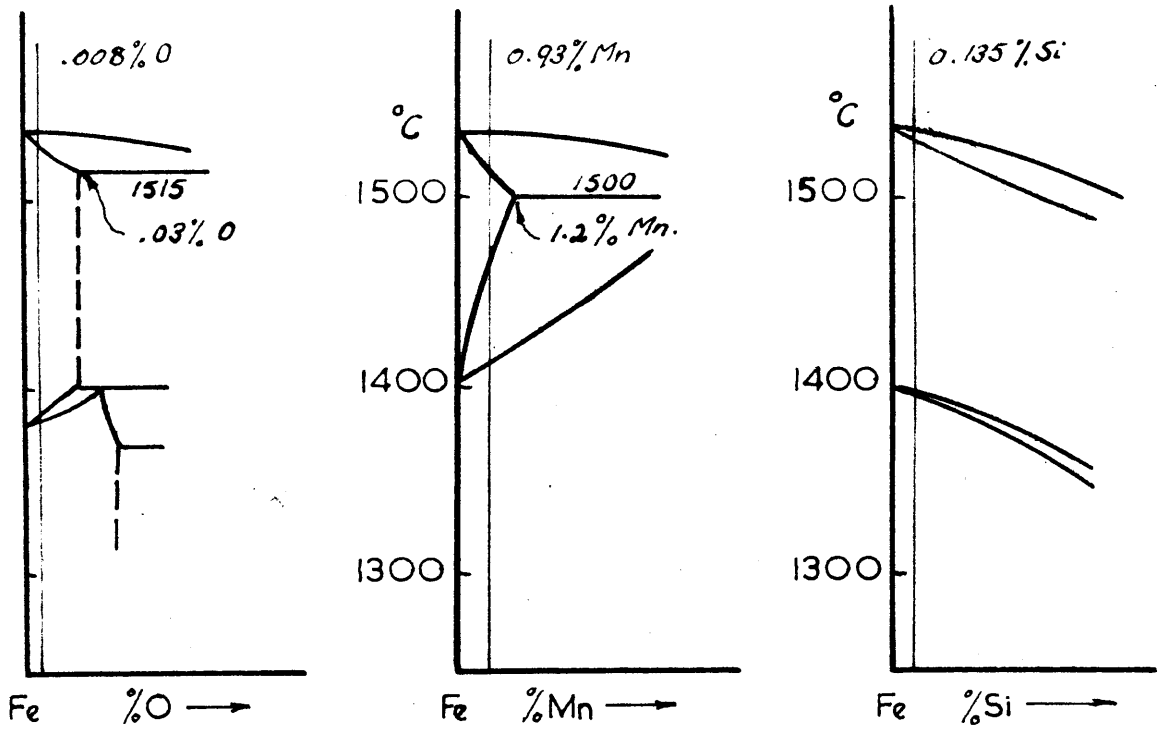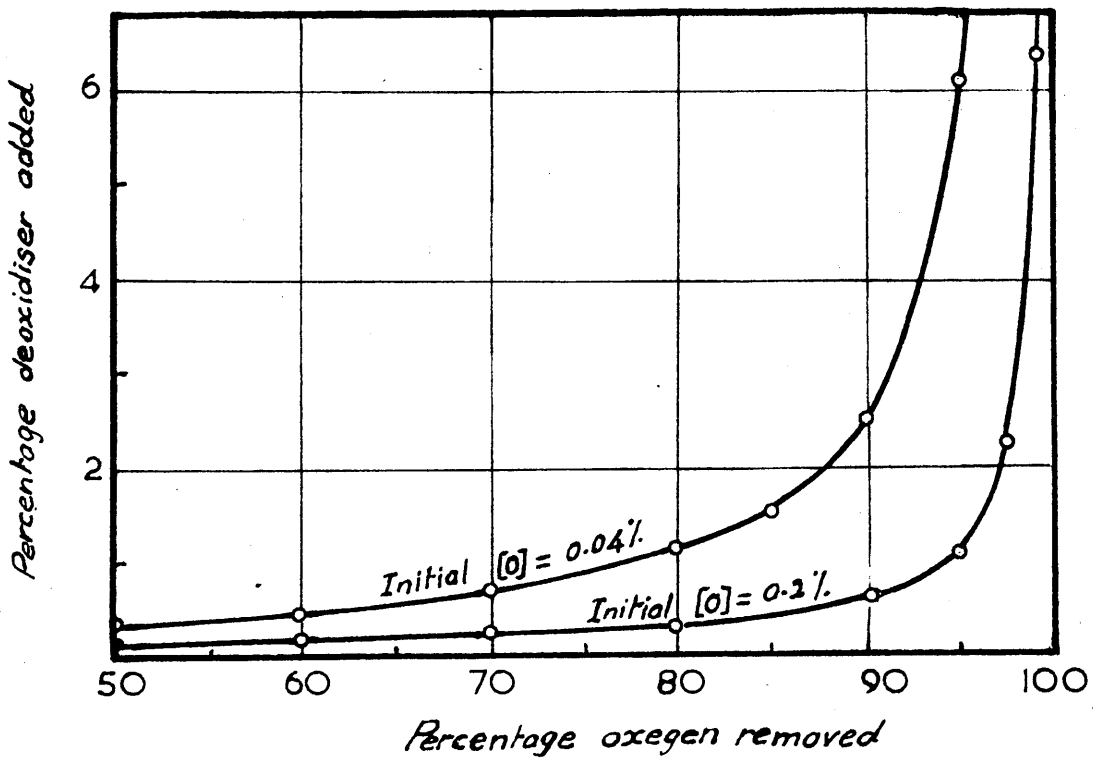
FIG. 81

This would mean finishing with iron containing 0.93 per cent manganese, 0.135 per cent silicon and 0.002 per cent oxygen. In practice such manganese contents would usually be unsuitable, so that aluminium might be used as an additional deoxidiser.

It should be mentioned here that on **freezing a** marked increase of deoxidation is to be expected due to the great influence of solidification on the deoxidation equilibria. (Deoxidation also increases with fall of temperature).

The interaction which occurs between liquid iron, dissolved oxygen and dissolved deoxidising elements is very complex . To explain this on a qualitative basis, the iron corners of the, three binaries Fe-O, Fe-Si and Fe-Mn are given in Fig.80. On freezing the above melt containing $[Mn]$ = 0.93, $[Si]$ = 0.135, $[O]$ = 0.008, the solid separating will contain a much smaller percentage of these elements than was present in the original melt, as shown by the binary diagrams, while the remaining liquid becomes richer in manganese, silicon and oxygen. Their concentration will now exceed the equilib: ;rium value and the deoxidation reactions will proceed further.

$$\underline{Mn} + \underline{O} \longrightarrow (MnO)$$
$$\underline{Si} + 2\underline{O} \longrightarrow (SiO_2)$$
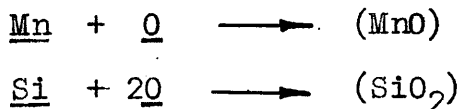
Whether the products are trapped between the dendrites of the freezing metal or escape and rise to the surface will depend on a number of factors such as cooling rate, the presence or absence of rimming action and mould design.

Tables/

Tables 25a & b show the amount of deoxidiser needed to remove different percentages of the oxygen present in

a) iron containing 0.04 per cent oxygen at 1550°C

b) iron saturated with oxygen at 1550°C.

calculated as above on the basis of 1000 gm. metal.

In Fig.81 the percentage of deoxidiser used (compared with the total amount of metal) is plotted against the per; :centage of oxygen removed. The curves show that for metal originally containing 0.04 per cent oxygen, 80 per cent is removed by a silicon-manganese deoxidiser amounting to 1 per cent of the weight of the iron. The curve after this point rises very steeply, so that a further 1.5 per cent of deoxidiser is required to remove 10 per cent more oxygen. Similarly in the second case, 95 per cent of the oxygen is removed by 1 per cent of deoxidiser. A further 4.8 per cent deoxidiser is needed to remove 99 per cent of the oxygen. The curves thus indicate how far the deoxidation process can be carried out economically.

Table 25a /

Table 25a.

Initial oxygen content = 0.04 per cent.

% removal	Deoxidiser (wt)				%age Deoxidiser	Comp. of inclusion.			Wt. of Incl.	Final Anal. of Steel.		
	Mn	Si	Mn+Si	$\frac{Mn}{Si}$		FeO%	MnO%	SiO$_2$%		[Mn]	[Si]	[O]
10	1.48	0.087	1.57	17.0	0.16	19	41	40	0.115	0.144	0.0065	0.036
20	1.78	0.123	1.9	14.0	0.19	17	43	40	0.23	0.17	0.008	0.032
30	2.12	0.167	2.29	12.7	0.23	15	45	40	0.345	0.20	0.0102	0.028
40	2.67	0.23	2.90	11.6	0.29	12.5	47.5	40	0.46	0.25	0.0144	0.024
50	3.32	0.31	3.73	10.7	0.37	10.5	49.5	40	0.51	0.31	0.020	0.02
60	4.28	0.43	4.71	9.9	0.47	8.5	51.5	40	0.69	0.40	0.030	0.016
70	6.34	0.76	7.1	8.3	0.71	6	54	40	0.80	0.60	0.061	0.012
80	9.7	1.52	11.22	6.4	1.12	4	56	40	0.92	0.93	0.135	0.008
85	13.13	2.57	15.7	5.1	1.57	3	57	40	0.98	1.27	0.24	0.006
90	19.76	5.49	15.7	3.6	2.52	2	58	40	1.03	1.93	0.53	0.004
95	39.8	21.3	61.1	1.87	6.11	1	59	40	1.09	3.93	2.11	0.002
99	199.5	52.5	724.5	0.38	72.4	0.2	59.8	40	1.14	19.9	52.5	0.0004

Table 25b.

Initial oxygen content = 0.2 per cent.

% O removal	Deoxidiser Mn	Si	Mn+Si	$\frac{Mn}{Si}$	%age Deoxid	Comp. of inclusion FeO	MnO	SiO2	Wt. of Incl.	Final Anal. of Steel Mn	Si	O.
60	0.77	0.66	1.43	1.2	0.14	42	18	40	3.44	0.029	0.0015	0.08
70	1.49	0.78	2.27	1.91	0.23	31.5	28.5	40	4.01	0.06	0.0025	0.06
80	2.625	0.86	3.49	3.05	0.35	21	39	40	4.58	0.124	0.0053	0.04
90	5.12	1.17	6.29	4.38	0.63	10.5	49.5	40	5.17	0.314	0.020	0.02
95	9.63	1.88	11.51	5.12	1.15	5	55	40	5.46	0.73	0.086	0.01
97.5	17.8	4.46	22.3	3.99	2.23	2.5	57.5	40	5.60	1.53	0.341	0.005
99	41.9	22.2	64.1	1.89	6.41	1	59	40	5.69	3.93	2.11	0.002
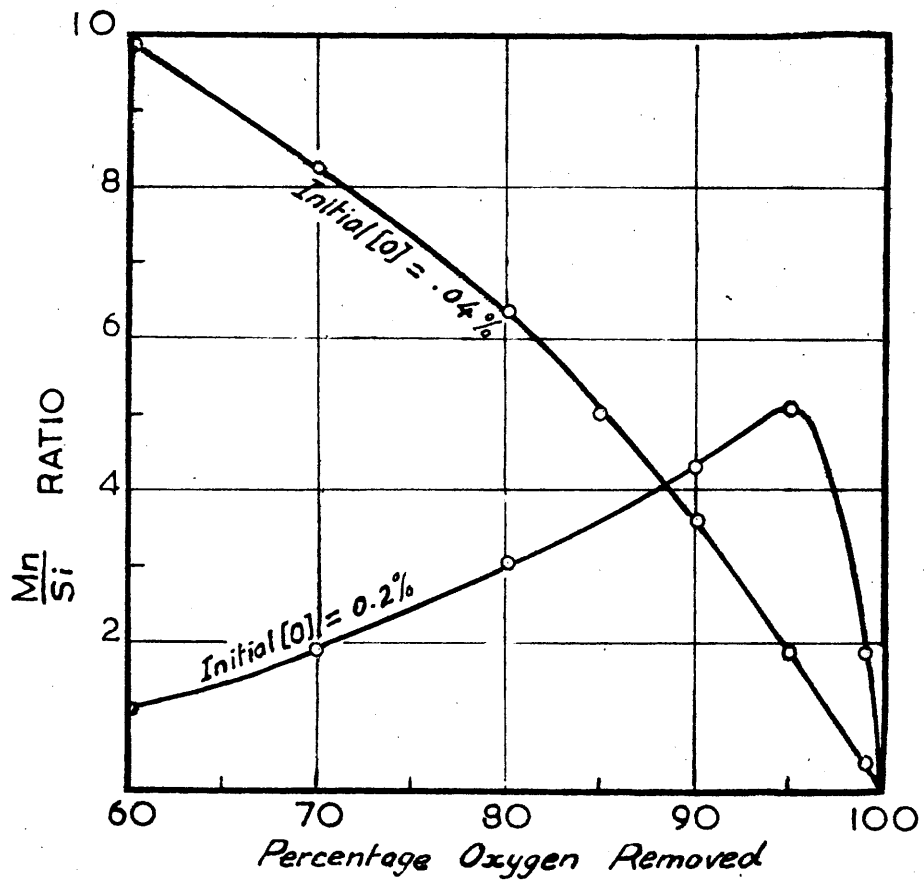
FIG. 82

Tables 25a and b also show that the most suitable manganese-silicon ratio for the deoxidiser varies with the percentage of deoxidation required and the initial oxygen content. In the case of iron saturated with oxygen, the ratio rises to a maximum and then falls rapidly as the per: :centage of deoxidation increases, the maximum occurring at about 95 per cent removal of oxygen as shown in Fig.82. This is because at high levels of deoxidation the silicon content of the metal (which depends on $(FeO)^2$) rises very rapidly compared with manganese and a large amount of silicon is required in the deoxidiser to satisfy this demand. For lower percentages of oxygen removed, the deoxidation product contains more FeO and as the silica content has been fixed at 40 per cent, FeO must increase at the expense of MnO. As the equilibrium content of manganese in the iron is also affected by the decreasing MnO/FeO ratio, less manganese is required for both slag and metal so once again the corresponding Mn/Si ratio decreases.

As in case (a) (iron originally containing 0.04 per cent oxygen) the FeO content of the slag never rises very high, the second effect is hardly noticeable and the Mn/Si ratio increases continuously with decreasing amount of oxygen removed.

Herty and Fitterer[116] have established by means of laboratory low carbon melts that fluid deoxidation products can be obtained with deoxidisers with Mn/Si ratios from 4 : 1 to/
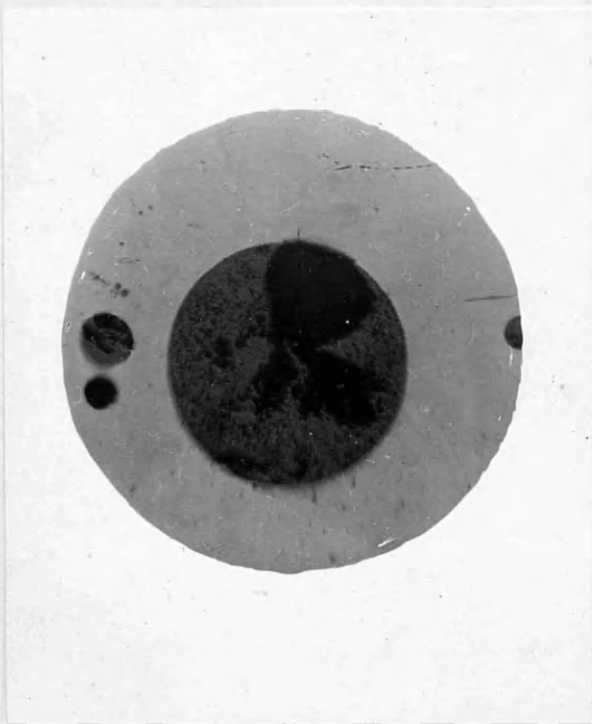
a - x 40
b - x 1500

Fig. 83 - FeO - MnO - SiO$_2$ Inclusion

to 7 : 1.   Addition of these alloys to iron containing oxygen resulted in the formation of large silicate inclusions.   These ratios have been supported by Korber and Oelsen[77].   The above calculations show that other ratios can give very fluid deoxidation products, although for practical amounts of deoxidation (e.g., removal of 80-90 per cent of oxygen from iron containing about 0.04 per cent oxygen) the present work indicates that the most suitable ratios lie between 3 : 1 and 6 : 1.   Such deoxidisers will give very fluid inclusions containing up to 20 per cent FeO.

This has actually been demonstrated in the course of the present work.   Fig.83a shows an inclusion produced by adding a deoxidiser containing Mn and Si in the ratio 4 : 1 to iron saturated with oxygen.   The ingot was allowed to cool slowly in the furnace.   Very large inclusions were produced, visible to the naked eye.   Such large inclusions probably grew from smaller ones during cooling either by coalescence with other small inclusions, according to Herty[17] or by progressive precipitation of deoxidation products on the inclusions already present, according to Sims and Lillieqvist[18] The spherical shape of the inclusions almost certainly indicates that they were liquid at the freezing point of the metal.

The same inclusion at a much higher magnification shown in Fig.83b shows a small amount of primary oxide phase and oxide-orthosilicate eutectic.   Its melting point would be about/

about 1300°C.   The high MnO content of this inclusion is in accord with the fact that the percentage addition of deoxidiser was 4 per cent corresponding to about 98 - 99 per cent removal of oxygen.   To obtain an inclusion contain: :ing 40 per cent SiO_2 would require a deoxidiser with a Mn/Si ratio of about 2, according to Fig.82.   The use of a higher ratio than 2 would, therefore, give rise to inclusions containing less SiO_2 than 40 per cent, as was the case here when a 4 : 1 ratio was used.

A C K N O W L E D G E M E N T. S.

The author wishes to record his thanks to
Professor R. Hay for his friendly criticism and advice.
He is also very much indebted to Dr. P.T. Carter for
his unfailing help and assistance during the course of
this research.

Thanks are also due to Mr. H.A. Sloman of the
National Physical Laboratories for his helpful advice
during the construction of the Vacuum Fusion Apparatus.

REFERENCES.

1. Christie, G.E.:   Private communication.

2. Carter, P.T. :   Discussions of the Faraday Society, 1948,
                         No.4, p.307.

3. Vacher, H.C., and   Trans. A.I.M.M.E., 1931, Vol.95, p.124.
   Hamilton, E.H. :

4. Phragmen, G., and   Jernkontarets Ann., 1939, vol.123,
   Kalling, B.   :   p.199.

5. Marshall, S. and   Trans. Am. Soc. Metals, 1942, vol.30,
   Chipman, J.   :   p.695.

6. Chipman, J.   :   Metal Progress, August, 1949, p.211.

7. Zapffe, C.A., and   Trans A.I.M.M.E., 1943, vol.154, p.192.
   Sims, C.E.   :

8. Richardson, F.D.:   J.I.& S.I., 1950, vol.166, No.2, p.137.

9. Körber, F., and   Mitt. Kaiser - Wilhelm Inst. Eisenfors:
   Oelsen, W.   :   :chung, 1935, vol.17, p.39.

10. Herasymenko, P.,:   J.I.& S.I., December, 1947, vol.157,
                        No.3, p.515.

11. Fornander, S., :   Discussions of the Faraday Society, 1948,
                        No.4, p.296.

12. Carter, P.T.,   :   Discussions of the Faraday Society, 1948,
                        No.4, p.342.

13. Speight, G.E., :   Private communication.

14. Chipman, J.,   :   J. of Am. Chem. Soc., 1933, vol.55, p.3131.

15. Goodeve, Sir Charles F. : Discussions of the Faraday Society
                              1948, No.4, p.9.

16. I.& S.I., Sixth Report on the heterogeneity of steel ingots
                              1935, p.47.

17. Herty, C.H., Jr.,   Cooperative Bulletin No.38, U.S.
    and others.   :   Bureau of Mines.

18. Sims, C.E., and   Trans A.I.M.M.E., 1930, vol.100, p.154.
    Lilliegvist, G.A.:

19. Sosman, R.B., and   Trans A.I.M.M.E., 1930, vol.100, p.186
    Kearny, N.J

20. /

20. Dorinckel, F., : Metallurgie, 1911, p.201.

21. Benedicks, C., and "Non-Metallic Inclusions in Steel"
    Lofquist, H. : (Chapman and Hall, London, 1930).

22. Greig, J.W. : Am. J. of Science, 1927, vol.13, p.133.

23. Herty, C.H., Jr.,: Metals and Alloys, 1930, p.883.

24. White, J., J. Roy. Tech. College, Glasgow,
    Howat, D.D., and : 1934, p.231.
    Hay, R.

25. Glaser, O. : Centralblatt fur mineralogie, 1926, p.81.

26. Jager, F.M., and Kon. Acad. V. Wetensch. Amersterdam,
    Von Klooster,H.S. : 1915, vol.24, p.921.

27. Wülfing, A. und Bericht der Heidelberger Akademie
    Hofmann-Degenfeld.: Math.-Phys.Klasse. 1919, No.14.

28. Whiteley, J.H., and J.of I.& S.I. 1919 vol.99, p.199.
    Hallimond, A.F. :

29. Von Keil, O. and Stahl und Eisen, 1925, vol.45, p.890.
    Demmann, A. :

30. Greig, J.W. : Am. J. of Science, 1927, vol.14, p.473.

31. Herty, C.H., Jr., Ind. and Eng.Chem., 1929, vol.21, p.
    and Fitterer,G.R. :

32. Bowen, N.L., and Am. J. of Science, 1932, vol.24, p.
    Schairer, J.F. :

33. Hay, R., Howat,D.D. J.of West of Scotland I.& S.I.,
    and White, J. : 1933-34, vol.41, p.97.

34. Ibrahim, M. : Ph.D. Thesis, Glasgow University 1950.

35. Bowen, N.L. : Am.J. of Science, 1935, vol.30, p.481.

36. Oberhoffer, P., and St. Eisen, 1921, vol.41, p.1449.
    Von Keil, O. :

37. Herty, C.H., Jr., : Metals and alloys, 1930, p.885.

38. Daniloff, B.N. : Unpublished Thesis, Carnegie Inst. of
    Technology, 1930.

39. Andrew, J.H., J.of I.& S.I., 1931 No.II, p.283.
    Maddocks, W.R., :
    and Howat, D.

40. White, J.,   : J.of I.& S.I., 1943, No.2, p.579.

41. Whiteley, J.H. : Seventh Report on the Heterogeneity of steel Ingots. The I.& S.I., 1937, Special Report No.16, p.23.

42. Jay, A.H., and Andrews,K.W. : J.of I.& S.I., 1945, vol.152, p.15.

43. Petterssen, H. : Jernkonterets Annaler, 1946, vol.130 p.653.

44. White, J. and Ford, W.F., : J.I.& S.I., 1946, vol.153, No.1, p.353

45. Carter, P.T., and Ibrahim, M. : Society of Glass Technology. In press.

46. Richardson, F.D., and Jeffes, J.H. : J.of I.& S.I. 1948, vol.160, No.3 p.261.

47. Kitchener, J.A., and Bockris ,J.O'M.: Discussions of the Faraday Society, 1948, No.4, p.91.

48. Maddocks, W.R. : Carnegie Memoirs, 1935, vol.24, p.51.

49. Rait, J. McMillan,Q.C., and Hay, R. : J.of the Roy.Tech. College, Glasgow, 1939, vol.4, p.449.

50. Bockris, J.O'm., Kitchener, J.A. Ignatowicz,S., and Tomlinson, J.W. : Discussions of the Faraday Society, 1948, No.4, p.264.

51. Carter, P.T., and Harris, I. : J. of the Physical Society, 1950.

52. Hart, R.H., and Rennie, R., : A.R.T.C., Thesis, the Royal Tech. College, Glasgow, 1950.

53. Harstigen : A.S.T.M. Card Index.

54. Ross, C.S., and Kerr, P.F., : Am. Min., 1932, vol.17, p.11.

55. Murray, P., and White, J. : Discussions of the Faraday Society, 1948, No.4, p.287.

55a. Warren, B.E., and Pincus, A.G. : J. of Am. Ceram. Society, 1940, vol.23 p.301.

56. Herty, C.H., Jr. Conley, J.E. and Royer, M.B. : Bureau of Mines, Tech. paper No.523.

57. Hay, R., White J.,: J.of the West of Scotland I.& S.I.,
    and McIntosh,A.B. 1934-35, vol.42, p.99.

58. Perutz, M.   : Mineralogical magazine, 1935-37, vol.24,
                          p.573.

59. Sundius, N.   : Mineralogical Abstracts, 1929-31, vol.4,
                          p.527; 1932-34, vol.5, p.143.

60. Wentrup, H.,   : Tech.Mitt. Krupp, 1937, vol.5, p.131.

61. Bell, H.   : Private communication.

62. Chipman, J. : Discussions of the Faraday Society, 1948,
                          No.4, p.23.

63. Richardson,F.D.   : J.of I.& S.I., 1950, vol.166, No.3,
    Jeffes J, and   p.213.
    Withers, G.

64. Richardson,F.D.,   : Discussions of the Faraday Society,
                          1948, No.4, p.244.

65. Zachariasen, W.H. : J.Am. Chem. Socy., 1932, vol.54, p.3841.

66. Warren, B.E.   : J.App.Phys.,1937,vol.8, p.645; 1942,vol.13,
                                                            p.802.
67. King, T.B.   : Ph.D. Thesis, Glasgow University, 1951.

68. Towers, H. and Trans. of British Ceramic Society, 1950,
    Kay, J.   : vol.49, p.341.

69. Losana, P.   : Atti delle Raele Accad. Sci. Torino,
                          1942-43, vol.78, p.194.

70. Urbain, G.   : Private communication.

71. Guggenheim,E.A.,   : Discussions of the Faraday Society,
                          1948, No.4, p.317.

72. Carter, P.T.   : Discussions of the Faraday Society, 1948,
                          No.4, p.326.

73. Colclough, T.P.,   : J.I.& S.I., 1920, vol.No.1, p.267.

74. Krings, W., and   : Zeitschrift fur anorganische Chemie,
    Schackmann, H.,   1932, vol.206, p.356.

75. Schenck, H.,   : "Physical Chemistry of Steel Making"
                          published by B.I.S.R.A.

76. Taylor, C.R., and : Trans. A.I.M.M.E., 1941, vol.154,
    Chipman, J.,   p.228.

77. White, J.   : The Iron and Steel Institute, Carnegie,
                          Scholarship Memoirs, 1938, vol.27, p.1.

78. Körber F., and: Mitteilungen aus dem Kaiser-Wilhelm-
    Oelsen, W.   Institut fur Eisenforschung,1933, vol.15,
                          p.271.

79. Darken, L.S., and: Trans. A.I.M.M.E., 1942, vol.150,
    Larsen, B.M.   p.87.

80. Herasymenko, P., : Trans. Faraday Soc., 1938, vol.34, p.1245

81. Tempkin, M.   : Acta. Physicoehim, 1945, vol.20, 411.

82. Samarin, A.M.,: Acta Physicochim, 1945, vol.20, 421.
    Tempkin, and
    Schwarzmann.

83. Herasymenko, P., :J. of S.I., 1950, vol.166, No.3, p.169.
    and Speight, G.E.

84. Chang, L.C., and : Met. Tech., Oct. 1946, Technical
    Derge, G.   Publication No.2101.

85. Hildebrand, J.M.: Proc. Nat. Acad. Sci. 1927, vol.13, p.267.

86. Rey, M.   : Discussions of the Faraday Society, 1948,
                      No.4, p.257.

87. Oberhoffer, P.and: Stahl u. Eisen, 1927, vol.47, p.1526.
    Schenck, H.

88. Tammann, G. and : Archiv. Eishenhüttenwesen, 1932,
    Oelsen, W.   vol.5, p.75.

89. Herty, C.H.,Jr. : Trans.A.I.M.M.E.,1926,vol.73,p.1107.

90. Körber, F., and : Mitt. Kais. Wilhelm Inst. Eisenforsch.,
    Oelsen, W.   Dussledorf, 1932, vol.14, p.181.

91. Krings, W., and : Ztsch. anorg. allgem.Chemie, 1931,
    Schackmann, H.   vol.202, 99; 1932, vol.206, p.337.

92. Chipman, J.,   : J. of Metals,   Feb.1950, p.341.
    Gero, N., and
    Winkler, T.B.

93. Hilty, D.C., and : J. of Metals, Feb.1950, p.414.
    Crafts, W.

94. Hilty, D.C. and : J. of Metals, Feb.1950, p.425.
    Crafts, W.

95. Barrett, E.P.,   :   Trans. A.I.M.M.E., 1939, vol.135, p.88.
    Holbrook, W.F.,
    and Wood, C.E.

96. Winkler, T.B., and: Trans. A.I.M.M.E., 1946, vol.167,
    Chipman, J.   p.111.

97. Wentrup, H., and : Archiv fur das Eisenhüttenwesen, 1939-40
    Hieber, G.   vol.13, p.69.

98. Dancy, C.   : Trans.Brit. Ceramic Society, 1950,
                           vol.49, p.360.

99. Smith, T.B.   :"Analytical Processes" Edward Arnold &
                           Co. London, 1940.

100. Reeve, L.   :   Trans. A.I.M.M.E., 1934, vol.113, p.82.

101. Oberhoffer, P. and : Stahl und Eisen, various references
     co-workers.   from 1922 to 1929.

102. Jordan, L. and : Bureau of Standards, Scientific paper
     Eckman, J.R.   No.514, 1925.

103. Thompson, J.G. : J.of Research, National Bureau of
     Vacher, H.C.,   Standards, 1937, vol.18, p.259.
     and Bright,H.A.

104. Sloman, H.A.   : I.& S.I. Sixth report of the heterogeneity
                        of steel ingots, 1935, p.71.

105. Sloman, H.A.   : I.& S.I. Seventh report of the heterogeneity
                        of steel ingots, 1937, p.82.

106. Sloman, H.A.   : I.& S.I. Eighth report of the heterogeneity
                        of steel ingots, 1939, p.48.

107. Sloman, H.A.   : Third report of the oxygen sub-committee.
                        J.I.& S.I. 1941, Vol.143, No.1.

108. Thanheiser and : Arch. Eisenhüttenw, 1935 36, vol.9.
     Brauns.   p.035.

109. Thompson, J.G. : J.of Research, National Bureau of
     and Holm,V.C.F.   Standards, 1938, vol.21, p.87.

110. Mallett, M.W.   : Trans.Am.Society for metals, 1949,
                        vol.41, p.870.

111. Hurst, J.E. and: J.I.& S.I. 1948, vol.159, No.2, p.130.
     Riley, R.V.

112. Ambler, H.R.   : The Analyst, 1929, vol.54 , p.517.

113. Tammann, G., and : Archiv. Eisenhüttenwesen, 1932, vol.5
     Oelsen, W.   p.75.

114. Huggins, M.L.   : J. Opt. Socy. Am. 1940, vol.30, p.420.

115. Zintl, E., and   : Z. anorg. Chemie, 1938, vol.236,
     Marawietz,   p.385.

116. Herty, C.H. Jr., : U.S. Bureau of Mines, Report of
     and Fitterer,G.R.   Investigations, 1930, No.3054 and
                          1931, No.3081.